Development of Glutamate Sensor Based on Nickel Oxide Nano Particle

by

Sumon Chakrabarty

A thesis submitted in partial fulfillment of the requirements for the degree of
Master of Science in Chemistry

Khulna University of Engineering & Technology
Khulna 9203, Bangladesh.

August 2016

Declaration

This is to certify that the thesis work entitled “Development of Glutamate Sensor Based on Nickel Oxide Nano Particle” has been carried out by Sumon Chakrabarty in the Department of Chemistry, Khulna University of Engineering & Technology, Khulna, Bangladesh. The above thesis work has not been submitted anywhere for the award of any degree or diploma.

Signature of Supervisor

Signature of Candidate

Acknowledgements

Firstly I would like to express my gratitude to my supervisor **Dr. A.B.M. Mamun Jamal**, Assistant Professor, Department of Chemistry, Khulna University of Engineering & Technology, for his endless enthusiasm and support throughout my studies. He had helped me at each and every point of the thesis work with his dedication, comments, suggestions and guidance which put me on the right path to fulfill the requirement, without which this situation was impossible to overcome. He also friendly supported me a lot in my daily life which I am truly appreciated.

I would like to thank Prof. Dr. Md. Abdul Motin, Head, the Department of Chemistry, KUET and the staff of the department for their continuous support during my thesis work. I would like to give my special thanks to Prof. Dr. Mohammad Abu Yousuf, Department of Chemistry, KUET for his excellent support, laboratory facilities, advice and enthusiasm throughout my M.Sc. I would like to thanks University Grant Commission and Khulna University of Engineering & Technology for funding my research.

I also want to express my all thanks, gratefulness and appreciations to my fellow researchers in the department for all the support they have done to me during this one and half year period.

Huge thanks go to my family for giving me inspiration, blessing and encouragement throughout the period of study.

Sumon Chakrabarty

Abstract

L-glutamic acid is one of the 20 standard amino acids used by all organisms. It plays an important role in clinical applications and in food processing and well known as a flavor enhancer commonly found in various foods. The excessive intake of this flavor enhancer can cause toxic effect to the human health. Therefore, development of sensors or biosensors for the determination of glutamate has been of great interest over the past two decades owing to its importance in food and biomedical industries.

In this study nickel oxide nanocrystal and nickel oxide hollowsphere have synthesized by using sol-gel and hydrothermal methods. Morphological characterization of nickel oxide particle was carried out using scanning electron microscopy (SEM) and X-ray diffraction (XRD). The crystallite size of nickel oxide prepared by sol-gel method has been found 60 nm. Nickel oxide nanocrystal shows higher selectivity towards glutamate detection compare to nickel oxide hollowsphere. The enzyme-free sensor has been fabricated through modification of glassy carbon using the mixture of nickel oxide nanocrystals and citosan (NiO/GCE). Cyclic voltammetry (CV) and amperometry were used to investigate the electrochemical behavior and catalytic properties of the assembled sensor for glutamate electro-oxidation in alkaline media. It has been found that NiO/GCE showed remarkably enhanced electrocatalytic activity towards glutamate and the electrochemical reaction is diffusion controlled. The sensitivity of NiO/ GCE has been found to be 11 $\mu A/mM/cm^2$. Under optimal detection conditions, the sensor exhibited linear behavior for glutamate detection in the concentration up to 8 mM with a limit of detection of 272 μM. The interference study of NiO/GCE has been found a significant current response for glutamate compared to the uric acid and ascorbic acid. The stability of NiO/GCE has been studied over a period of one week and found to retain 65% of its original activity towards glutamate detection. Experimental results show that NiO/GCE has significant promise for fabricating cost effective, enzyme-less, sensitive, stable and selective sensor platform.

Contents

LIST OF TABLES

LIST OF FIGURES

CHAPTER I

Introduction

1.1 General

Electroanalytical chemistry, also known as electroanalysis, lies at the interface between analytical science and electrochemistry. It is concerned with the development, characterization and application of chemical analysis methods employing electrochemical phenomena. It has major significance in modern analytical science, enabling measurements of the smallest chemical species, right up to the macromolecules of importance in modern technology.

Today, the electrochemical sensor plays an essential analytical role in the fields of environmental conservation and monitoring, disaster and disease prevention, and industrial analysis. A typical chemical sensor is a device that transforms chemical information in a selective and reversible way, ranging from the concentration of a specific sample component to total composition analysis, into an analytically useful signal. A huge research effort has taken place over the several years to achieve electrochemical sensors with attractive qualities including rapid response, low cost, miniaturisable, superior sensitivity and selectivity, and appropriate detection limits. In the highly diverse field of chemical (and biochemical) sensing, the sensor is governed by both the aspect of the environment it is measuring and the matrix in which it is in. As well as sensors that use electrochemistry as the type of energy transfer that they detect, optical [1], thermal [2] and mass-based [3] sensors are also well-developed. From an analytical perspective, electrochemistry is appealing as it directly converts chemical information into an electrical signal with remarkable detectability, experimental simplicity and low cost.

There is no need for sophisticated instrumentation, e.g., optics. A very attractive feature of electrochemistry is that it depends on a surface phenomenon, not an optical path length, and thus sample volumes can be very small, lending itself to miniaturisation. The interest

in electrochemical sensors continues unabated today, stimulated by the wide range of potential applications. Their impact is most clearly illustrated in the widespread use of electrochemical sensors seen in daily life, where they continue to meet the expanding need for rapid, simple and economic methods of determination of numerous analytes [4-6].

Through the refinement of existing sensing technologies along with the development of innovative functional sensor materials including nano and biological materials [7-10], improved data analysis [11], and sensor fabrication and miniaturisation [12-14], opportunities for the construction of new generation sensors with much improved performances are emerging. Two branches of electrochemical sensors are developing: sensors with increased specificity and sensors capable of simultaneous/multiplex determination. In both of these branches, the ability to operate in complex biological matrixes will remain critical, forcing researchers to solve problems of biocompatibility and stability [15].

For many years, food additives have been used for flavoring, coloring and extension of the useful shelf-life of food, as well as the promotion of food safety [16]. Flavoring systems are very important in savory food manufacturing. Flavorings can play an important nutritional role, particularly in foods that are not very flavorful, by providing the needed appeal [17]. Foods and ingredients high in free amino acids or made up of protein have been used in cooking for many centuries, in many cultures, in order to enhance the sensory qualities of various foods [18].

Glutamate is one of the most common amino acids found in nature. It is the main component of many proteins and peptides, is present in most tissues and virtually every food contains glutamate. Glutamate is also produced in the body and plays an essential role in human metabolism [19-21]. It is a major component of most natural protein foods such as meat, fish, milk and some vegetables. In the early 1900s, researchers isolated an ingredient (glutamate) in plants (i.e. seaweed) that is the essential taste component responsible for greatly enhancing flavor [19, 21]. From then glutamate is being widely used in the food industry as flavor enhancer, and commonly used as its sodium salt (monosodium glutamate).

Monosodum glutamate (MSG) has a toxic effect on the testis by causing a significant oligozoospermia and increase abnormal sperm morphology in a dose-dependent fashion in male living beings [22]. It has been implicated in male infertility by causing testicular hemorrhage, degeneration and alteration of sperm cell population and morphology [23]. It has been reported that MSG has neurotoxic effects resulting in brain cell damage, retinal degeneration, and endocrine disorder. Some of the pathological conditions that are attributed with the disease, such as addiction, stroke, epilepsy, brain trauma, neuropathic pain, anxiety, depression [24], schizophrenia [25], Parkinson's disease [26], Al-zheimer's disease [27], Huntington's disease, and amyotrophic lateral sclerosis. It can be stated that MSG is the cause of such varied conditions as epilepsy and Al-zheimer's disease, although there may be concerns of its involvement in its etiology [28].

Due to glutamate's ubiquity throughout the human body and its central metabolic role; it is an excellent biomarker for toxicity. Many pharmaceutical compounds act upon disease causing cells by inducing cytoxicity via apoptosis and/or necrosis. In a loss of cell membrane integrity leading to the release of its cell contents, which includes glutamate [29]. So it is very important to detect glutamate fluctuation.

Electrochemical screening techniques are the most popular compare to other central laboratory based techniques such as spectrophotometric [30] or chromatographic [31] techniques. It is due to the growing demand for development of in situ, portable, cost effective methodology, where electrochemical techniques have proven advantages for such applications. However, challenges are attributed to such developments are selectivity, sensitivity, response time, stability, biocompatibility and reproducibility. Trends for researchers and manufacturers working with the micro and nanostructured materials as sensing platform is growing popularity due to the higher sensitivity and lower noise, can be used for in situ technology, as well as more suitable towards biocompatibility, improve response time, stability and reproducibility.

Many studies about providing suitable coating on the electrodes have been investigated, Electron transfer chemical and electrocatalysis properties are very important for them. Exact determination of glutamate concentration is necessary for food industry [32]. Chitosan include excellent biocompatibility, biodegradability, nontoxicity, highmechanical

strength, good adhesion and cheap properties, therefore it has been used as an immobilization matrix [33].

In this work, a film of nickel oxide nanoparticle + chitosan modified glassy carbon electrode (NiO/GCE) electrode was prepared for oxidation of glutamate without using any enzyme. The electrochemical properties of this sensor were investigated. This sensor exhibited rapid response, low detection limit and broad linear range.

1.2 Glutamate

Glutamate is one of the most common amino acids found in nature. It is the main component of many proteins and peptides, and is present in most tissues. Glutamate is also produced in the body and plays an essential role in human metabolism.

Monosodium glutamate is the sodium salt of glutamic acid, one of the most abundant naturally occurring non-essential amino acids. It is found in tomatoes, parmesan chees, potatoes, mushrooms, and other vegetables and fruits [34].

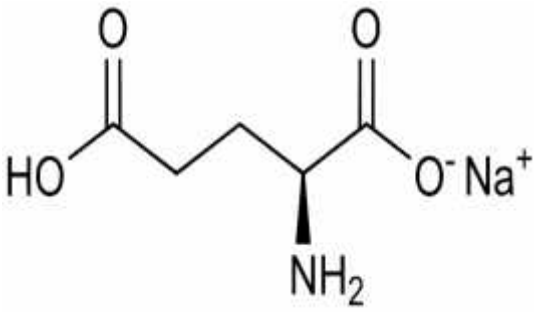

Fig.1.1: Structure of monosodium glutamate.

Glutamate is considered to be the primary neurotransmitter in the mammalian brain and facilitates normal brain function [35]. It is a non-essential endogenous excitatory amino acid that is synthesized in neurons, from precursors such as glutamine and 2-oxoglutarate. Along with aspartate and homocysteine, glutamate contributes to excitatoryneurotrans - mission in the central nervous system (CNS), whilst its immediate precursor gamma – amino butyric acid (GABA) acts as an endogenous inhibitory neurotransmitter [36].

Neurotoxicity, which causes damage to brain tissue, can induce by glutamate at high concentrations.

In cellular metabolism, glutamate also contributes to the urea cycle and tricarboxylic acid cycle (TCA)/Krebs cycle. It plays a vital role in the assimilation of NH^{4+} [37]. Glutamate is synthesised from $NH^{4+}$and alpha-ketoglutarate by glutamate dehydrogenase (GLDH). The process is a reversible reaction, whereby glutamate can also be converted to alpha - ketoglutarate by oxidative deamination. The reaction can only occur in the presence of the coenzyme nicotine adenine dinucleotide (NAD^{+}). The direction of the reaction is primarily dependent on the relative concentrations of glutamate, alpha-ketoglutarate, ammonia and the ratio of oxidized to reduce coenzymes.

Intracellular glutamate levels outside of the brain are typically 2 –5 mmol/L, whilst extracellular concentrations are ~0.05 mmol/L [38] and is present in high concentrations throughout the liver, brain, kidney and skeletal muscle [39]. Glutamate has a significant role in the disposal of ammonia, which is typically produced from the digestion of dietary amino acids, protein and the ammonia produced by intestinal tract bacteria. Glutamate can also dispose of ammonia by being converted to glutamine by glutamine synthase.

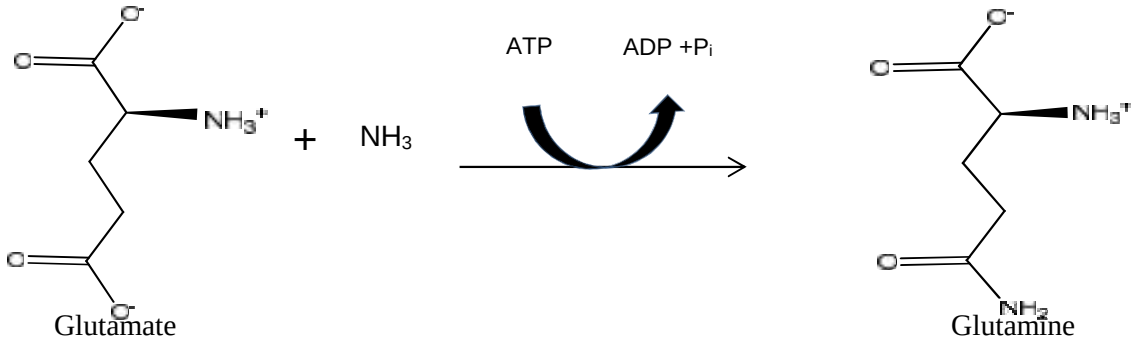

Glutamate Glutamine

1.2.1 Glutamate natural occurrence

Glutamate, one of the most common amino acids found in nature, is present in many proteins and peptides and most tissues. Glutamate is also produced in the body and binds with other amino acids to form a structural protein [40]. When glutamate bounds to protein

molecule, it is tasteless and does not provide umami taste to food. However, protein hydrolysis during fermentation, aging, ripening and heat cooking process will liberate free glutamate [41].

Glutamate is a crucial component of the taste of cheese, sea foods, meat broths, and other foods [42]. They reported measured free glutamic acid, which present naturally in different foods, such as meat, poultry, seafood and vegetables (Table 1.1). Seaweed, cheese,fish sauce, soy sauce, fermented beans (locust beans and soybeans) and tomato showed high levels of free glutamic acid. Konosu, Hayashi, and Yamaguchi [43] showed that the characteristic tastes of many natural foods are reproduced by mixing amino acids, umami taste substances and salts in appropriate ratios.

Table1.1 : Natural glutamate content of foods.

Food items	Free glutamic acid (mg/100g)
Meat and poultry	
Beef	10
Pork	9
Chicken	22
Vegetables	
Cabbage	50
Tomato	246
Corn	106
Green peas	106
Onion	51
Potato	10
Mushroom	42
Fruits	
Avocado	18
Apple	4
Grape	5
Kiwi	5

1.3 Electrochemical sensors

Electrochemical sensors are the devices, which are composed of an active sensing material with a signal transducer. The role of these two important components in sensors is to transmit the signal without any amplification from a selective compound or from a change in a reaction. These devices produce any one of the signals as electrical, thermal or optical output signals which could be converted into digital signals for further processing. One of the ways of classifying sensors is done based on these output signals. Among these, electrochemical sensors have more advantage over the others because; in these, the electrodes can sense the materials which are present within the host without doing any damage to the host system. On the other hand, sensors can be broadly classified into two categories as chemical sensors and biosensors. The biosensors can be defined in terms of sensing aspects, where these sensors can sense biochemical compounds such as biological proteins, nucleotides and even tissues [44].

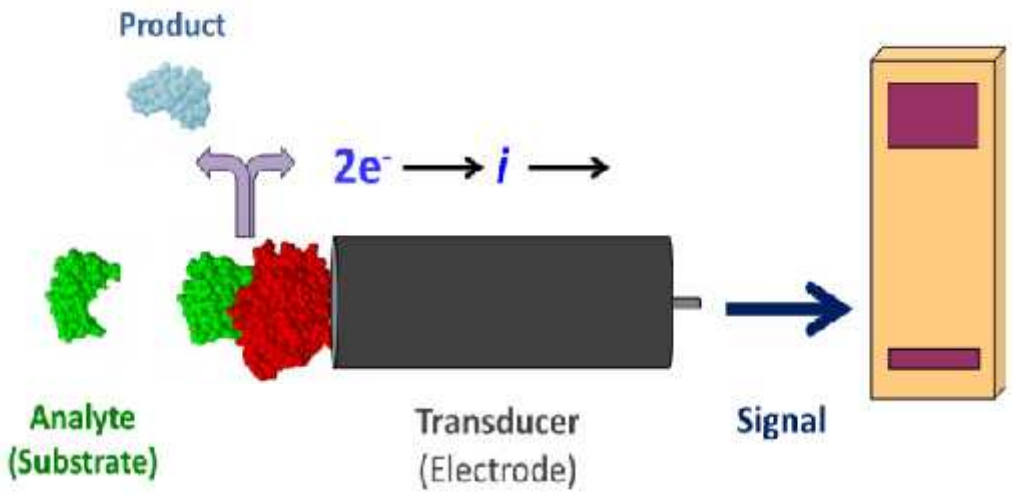

Fig.1.2: Mecanism of electrochemical sensor.

Depending on the exact mode of signal transduction, electrochemical sensors can use a range of modes of detection such as potentiometric, voltammetric and conductimetric. Each principle requires a specific design of the electrochemical cell. Potentiometric sensors are very attractive for field operations because of their high selectivity, simplicity

and low cost. They are, however, less sensitive and often slower than their voltammetric counterparts. Examples of transduction techniques include:

- Potentiometric – The measurement of the potential at zero current. The potential is proportional to the logarithm of the concentration of the substance being determined.

- Voltammetric – Increasing or decrease the potential that is applied to a cell until the oxidation or reduction of the analyte occurs. This generates a rise in current that is proportional to the concentration of the electroactive potential. Once the desired stable oxidation/reduction potential is known, stepping the potential directly to that value and observing the current is known as amperometry.

- Conductiometric – Observing changes in electrical conductivity of the solution. [45]

The selection and development of an active material is a challenge. The active sensing materials may be of any kind as whichever acts as a catalyst for sensing a particular analyte or a set of analytes. The recent development in the nanotechnology has paved the way for large number of new materials and devices of desirable properties which have useful functions for numerous electrochemical sensor and biosensor applications [5].

Basically by creating nanostructure, it is possible to control the fundamental properties of materials even without changing their chemical composition. In this way the attractive world of low dimensional systems, together with the current tendencies on the fabrication of functional nanostructured arrays could play a key role in the new trends of nanotechnology [12, 46, 47].

Further, the nanostructures can be used for both efficient transport of electrons and optical excitation, and these two factors make them critical to the function and integration of nanoscale devices [48-50]. In fact, nano systems are the smallest dimension structures that can be used for efficient transport of electrons and are thus critical to the function and integration of these nanoscale devices.

1.3.1 Chemically modified electrodes

Chemically modified electrodes (CMEs) comprise a relatively modem approach to electrode systems a wide spectrum of basic electrochemical investigations, including the relationship of heterogeneous electron transfer and chemical reactivity to electrode surface chemistry, electrostatic phenomena at electrode surfaces, and electron and ionic transport phenomena in polymers, and the design of electrochemical devices and systems for applications in chemical sensing, energy conversion and storage, molecular electronics, electrochromic displays, corrosion protection, and electro-organic syntheses. Compared with other electrode concepts in electrochemistry, the distinguishing feature of a CME is that a generally quite thin film (from a molecular monolayer to perhaps a few micrometers-thick multilayer) of a selected chemical is bonded to or coated on the electrode surface to endow the electrode with the chemical, electrochemical, optical, electrical, transport, and other desirable properties of the film in a rational, chemically designed manner [51].

The range of electrode surface properties includes, but is more diverse than, that of ion-selective electrodes (ISEs) which also involve, in their highest forms, rational design of the phase-boundary, partition and transport properties of membranes on or between electrodes. While CMEs can operate both amperometrically (or voltammetrically) and potentiometri-cally, they are generally used amperometrically, a faradaic (charge transfer) reaction being the basis of experimental measurement or study, whereas ISEs are generally used in potentiometric formats where a phase-boundary potential (interfacial potential difference) is the measured quantity [52]. Gas-sensing electrodes (e.g., for $C0_2$, NH_3, NOx) are also potentiometrically based [53] although the oxygen electrode, which functions amperometri -cally, is an exception [54]. Chemically sensitive field effect transistors (CHEMFETs) are basically non-faradaic electrode systems in which electric field variations in the semiconductor gate region control the magnitude of the source drain current [55]. Enzyme-based electrodes detect the product(s) of a reaction between an immobilized enzyme layer and a reaction substrate in many ways, including both amperometric and potentiometric means. The distinction between CMEs and amperometric enzyme-modified electrodes is thus very narrow, the latter being based on a natural biological catalyst, but also with a rational (bio)molecular electrode design goal in mind.

1.3.2 General methods of modification of electrodes

The concept of chemically modified electrodes (CMEs) is one of the exciting developments in the field of electroanalytical chemistry. Many different strategies have been employed for the modification of the electrode surface. The motivations behind the modifications of the electrode surface are: (i) improved electrocatalysis, (ii) freedom from surface fouling and (iii) prevention of undesirable reactions competing kinetically with the desired electrode process [56]. The increasing demand for it has led to the development of a rapid, simple and non-separation method for the simultaneous determination of isomers where the CMEs have emerged as an efficient and versatile approach, and have attracted considerable attention over the past decades due to its advantages in terms of reduced costs, automatic and fast analysis, high sensitivity and selectivity [57-61]. There are numerous techniques that may be used to modify electrode surfaces. Amongvarious CMEs, polymer-modified electrodes (PMEs) are promising approach to determination. Some modification processes are-

Covalent Bonding: This method employs a linking agent (e.g. an organosilane) to covalently attach one of several monomolecular layers of the chemical modifier to the electrode surface [59].

Drop-Dry Coating(or solvent evaporation):A few drops of the polymer, modifier or catalyst solution are dropped onto the electrode surface and left to stand to allow the solvent to dry out [60].

Dry-Dip Coating: The electrode is immersed in a solution of the polymer, modifier or catalyst for a period sufficient for spontaneous film formation to occur by adsorption. The electrode is then removed from solution and the solvent is allowed to dry out [57].

Composite: The chemical modifier is simply mixed with an electrode matrix material, as in the case of an electron-transfer mediator (electrocatalyst) combined with the carbon particles (plus binder) of a carbon paste electrode. Alternatively, intercalation matrices such as certain Langmuir-Blodgett films, zeolites, clays and molecular sieves can be used to contain the modifier [61].

Spin-Coating(or Spin-Casting): it is also called spin casting, a droplet of a dilute solution of the polymer is applied to the surface of a rotating electrode. Excess solution is spun off the surface and the remaining thin polymer film is allowed to dry. Multiple layers are applied in the same way until the desired thickness is obtained. This procedure typically produces pinhole-free thin films for example, oxide xerogel film electrodes prepared by spin-coating a viscous gel on an indium oxide substrate [57].

Electrodeposition: In this technique the electrode is immersed in a concentrated solution ($\sim 10^{-3}$ $molL^{-1}$) of the polymer, modifier or catalyst followed by repetitive voltammetry scans. The first and second scans are similar, subsequent scans decrease with the peak current. For example, electrochemical deposition of poly (o-toluidine) on activated carbon fibre [61].

Electropolymerisation: A solution of monomer is oxidized or reduced to an activated form that polymerizes to form a polymer film directly on the electrode surface. This procedure results in few pinholes since polymerization would be accentuated at exposed (pinhole) sites at the electrode surface. Unless the polymer film itself is redox active, electrode passivation occurs and further film growth is prevented.

In this technique the electrode is immersed in a polymer, modifier or catalyst solution and layers of the electropolimerized material builds on the electrode surface. Generally, the peak current increases with each voltammetry scan such that there is a noticeable difference between the first and final scans indicating the presence of the polymerized material. For example, electropolymerization of aniline on platinum electrode perturbations.

Chitosan: Chitosan is a derivative of chitin, which is one of the world's most plentiful organic resources and is derived from the shells of crustaceans. It is a linear polyaminosaccharaide composed of randomly distributed β-(1,4)-linked D-glucosamine and N-acetyl-D-glucosamine groups. Due to its structure, chitosan possesses good adhesion and cheap properties, therefore it has been used as an immobilization matrix. Although it has poor electrical conductivity, but it usually has been combined with carbon nanotubes, redox mediator and metal nanoparticles [62].

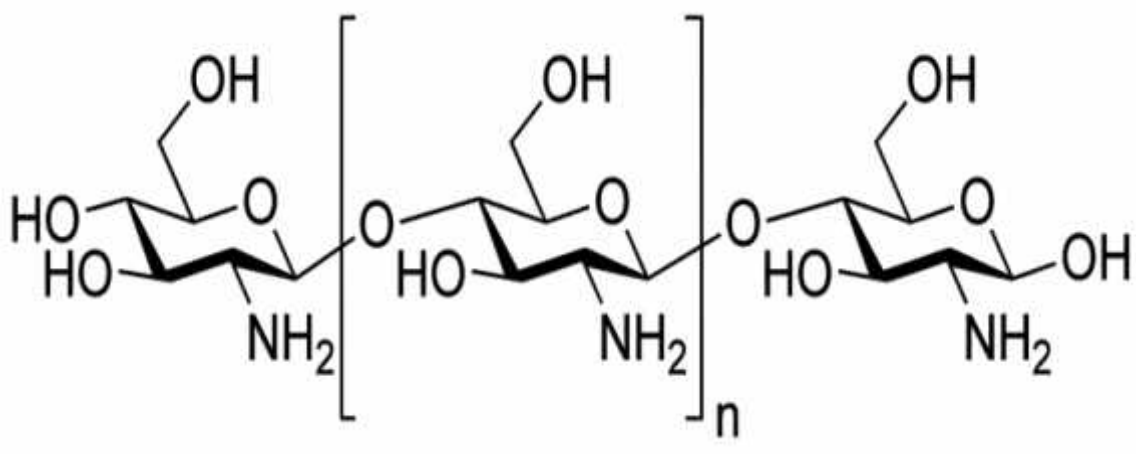

Fig 1.3: Structure of chitosan.

Chitosan is soluble in aqueous acidic media at pH < 6.5. When dissolved, it bears a high positive charge on its amino groups. Chitosan has gel-forming properties as a result of its ability to adhere to negatively charged surfaces and aggregate polyanionic compounds.

1.3.3 Electrochemical glutamate sensors

A lot of research in glutamate sensors has focused on electrochemical methods. Electrochemical sensors can be produced very cheaply, allow for miniaturization and are well-known, so they are easy to use. Most electrochemical glutamate sensors rely heavily on the use of enzymatic reactions. Glutamate reacts with an immobilized enzyme (most commonly glutamate oxidase or) to form reactants that can be amperometrically sensed. Two different classes of amperometric sensors can be distiguished. The first class uses the enzyme glutamate oxidase to turn glutamate into among other things hydrogen peroxide. The second class relies on an additional redox reaction with additional enzymes, such as horseradish peroxidase.

$$\textbf{L-glutamate} + O_2 + H_2O \longrightarrow \textbf{2-oxoglutarate} + NH_3 + H_2O_2$$

There have been many subsequent sensors that rely on the same enzymatic reaction for glutamate sensing. Most sensors now a days use a combination bovine serum albumin (BSA) and glutaraldehyde to immobilize the oxidase on the electrode. While this reaction

is very specific for glutamate, it also requires a sufficient concentration of oxygen. It is therefore not unlikely that a sensor will deprive the brain of its oxygen, which is not favourable, especially since glutamate concentration is strongly associated with ischemia [63].

The use of enzymes for electrochemical sensing dramatically increases sensor costs, making mass production undesirable [64]. In order to overcome this problem, recently introduced a Ni-nanowire electrode which senses glutamate without the use of enzymes [65]. The sensor exploits the high catalytic activity of nickel to carbohydrates. This method achieves high sensitivity, but additional research is necessary to prevent interference by glucose. So far, no other non-enzymatic glutamate sensors have been found in literature, but the results obtained by Jamal show great potential for the development of non-enzymatic sensors.

Recent advances in micro and nano fabrication may result in new non-enzymatic electrodes that can be produced more cost-effective. The development of a new potentiometric glutamate sensor with good sensitivity and selectivity [66] also has potential for further improvement of electrochemical glutamate sensing.

One of the problems with electrochemical sensing of glutamate is the presence of other chemical species which interfere with the reactions and can potentially destroy the electrode. In the brain the most important are ascorbic acid (AA) and uric acid (UA). In order to overcome this problem, many sensors use a membrane that is capable of rejecting these unwanted species, A report by Wahono discusses the advantages and disadvantages of several permselective membranes, and reported that Nafion TM or mono-Phenylenediamine (m-PD)were the most optimal, where m-PD had the best rejection and Nafion was more biocompatible [64]. The sensors that were reviewed have all incorporated Nafion as their rejecting membrane. Most authors included a selectivity study where the sensitivity to Glutamate is compared with the sensitivity to various other species, most importantly AA and UA. All find similar values of above 200, making them suitable for reliable glutamate sensing.

1.4 Fundamentals of electrochemistry and various electro-analytical techniques

1.4.1 Faradaic currents

The Faradaic current is the current that flows through an electrochemical cell that is generated by the change in oxidation state of the electroactive species occurring at the electrode surface, combined with the current contribution due to the charge transfer between the electrode and the background analyte present in solution. The faradaic current obeys Faraday's law.

1.4.2 Charging currents and the electrical double layer

The application of a potential to the electrode surface causes ions near the electrode surface to migrate towards or away from the electrode depending on the respective charge of the electrode and the ions. This forms an electrical double layer, comprised of the electrical charge at the surface of the electrode and the charge of the ions in the solution near the electrode. This double layer leads to the generation of a non-faradaic charging current.

The electrical double layer is an array of charged particles and orientated dipoles. It is composed of two layers; the layer closest to the electrode is known as the inner Helmholtz plane (IHP) and the outer Helmholtz plane (OHP) (Fig 1.4). The planes were discovered by Hermann von Helmholtz in 1853. The IHP is composed of solvent molecules and specifically adsorbed ions, whilst the OHP represents the imagined out er layer closest to the electrode that passes through the centre of solvated ions, but is separated by the molecules at the IHP [67]. These layers are both held at the surface of the electrode. The behaviour of the interface between the electrode and the solution is similar to that of a capacitor.

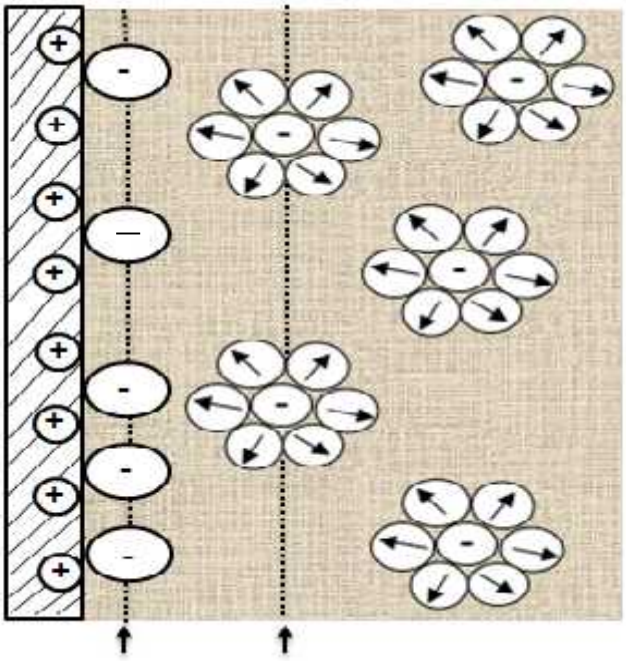

Fig 1.4: Schematic representation of the electrical double layer.

Beyond the double layer, is a diffuse layer of scattered ions that extents into the bulk solution. These ions are ordered relative to the coulombic forces acting upon them and the random motion of the solution by thermal motion. The balance of the electrostatic forces on ions at the surface of the electrode, which are repelled or attracted dependent on their charge, is counterbalanced by the random motion of the diffuse layer. This causes a non-uniform distribution of ions near the electrode surface. As a result, the field strength of the potential applied to the electrode diminishes rapidly, thereby causing the double layer to be extremely thin at 10 – 20 nanometers in thickness. It is also essential to use a high electrolyte concentration, typically a 100 fold greater than that of the analyte, as this concentrates the charge at the Helmholtz planes, therefore ensuring that diffusion is the dominant mechanism for mass transport [68].

1 .4.3 Mass transfer process in voltammetry

Mass transfer is the movement of material from one location to another in solution. In electrochemical systems, three modes of mass transport are generally considered which a substance may be carried to the electrode surface from bulk solution including diffusion, convection and migration. Any of these or more than one might be operating in a given experiment which is depended on the experimental conditions.

In general, there are three types of mass transfer processes:

- Migration
- Diffusion
- Convection

Migration

Migration is the movement of ions through a solution as a result of electrostatic attraction between the ions and the electrodes. It is the primary cause of mass transfer in the bulk of the solution in a cell. This motion of charged particle through solution, induced by the charges on the electrodes is called migration . This charge movement constitutes a current. This current is called migration current. The larger the number of different kinds of ions in a given solution, the smaller is the fraction of the total charge that is carried by a particular species. Electrolysis is carried out with a large excess of inert electrolyte in the solution so the current of electrons through the external circuit can be balanced by the passage of ions through the solution between the electrodes, and a minimal amount of the electroactive species will be transported by migration. Migration is the movement of charged species due to a potential gradient. In voltammetric experiments, migration is undesirable but can be eliminated by the addition of a large excess of supporting electrolytes in the electrolysis solution. The effect of migration is applied zero by a factor of fifty to hundred ions excess of an inert supporting electrolyte.

Diffusion

Diffusion refers to the process by which molecules intermingle as a result of their kinetic energy of random motion. Whereas a concentration difference between two regions of a solution, ions or molecules move from the more concentrated region to the dilute and leads to a disappearance of the concentration difference.

The one kind of mode of mass transfer is diffusion to an electrode surface in an electrochemical cell. The rate of diffusion is directly proportional to the concentration difference. When the potential is applied, the cations are reduced at the electrode surface

and the concentration is decreased at the surface film. Hence a concentration gradient is produced. Finally, the result is that the rates of diffusion current become larger.

Convection

By mechanical way reactants can also be transferred to or from an electrode. Thus forced convection is the movement of a substance through solution by stirring or agitation. This will tend to decrease the thickness of the diffuse layer at an electrode surface and thus decrease concentration polarization. Natural convection resulting from temperature or density differences also contributes to the transport of species to and from the electrode . At the same time a type of current is produced. This current is called convection current. Removing the stirring and heating can eliminate this current. Convection is a far more efficient means of mass transport than diffusion.

1.4.4 Electrochemical setup

Electrochemical cell

Typically electrochemical reactions take place in an electrochemical cell (Fig1.5) which is made from quartz or glass, into which the sample solution is added. The sample solution must be of sufficient depth to cover the two or three electrodes utilised. Variables such as temperature can be controlled by utilising a water jacket cell, which is connected to a thermostatically controlled water bath. Experiments such as amperometry require stirring, thus a magnetic stirrer bar can sit at the bottom of the solution, which is controlled by a magnetic stirrer that sits underneath the electrochemical cell. The stirrer geometry should allow for consistent stirring.

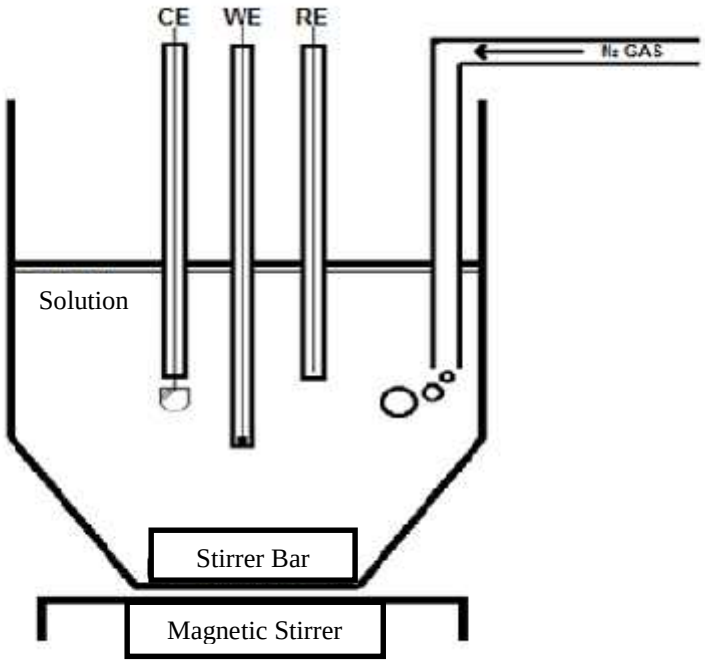

Fig. 1.5: Schematic diagram of a voltammetric cell based on a three electrode system. CE: counter electrode, WE: working electrode, RE: reference electrode.

Working electrode (WE)

The working electrode (WE) is the location at which the reaction of interest takes place. The working electrode must be made of a material that is stable in the electrolyte medium utilised during the experiment, eg: carbon. This is to ensure that the electrode does not corrode or become fouled, thereby altering the surface area, and to prevent other compounds reducing in the potential range of interest. Working electrodes should have high surface reproducibility with a uniform distribution of potential across the surface to prevent IR drop. The background current within the potential region of interest should be low. The cost, availability and toxicity of the material should also be considered.

Reference electrode

A reference electrode acts as a half-cell which has a stable and accurately maintained potential which is used a reference for the measurement of voltage applied by the counter electrode (CE). It is potentiometric and thus has zero current flowing through it. The potentiostat compensates if a difference in voltage is detected between the AE and WE and

adjusts the output accordingly until the difference is zero, this action is known as feedback [69]. An example of a commonly used reference electrode the silver -silver chloride (Ag/AgCl). For applications such as chromoamperometry where small currents are flowing for short time periods, two electrode systems may be used, where the counter electrode assumes the role of RE and WE. Since current flowing through the reference electrode may alter its stability over time, three electrode systems with a counter electrode are often utilised in experimental situations, and for amperometric applications over prolonged time periods.

Counter electrode

The function of the counter electrode (CE) is to complete the circuit by applying a voltage difference respectively to the WE, thereby allowing charge to flow. The CE is composed of an inert material such as carbon or platinum.

Potentiostat

The instrument used to control the potential difference applied across the electrochemical cell is called a potentiostat. A potentiostat adjusts the voltage difference between the anode and the cathode in order to maintain a constant working electrode potential [70]. A potential is applied to the working electrode, resulting in a flow of charge towards the counter electrode. A potential drop (iR) is caused by the electrolyte conductivity, the distance between the electrodes, the magnitude of the current and resistance across the electrode material. If the iR drop is uncompensated, the reaction will no longer operate at the desired potential, and the reaction may cease. The reference electrode monitors the potential at the working electrode and feeds the value back to the opamp. If a difference in potential is observed between the RE and WE, the potential applied to the CE is altered to compensate. A second op-amp is used as a current-voltage converter to measure the flow of current, with a resistor used to output the voltage per unit current.

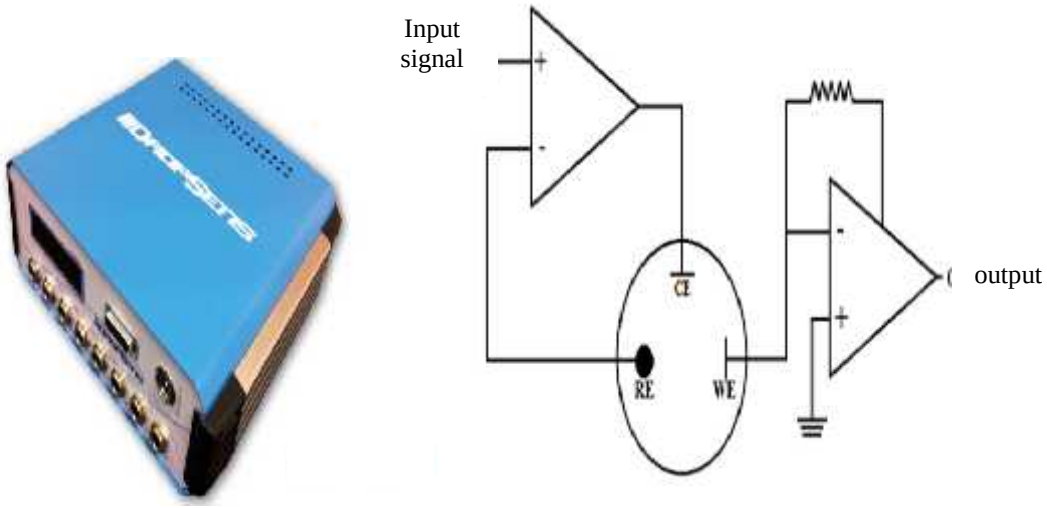

Fig. 1.6 : A potentiostat with circuit diagram of a three-electrode system.

1.4.5 Cyclic voltammetry (CV)

Cyclic voltammetry is a commonly used and versatile potentiodynamicelectroanalytical technique used to study redox systems, the reversibility of the reaction, the stoichiometry of a system and the diffusion coefficient of an analyte. These can be used to determine the electrochemical characteristics and identity of an unknown compound.

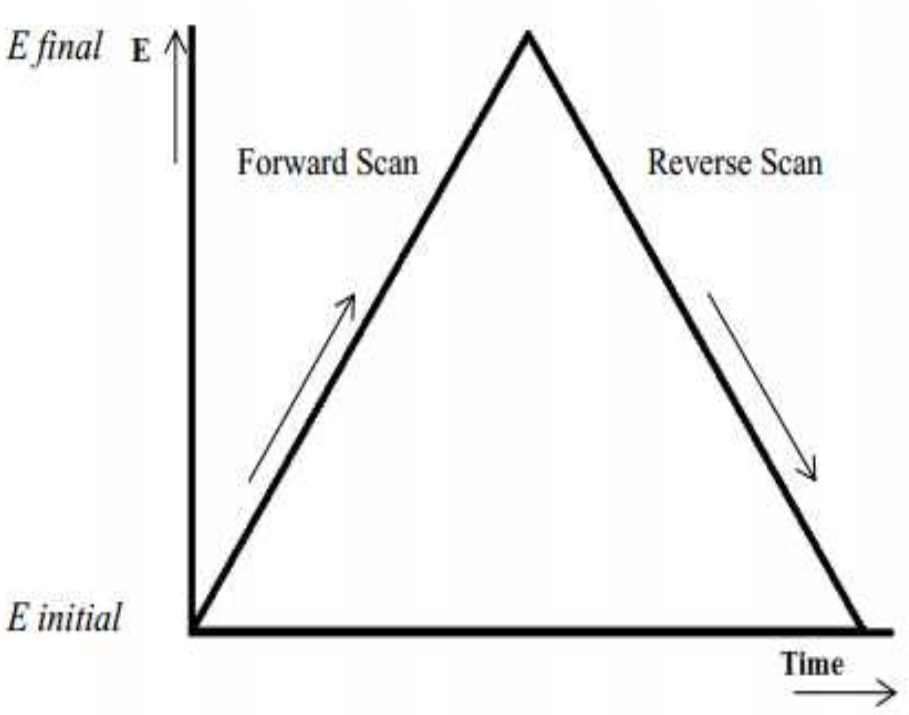

Figure 1.7: Cyclic voltammetry input waveform.

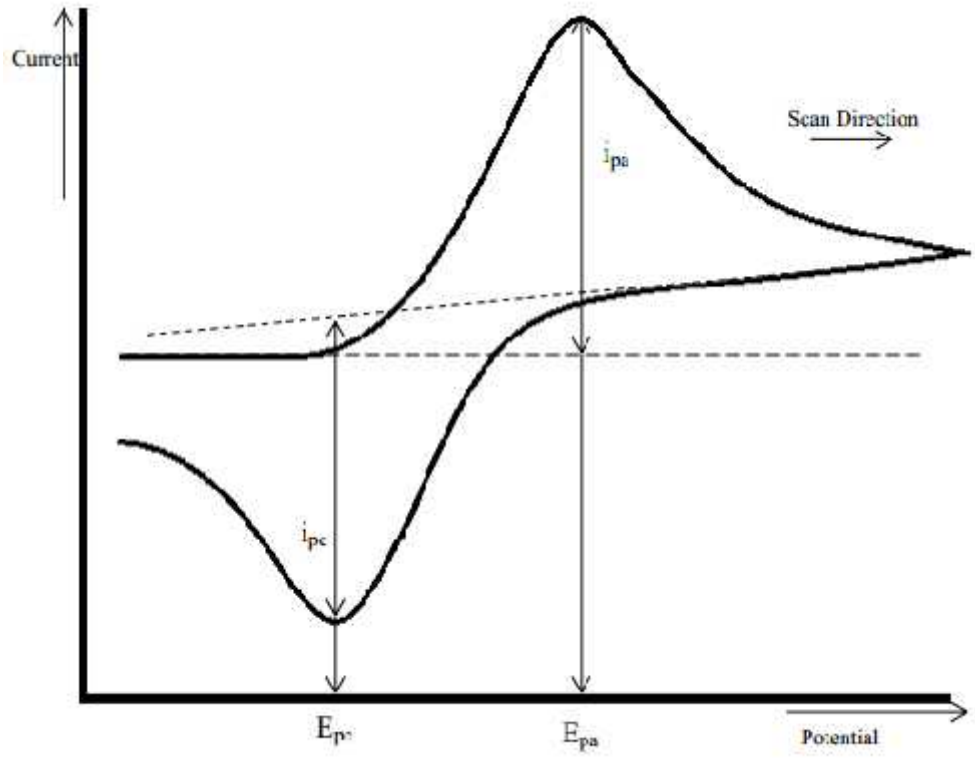

Fig 1.8: Typical Cyclic Voltammogram response for a reversible redox couple.

Cyclic voltammograms are characterized by six important parameters.

- The cathodic (E_{pc}) and anodic (E_{pa}) peak potentials
- The cathodic (i_{pc}) and anodic (i_{pa}) peak currents
- The cathodic half-peak potential ($E_{p/2}$)
- The half wave potential ($E_{1/2}$)

Cyclic voltammetry linearly applies a triangular potential ramp to the working electrode at a defined scan rate until it has reached a set switching potential as shown in Fig 1.7. Once the switching potential on the triangular excitation potential ramp is reached, it begins a scan in the reverse direction. During the potential sweep, the current is measured resulting from the potential applied. The resulting plot of current vs. potential is known as a cyclic voltammogram, as illustrated in Fig. 1.8.

The two peak currents (i_{pc}/i_{pa}) and two peak potentials (E_{pc}/E_{pa}) form the basis for the analysis of the cyclic voltammetric response to the analyte. The shape of the

voltammogram is due to the concentration of the reactant (R) or product (P) at the electrode surface during the scan. Ideally, the scan begins at a potential of negligible current flow whereby the analyte is neither oxidized nor reduced. As the potential is ramped linearly, electron transfer between the electrode and the analyte in the solution begins to occur; this leads to an accumulation of product and a depletion of the reactant. The ramp increases in accordance to the Nernst Equation.

$$E = E^0 + \frac{0.059}{n} log \frac{[OX]}{[Red]}$$

Where E is the applied potential and E^0 the formal potential; [OX] and [Red] represent surface concentrations at the electrode solution interface, not bulk solution concentrations. Note that the Nernst equation may or may not be obeyed depending on the system or on the experimental conditions.

At the peak of the anodic wave the reaction becomes diffusion controlled, as the diffusion layer has grown sufficiently from the electrode that the flux of the product to the electrode is too slow to satisfy the Nernst equation. As a result, the concentrat ion of the reactant at the surface reaches zero. Subsequently, the rate of diffusion then decreases, reducing the current flow, in accordance with the Cottrell equation. Once the potential ramp has reached the switching potential, the potential is ramped in the opposite direction resulting in a cathodic potential being applied.

The peak current for a reversible system is described by the Randles-Sevcik equation [71]. The current is directly proportional to the concentration and increases in respect to the square root of the scan rate. This dependence on scan rate implies the reaction at the electrode is controlled by mass transport. The equation applies at standard temperatures. (25°C, n = number of electrons involved, A = electrode area, D = diffusion coefficient, CB= bulk electrode concentration and v = scan rate).

$$i_p = (2.69 * 10^5)\, n^{\frac{3}{2}} A D^{\frac{3}{2}} C_B v^{\frac{1}{2}}$$

The reversibility of a electrochemically reversible couple can be identified by the measurement of the potential difference the two peak potentials. An electrochemically reversible system based on a one electron transfer process is denoted in equation A fast one electron transfer exhibits a ΔEp of 59 mV.

$$\Delta E_p = E_{pa} - E_{pc} = \frac{59}{n}\ \text{mV}$$

1.4.6 Amperometry

A fixed potential is applied to an electrode against a reference electrode (Fig 1.9) until a steady state current is generated. This is achieved more readily in a stirred solution due to the greater efficiency of mass transport. Stirring also ensures that the concentration gradient at the working electrode is constant. Once steady state is achieved, standard additions of the analyte of interest are added into the voltammetric cell. The additions result in increases in current, with each addition occurring after steady state has been achieved, the magnitude of the current is proportional to the concentration of the analyte, which in turn is proportional to the rate of the redox reaction at the working electrode surface. An example of a typical amperometric plot is shown in Figure 1.9 b.

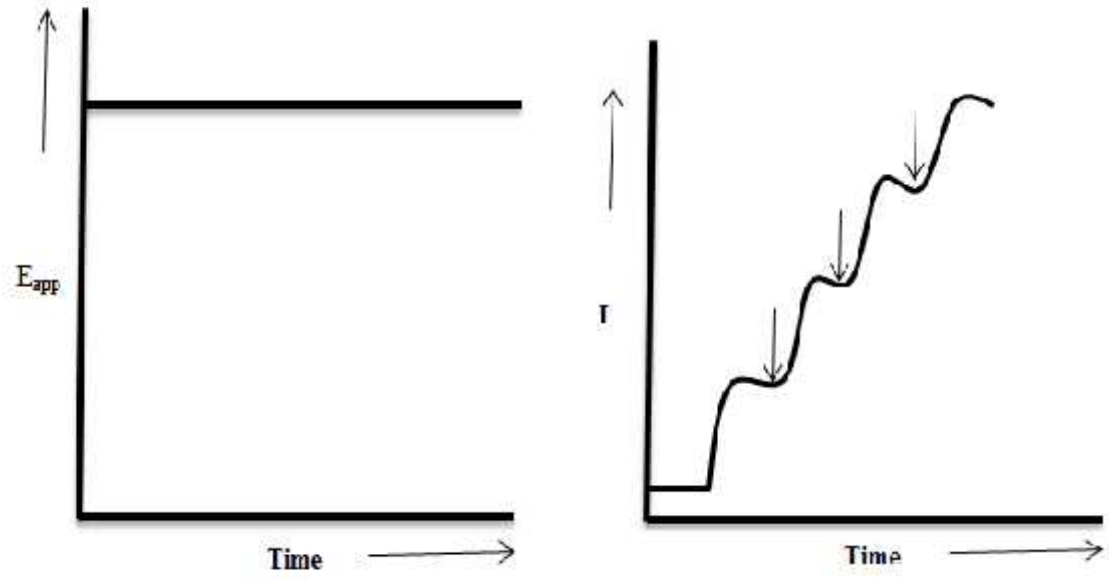

Figure 1.9: (a) Current waveform for amperometric experiments. (b) A typical amperometric plot in stirred solution. Arrows indicate additions of the target analyte.

1.4.7 Chronoamperometry

Chronoamperometry differs from amperometry by being conducted in a quiescent, unstirred solution. A sufficient E_{app} is applied to drive a redox reaction at the surface (Figure 1.10a); this generates a large current which decays rapidly as the concentration of the analyte is depleted at the electrode surface due to the diffusion (Fig 1.10b).

The variation in the magnitude of current with time for a planar electrode is described by the Cottrell equation [72], which is derived from Fick's second law. The equation is described as follows; nrepresents the number of electrons, F is the Faraday constant, A is the electrode area (cm^2), C^o is the bulk electrolyte concentration (mol/cm^3), t is time (seconds) and D is the diffusion coefficient (cm^2/s).

$$i_t = \frac{nFAC^0D^{\frac{1}{2}}}{\pi^{\frac{1}{2}}t^{\frac{1}{2}}}$$

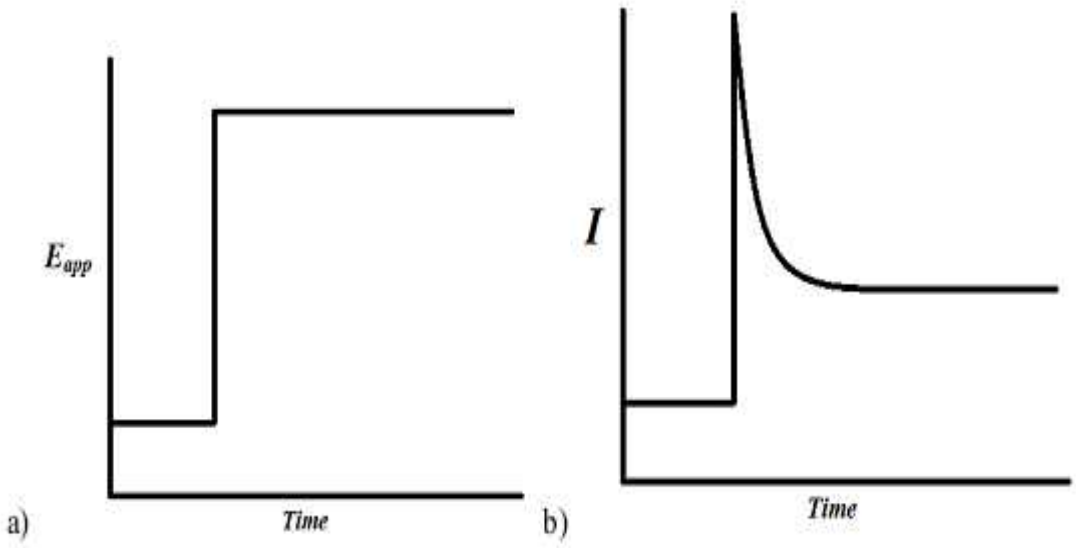

Fig1.10: a) excitation waveform b) current response output generated from the excitation waveform.

1.5 Sensor characterization

1.5.1 Scanning electron microscopy (SEM)

The scanning electron microscope (SEM) is a powerful and frequently used instrument, in both academia and industry, to study, for example, surface topography, composition, crystallography and properties on a local scale. The spatial resolution is better than that of the optical microscope although not quite as good as for the transmission electron microscope (TEM). The SEM has an extremely large depth of focus and is therefore well suited for topographic imaging.

Besides surface topographic studies the SEM can also be used for determining thechemical composition of a material, its fluorescent properties, the formation of magnetic domains and so on.

The specimen is bombarded by a convergent electron beam, which is scanned across thesurface. This electron beam generates a number of different types of signals, which areemitted from the area of the specimen where the electron beam is impinging (Fig. 1.11).

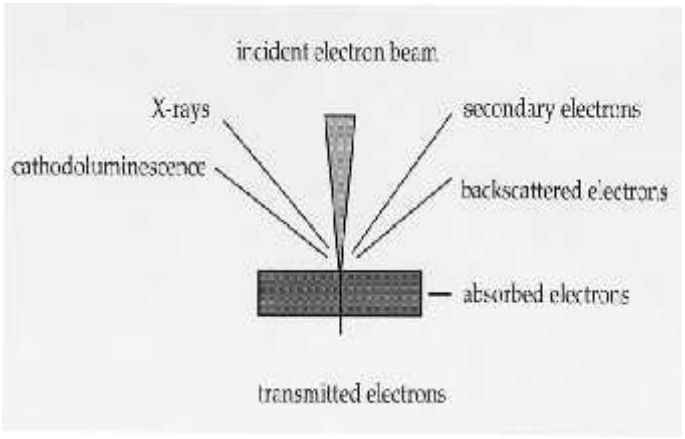

Fig 1.11: Example of some of the different types of signals produced when high-energy electron impinges on a material.

The induced signals are detected and the intensity of one of the signals (at a time) isamplified and used to as the intensity of a pixel on the image on the computer screen.The electron beam then moves to next position on the sample and the detected intensitygives the intensity in the second pixel and so on.

The working principle of the SEM is shown in Figure 1.12. For improved signal-to-noise ratio in the image, one can use a slower scan speed. This means that the electron beam stays a longer time at one position on the sample surface before moving to the next. This gives a higher detected signal and increased signal-to-noise ratio [73].

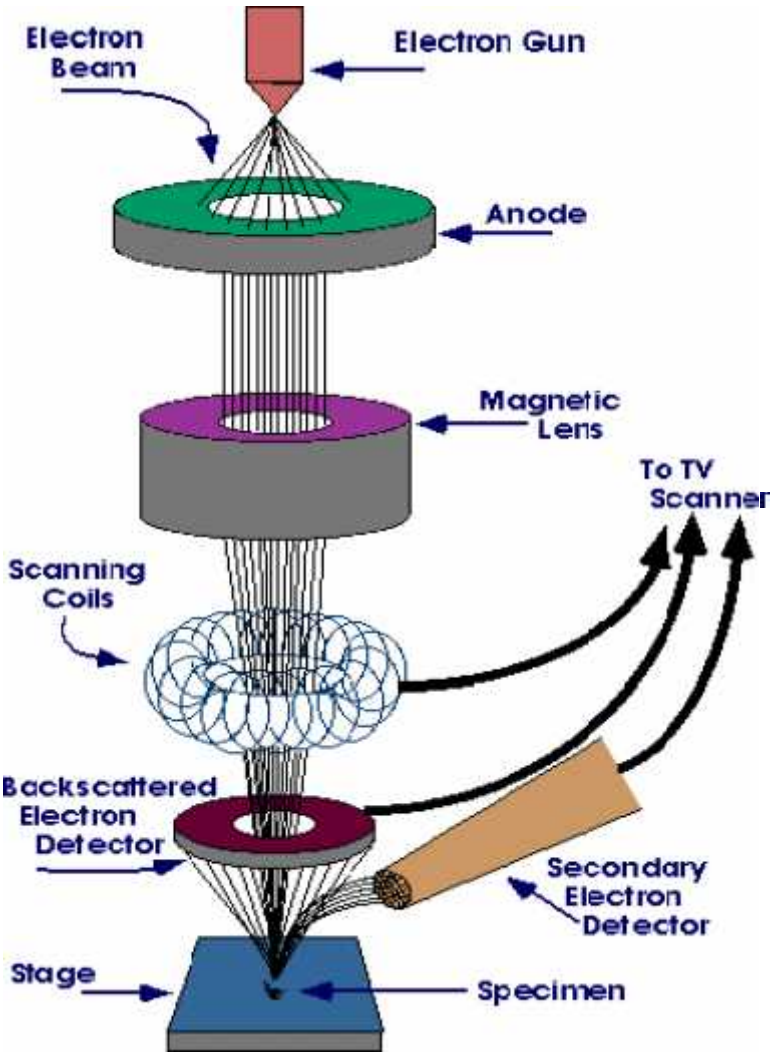

Fig. 1.12: Schematic diagram of a SEM.

1.5.2 X-ray diffraction (XRD)

X-ray diffraction (XRD) relies on the dual wave/particle nature of X-rays to obtain information about the structure of crystalline materials. A primary use of the technique is the identification and characterization of compounds based on their diffraction pattern. The dominant effect that occurs when an incident beam of monochromatic X-rays interacts

with a target material is scattering of those X-rays from atoms within the target material. In materials with regular structure (i.e. crystalline), the scattered X-rays undergo constructive and destructive interference. This is the process of diffraction. The diffraction of X-rays by crystals is described by Bragg's Law, n(lambda) = 2d sin(theta). The directions of possible diffractions depend on the size and shape of the unit cell of the material. The intensities of the diffracted waves depend on the kind and arrangement of atoms in the crystal structure. However, most materials are not single crystals, but are composed of many tiny crystallites in all possible orientations called a polycrystalline aggregate or powder. When a powder with randomly oriented crystallites is placed in an X-ray beam, the beam will see all possible interatomic planes. If the experimental angle is systematically changed, all possible diffraction peaks from the powder will be detected.

The parafocusing (or Bragg-Brentano) diffractometer is the most common geometry for diffraction instruments.This geometry offers the advantages of high resolution and high beam intensity analysis at the cost of very precise alignment requirements and carefully prepared samples. Additionally, this geometry requires that the source-to-sample distance be constant and equal to the sample-to-detector distance. Alignment errors often lead to difficulties in phase identification and improper quantification. A mis-positioned sample can lead to unacceptable specimen displacement errors. Sample flatness, roughness, and positioning constraints preclude in-line sample measurement. Additionally, traditional XRD systems are often based on bulky equipment with high power requirements as well as employing high powered X-ray sources to increase X-ray flux on the sample, therefore increasing the detected diffraction signals from the sample. These sources also have large excitation areas, which are often disadvantageous for the diffraction analysis of small samples or small sample features.

Chapter I serves as an introduction to both the physiological significance of glutamate and the fundamental principles underpinning the electrochemical techniques used throughout this thesis. In the next chapter we will discuss about literature review about glutamate sensors.

1.6 Objectives of the present work

The objectives of this research are to develop a glutamate sensor and also to study the sensitivity, selectivity, stability of this sensor using various electrochemical techniques.

The specific aims are:

i) To synthesize nickel oxide nanocrystal by sol-gel method.

ii) To synthesize nickel oxide hollow spheres (NiO-HSs) by hydrothermal method.

iii) To modified glassy carbon electrode with nickel oxide nanoparticle.

iv) To characterize the sensor using electrochemical methods, X-ray diffraction and Scanning Electron Microscope.

v) To test and validate the modified sensor for the glutamate detection.

CHAPTER II

Literature review

2.1 Introduction

Sensors and sensor arrays for the detection of chemical and biological substances have attracted much attention in recent years. The ultimate goal is to fabricate sensors that can determine the presence of a wide range of substances at relevant concentration levels with sufficient selectivity and sensitivity. Such research would ultimately produce technology that could be applicable in many segments including food processing, environment alremediation, agriculture, medical diagnostics and defense. The main requirements besides selectivity and sensitivity are fast response, low fabrication costs, robustness and portability. Hence intensive research activities around the world are focused on developing new sensing materials and technologies. With the development of nanotechnology, there is a growing demand for advanced electronics based on functional nanomaterials. Important characteristics and the quality parameters of nanosensors can be improved over the case of classically modeled sensors merely reduced in size.

Over the last decade significant progress has been made in the development of immobilized electrochemical sensors for monitoring glutamate. This review discusses evolution of glutamate sensor from first generation toward third generation based on micro and nanostructured sensor platforms for the industrial and clinical applications.

2.2 Advancement from first to third generation glutamate sensors

First generation enzyme-based electrochemical sensors were developed during the 1960s and early 1970s [74-76]. Detection is based on one-step redox reaction catalyzed by a specific oxidase, for example glucose oxidase or glutamate oxidase, where after the O_2 consumed or H_2O_2 produced during this oxidation is detected directly by the electrodes.

First generation glutamate sensors are relatively simple instruments (Figure 2.1). They consist of an electrode covered by a protection layer and an enzyme layer. Normally the electrode is a platinum cylinder or disk. In the Gerhardt group screen printed platinum recording site (15 x 333 µm, S_2 type) based on ceramic substrate [77, 78] was used as microelectrode. Carbon fiber is also often used as electrode material for first generation sensors. The surface of the electrode material is covered by protection and enzyme layers. The protection layer eliminates non-specific signals by preventing interference compounds to reach the bare electrode.

Different research groups use different orders of protection and enzyme layers: some research groups apply the protection layer under the enzyme layer, while other groups coat the protection layer on the outside of the enzyme layer. There are quite a few studies about the selection of the material for this protection layer, which will be later discussed in detail. The enzyme layer is normally composed of glutamate oxidase, a cross linker and a protein stabilizer.

First generation sensors mostly use glutaraldehyde as the cross linker and bovine serum albumin as the enzyme stabilizer. The amount of the most important composite of the sensors, glutamate oxidase, is quite high, ranging from 100 to 200 U/mL. In our laboratory, we find that 200 U/mL of glutamate oxidase produces the most stable sensors. The enzyme layer may also be applied in a number ways, such as manual coating, drop coating, dip coating and spray coating. Manual coating with microdrops (~ 1 µL) of enzyme mixture is predominantly used. After coating, a very thin yellow transparent layer of enzyme can be seen under a microscope.

On first generation sensors, glutamate is oxidized with glutamate oxidase and produces α-ketoglutarate and H_2O_2. At high potential, for example +700 mV for platinum, the electrode gains electrons from H_2O_2 and finally converts H_2O_2 into O_2. In a few cases, consumed O_2 is detected by its reduction on the electrode at very low potential, for example –650 mV [79].

Second generation sensors were developed in the 80s' and 90s' [80, 81] and possess a more complicated structure. A two-step redox reaction is involved in this type of sensors.

As with first generation sensors, a certain biological substance is first oxidized by O_2 on the surface of the sensors, and H_2O_2 is produced. The H_2O_2 is further reduced by a redox mediator. In this step, a second redox enzyme is required, normally peroxidase. Therefore in second generation sensors reduction/oxidation of the redox mediator is used to detect the analyte of interest. In general, these redox reactions are performed at a lower potential, which result in sensors with less sensitivity for interfering compounds.

Second generation glutamate sensors are composed of an electrode, an enzyme layer and an outside protection layer. Carbon fiber electrode (CFE), platinum and screen printed graphite-silver electrodes are often used in these sensors [82, 83, 84].

The composition of the enzyme layer of the second generation sensors is more complicated, compared with that of the first generation ones since it is composed of glutamate oxidase (or glutamate dehydrogenase + NADH + NADH redox mediator), peroxidase, a cross linker, a redox mediator and sometimes ascorbic acid oxidase to prevent ascorbic acid (AA) interference. The redox mediator has to Sensors met certain criteria. Ideally, it should show reversible heterogeneous kinetics: have stable oxidized and reduced forms, should react rapidly with the second redox enzyme peroxidase, the potential applied for the regeneration of the oxidized mediator should below and pH independent, the reduced form should not react with O_2 [85] and it should be tightly anchored into the architecture of the biosensor. Soluble low-molecular weight metal complexes are mainly used for this purpose. The material of second generation electrodes also has to match with the redox mediator electrochemical property for optimizing electron transfer. For example, our cyclic voltammetric studies suggested that the CFE responds better to the oxidation-reduction of osmium complex used as the redox mediator than the platinum wire electrode. Therefore, attentions should be paid on the selection of materials with respect to their interactions and the efficiency of redox reactions in order to obtain better response. Since a large amount of redox mediator is involved in this enzyme layer, and it contains more composites, the thickness of the enzyme layer of second generation sensors is slightly larger than that of first generation sensors. The second generation sensors developed in our lab have an enzyme layer of about 5 µm thick.

A protection layer coats the outside of the sensors. It not only prevents non-specific electrochemical interferences reacting with redox mediators and electrodes, but also decreases biofouling of sensors. Biofouling, defined as unspecific attachment of biological material to electrode surfaces upon their exposure to brain tissue, can influence the performance of sensors, including decreasing sensitivity and increasing interference response.

In order to reduce the detection potential, second generation sensors work with a more complicated and longer reaction chain. Different redox mediators, such as Prussian Blue [84] and osmium polymer complex [86], lead to different subtypes of second generation sensors that have different electron transfer mechanisms. Here we use a hydrogel sensor previously developed by Kulagina et al. [87] as an example. These sensors consist of a CFE that is coated with a redox-hydrogel. The CFE has a diameter of 10 µm and a length of 300-400 µm. The hydrogel enzyme layer contains five components: glutamate oxidase; ascorbic acid oxidase; horseradish peroxidase, the second redox enzyme; osmium redox polymer (POs-EA), which is the redox mediator, it is composed of a poly(vinylpyridine) backbone complexed with osmium (bipyridine) chloride groups and partially quarternized with ethylamine groups; and poly(ethylene glycol) diglycidylether (PEDGE) as the cross linker, that covalently cross-links the enzymes with POs-EA at their amino groups via a ring-opening reaction. Finally, on the outside of the hydrogel layer a thin Nafion protection layer is applied to prevent biofouling. On these hydrogel-based second generation of sensors, the glutamate is firstly converted into α-ketoglutarate under glutamate oxidase catalysis and $H_2O_2$is produced in this step; then the H_2O_2 is further reduced by Os^{2+} into H_2O under catalysis of horseradish peroxidase, the Os^{2+} is oxidized into Os^{3+}on the CFE surface at –100 mV, the CFE losses electrons and the Os^{3+}gains these electrons to convert back into Os^{2+}. This way the osmium is recycled and acts as an electron transfer mediator.

$$\text{I. Glutamate} + O_2 \xrightarrow[\text{Horseradish peroxidase}]{\text{Glutamate oxidase}} \alpha\text{-ketoglutarate} + H_2O_2$$

$$\text{II. } 2Os^{2+} + 2H^{+} + H_2O_2 \longrightarrow 2Os^{3+} + H_2O$$

$$\text{III. } 2Os^{3+} + 2e^{-} \longrightarrow 2Os^{2+}$$

Third generation glutamate sensors were developed by jamal et. al. [88] based on the first generation principle, which has been found to be much superior compare to the sensor developed by [89] which was based on second generation principle. A complex entrapment method which consisted of drop-coating a 10µL mixture of GluOx (25U in 205µL), 2mg of BSA, 20µL of glutaraldehyde (2.5% w/v) and 10µL of Nafion (0.5%) onto a platinum nanoparticle modified gold nanowire array (PtNP-NAE) and allowing it to dry overnight under ambient conditions.

Recently [65] published an article for glutamate detection based on fabrication of nickel nanowire arrays and also modified a nickel nanowire array electrode with Pt and characterized their behavior for glutamate detection without using any enzyme. Pt particles were dispersed on Ni nanowires by a hydrothermal reduction method from a solution containing a platinum metal salt (5 mM $Na_2PtCl_6$6H2O) and a reducing agent (30 mM $NaBH_4$).

2.3 Oxygen dependency of the sensors

A glutamate biosensor [90] was successfully applied to the determination of MSG in soy sauce, tomato sauce, chicken Thai soup and chilli chicken. MSG levels compared very favourably with a spectrophotometric method (2 - 5% CoV based on n = 5). The biosensor was fabricated by mixing glutamate oxidase, BSA and glutaraldehyde, then spreading the mixture onto the surface of an O_2 permeable poly-carbonate membrane. The membrane was then attached to an oxygen probe using a push cap system and oxygen consumption was measured at an applied potential of -0.7 V; this is a considerably more negative operating potential compared to previously discussed biosensors.

In 2005 Colm P. McMahon et.al [91] was studied the oxygen dependence of the cylinder and disk biosensors over the same Glu concentration range 0-150 µM. GluOx-based first-generation biosensor in terms of an apparent Michaelis Menten constant for oxygen, $K_M(O_2)$ was used. The oxygen dependence was significantly greater for the cylinder-based electrode, $K_M(O_2)$ = 12 ± 1 µM compared with 3 ± 1 µM for PtD/GluOx/PPD-BSA.

Wiete H.Oldenzia et.al [92] the oxygen dependency of the glutamate microsensor was investigated for two conditions: the oxygen dependency in the presence of glutamate (and in the presence of both glutamate and AA. To investigate the oxygen consumption of Glu-ox, the glutamate microsensor was placed in a small-volume beaker (slowly stirred and controlled at 37°C) and a glutamate concentration of 10µM was administered. Next, the pO_2 levels were varied. It was shown that the glutamate signal was barely affected by the altered pO_2 levels and that the sensitivity for glutamate decreased 9% when the pO_2 levels were decreased from 21 to 2%. In a following step, 200 µM AA was administered (not indicated) prior to a second application of glutamate. Now, both oxygen-consuming enzymes were active. It was shown that the output of the microsensor was profoundly affected by the pO_2 levels, and changes of 60% were observed when oxygen levels were varied from 21% to respectively 2 and 100%.

The higher oxygen dependency in the presence of AA is explained by the fact that, beside both oxygen-consuming enzymes being active, the concentration of AA-ox within the hydrogel is much higher than Glu-ox. In addition, when the activity of AA-ox is limited by oxygen deprivation, less AA will be scavenged, and in turn, a larger suppression of the glutamate signal occurs due to interference by AA in the redox cascade. It is concluded that pO_2 levels that are normally present in the brain limit the sensitivity of the microsensor only to a small extent. Therefore, it is unlikely that physiological fluctuations of pO_2 (2-7%) will influence the response of the microsensor.

2.4 The extracellular concentration of glutamate

The various studies using glutamate sensors have produced different values of basal extracellular glutamate concentrations. A device for the measurement of glutamate in brain extracellular fluid utilising a relatively simple fabrication procedure has been reported [93]. The procedure involved dipping a 60-µm radius Teflon coated platinum wire into a buffered solution containing glutamate oxidase and o-phenylenediamine (PPD), followed by a solution containing phosphatidylethanolamine (PEA) and bovine serum albumin (BSA). The glutamate oxidase was entrapped by the electro- polymerization of PPD on the surface of the electrode. The PPD and PEA was used to block out interferences.

The basal levels of glutamate detected by the sensors produced by Oldenziel et al. varied between 18.2 ± 9.3 µM and 23.6 ± 5.3 µM in striatum. This result is accordance with the observation by Kulagina et al.: 29 ± 9.0 µM in striatum. Lower levels were reported by Rahman et al. [94] 2.0 ± 0.5 µM in rat striatum. The basal values reported by the Gerhardt group displayed a large variation: 2-40 µM. This is partly explained by different anesthesia depth during measurement: the deeper the level of anesthesia, the lower the current output of the sensors [92]. In general micro dialysis studies have reported somewhat lower basal values (1-5 µM). Note that in all the experiments with the second generation glutamate sensors, post *in vivo* calibration was taken to correct the biofouling effect on sensors: their sensitivity decreased considerably. While for the first generation sensors from Pinnacle Technology and the Gerhardt group, pre-*in vivo* calibration was used to calculate the glutamate concentrations. Therefore, the glutamate basal levels observed in these first generation sensors could have been underestimated.

Mikhail B.Bogdanov [95] examined effects of high doses of monosodium glutamate (MSG) on extracellular glutamate levels in rat striata. Using *in vivo* microdialysis. Parenteral doses (0.5. 1.0and 2.0. but not 0.25. g/kg, i.p) caused dose and time-dependent increases, peaking after 40 min (at 174 ± 47%. 485 ± 99% and 1021 ± 301%of basal levels. respectively). In contrast. Dietary MSG (I.49 ± 0.10g/kg/h) was ineffective.

Kulagina et al. also suggested that the small size of the hydrogel based glutamate sensors causes less damage to the adjacent tissue, implicating that the implantation had less influence on neuronal activity; therefore the higher levels of glutamate might be explained by a more pronounced neuronal activity in the vicinity of the microsensors. In this regard it is of interest to compare the damage caused by the different sensors or microdialysis probes. Borland et al. [96] provided evidence that dopamine release was disrupted within 220 µm from microdialysis probes in tissue, whereas the damage caused by the hydrogel-based carbon fiber sensors was only seen within an area of 3 µm in diameter around the fibers. The damage caused by the Gerhardt sensors was substantial and seen at distances of 50 -100 µm around the sensors [77]. Therefore the significance and origin of basal glutamate levels detected by the currently available glutamate sensors need further investigation.

2.5 Sensitivity of the sensors

The sensitivity of glutamate sensors of various studies produced different result followed by different process. The sensors designed by Kulagina et al. [87] were applied in brains of anesthetized rats. In this work, high basal levels of glutamate were reported: 29 ± 9.0 µM in striatum. The synaptic origin of the recorded glutamate was demonstrated by local infusion of 200 nL of sodium-channel blocker tetrodotoxi (TTX) 100 µM, which induced a 25-85 % decrease in glutamate when compared with basal levels. A fouling effect was reported after *in vivo* experiments: the sensitivity of the sensors decreased by 50-65 %.

A selective biosensor for the determination of glutamate in food seasoning was developed by incorporating glutamate oxidase into a poly (carbamoyl) sulfonate (PCS) hydrogel [29]. The GluOx-PCS mixture was drop-coated onto the surface of a thick-film platinum electrode. Liquid samples (1, 10 and 100 µL) were diluted to 10 mL with phosphate buffer. The biosensor was then applied to determine the glutamate recovery from different concentrations of the sample. The results generated correlated favorably with an L-glutamate colorimetric test kit.

An interesting entrapment approach employing polymers to encapsulate GluOx onto a gold electrode has been reported [97]. The first step involved the immersion of a gold disc electrode in 3-mercaptopropionic acid (MPA) solution, followed by drop-coating layers of poly-L-lysine and poly (4-styrenesulfonate). Once dry, a mixture of GluOx and glutaraldehyde was drop-coated on to the surface to form a bilayer. The authors suggested that MPA increases the adhesion of the polyion complex to the gold surface by the electrostatic interaction between the carboxyl groups present on the MPA and the amino groups present on the poly-L-lysine. A response time of only 3 seconds was achieved after an addition of 20 nM glutamic acid, which gave a current of 0.037 nA (1.85 nA/µM). A linear response was observed between 20 and 200 µM.

Recently, Gholizadeh et al. [98] fabricated vertically aligned carbon nanotube nanoelectrode array (VACNT-NEA) by photolithography method. Glutamate dehydrogenase is covalently attached to the tip of CNTs. The voltammetric biosensor, based on high density VACNTs, exhibits a sensitivity of 0.976 mA $mM^{-1}cm^{-2}$ in the range

of 0.1−20 µM and 0.182 mA.mM^{-1}cm^{-2} in the range of 20−300 µM glutamate with a low detection limit of 57 nM. Using the fabricated VACNT-NEA, the sensitivity increases approximately to a value of 2.2 AmM^{-1}cm^{-2} in the range of 0.01 to 20 µM and to 0.1 A mM^{-1}cm^{-2} in the range of 20−300 µM glutamate. Using this electrode, a record low detection limit of 10 nM was achieved for glutamate.

Rahman et al. [94] have developed Pt needle-type (25 µm in diameter and ~ 300 µm long) glutamate sensors. The design is based on the covalent immobilization of glutamate oxidase onto a conducting polymer (CP) of 5, 2':5',2"-terthiophene-3'-carboxylic acid on the electrodes. Co-immobilizing ascorbate oxidase and coating the sensor surface with a cationic polymer, polyethyleneimine minimized the endogenous reducing agent interference. These biosensors efficiently detected glutamate through the oxidation of enzymatically generated H_2O_2 at +0.45 V vs. Ag/AgCl. The basal extracellular glutamate concentration in anesthetized animals was determined to be about 2.0 ± 0.5 µM in rat striatum based on the post *in vivo* calibration. The biofouling was about 29%. These sensors detected an increase of extracellular glutamate after repeated injections of cocaine. Unfortunately, to date there have been no further *in vivo* pharmacological evaluations (such as TTX-dependency) reported for these sensors. The study on which the Pinnacle sensors are based [99] reported a pronounced biofouling effect: the sensitivity to glutamate decreased by an average of 51.3 ± 4.7% after exposure to brain tissue, which is due to the absorption of endogenous species on the sensor surface.

Kate M. Wassum et al. [100] have developed silicon wafer-based platinum microelectrode arrays (MEAs) modified with glutamate oxidase (GluOx) for electro enzymatic detection of glutamate *in vivo*. The fabrication method is a complex, multi-step process whereby The MEA biosensors coated with PPy/Nafion/GluOx were sensitive to and selective for glutamate additions of increasing concentrations of glutamate produced corresponding and linear increases in current such that the sensitivity to glutamate was 2.46 +/- 0.48 pA/µM, and the limit of glutamate detection was 0.79 +/- 0.16 µM (11 electrodes on 5 probes) at twice the level of the noise.

A recent application of a micro glutamate biosensor for investigating artificial cerebrospinal Fluid (CSF) under hypoxic conditions was described [101]. The fabrication

method is a complex, multi-step process whereby glutamate oxidase is incorporated with chitosan and Ceria-titania nanoparticles.

The nanoparticles are able to store and release oxygen in its crystalline structure; it can supply O_2 to GluOx to generate H_2O_2 in the absence of environmental oxygen. Whilst the fabrication procedure is complex, the biosensor possesses superior sensitivity to previously discussed biosensors.

Jonathan C. Claussen, et al. [102] described two hybrid nanomaterial biosensor platforms, based on networks of single-walled carbon nanotubes (SWCNTs) enhanced with Pd nanocubes and Pt nanospheres and grown in situ from a porous anodic alumina (PAA) template (Fig. 2.8). These nanocube and nanosphere SWCNT networks are converted into glutamate biosensors by immobilizing the enzyme glutamate oxidase onto the electrode surface. The Pt nanosphere /SWCNT biosensor outperformed the Pd nanocube/SWCNT biosensor and previously reported similar nanomaterial-based biosensors by amperometrically monitoring glutamate concentrations with a wide linear sensing range (50 nM to1.6 mM) and a small detection limit (4.6nM,3σ). Furthermore the GluOx/Pt-SWCNT/PAA biosensor demonstrates a glutamate sensitivity (27.4 $mAmM^{-1}cm^{-2}$) that is nearly five times the sensitivity of the GluOx /Pd-SWCNT/PAA biosensor (5.5 $mA.mM^{-1}$ cm^{-2}).

The increased interest in glutamate measurement has led to the commercial development of an *in vivo* glutamate biosensor by Pinnacle Technology Inc. [99]; this has been successfully used for monitoring of real-time changes of glutamate concentrations in rodent brain. The biosensor employs an enzyme layer composed of GluOx and an "inner-selective" membrane, composed of an undisclosed material that eliminates interferences. The enzymatically generated hydrogen peroxide is monitored using platinum -iridium electrode. The biosensor possesses a linear range up to 50µM. The manufacturers indicate that the miniaturised biosensor requires calibration upon completion of an experiment in order to ensure the selectivity and integrity of the sensors.

A group at University of California, [103] recently reported their work on platinization of L-glutamate microbiosensors. Platinum-black was deposited on a Pt wire electrode (~

0.00122 cm^2) by cycling potential between -1.4 V and -2.0 V (vs. Ag/AgCl) at 500 mVs^{-1} in a plating solution of 1% chloroplatanic acid, 0.0025%HCl, 0.01%lead acetate in water. The solution was vigorously stirred during the deposition process. Pt-black modified microelectrodes were dip-coated with L-Glutamate oxidase (L-GluOx). A 80 ±10 $\mu AmM^{-1}cm^{-2}$ glutamate sensitivity was reported.

A novel biosensor fabrication technique was developed [104] which consisted of entrapping GLDH between layers of alternating poly (amidoamine) dendrimer encapsulated platinum nanoparticles (Pt-PAMAM) with multi-walled carbon nanotubes. PAMAM's were used to modify the surface of the glassy carbon electrode due to their excellent biocompatibility and chemical fixation properties. The procedure was repeated using positively charged Pt-PAMAM and negatively charged GLDH which were alternatively adsorbed onto the CNTs in a layer-by-layer process. The assembly process and enzyme immobilisation process is illustrated in.

In contrast to the above, a simpler and less time consuming method of fabricating a glutamate biosensor has been described [105] which involved incorporating GLDH and NAD^+ into carbon paste. The mixture was inserted in a holder, placed in to a solution containing O-phenylenediamine and subsequently electro polymerized. The o-phenylene di amine film is simultaneously able to prevent interferences and facilitate the amperometric detection of NADH at low applied potentials by acting as an electron mediator. The biosensor was used to determine glutamate in chicken bouillon cubes; the results compared favourably to those obtained using a spectrophotometric method (12.6 ± 0.3% (n = 5) and 12.3% respectively).

It appeared that the average sensitivity of the first generation sensors is about five times higher than that of the second generation sensors. One of the major disadvantages of these second generation sensors was their sensitivity to the interference by AA.

2.6 Selectivity of the sensors

The initial objective of glutamate sensor design to detect rapid changes in synaptic glutamate concentrations in the brain of freely moving animals – has not yet been fully

accomplished with the existing sensors. Comparing these two types of sensors, the first generation sensors possess a simpler structure than the second generation sensors and therefore they respond faster. One of the examples is the commercially available sensors developed by the Gerhardt group, which detect extracellular glutamate levels in the brain of freely moving animals in sub-second scale.

For studies into the real-time regulation of glutamate in the brain two key challenges remain: improving response time and addressing interference. Since glutamate transport cycle by glial cells is less than 100 ms, more accurate detection is highly desirable. The response time of the sensors depends mostly on the kinetics of the enzymes and diffusion speed of H_2O_2 to the electrode. Moreover, biofouling can induce an increase in response time and interference during long term implantation of sensors *in vivo*. Hence there is ongoing need to optimize the construction of glutamate amperometric sensors, with a particular focus on the construction of the enzyme application matrix and protection layer.
The selectivity of a GlOx/nano-CP/Pt micro biosensor for glutamate [74] was evaluated amperometrically in the presence of other biological compounds, such as ascorbate, dopamine, uric acid, acetaminophen, L-cysteine, and others amino acids. As described in the previous section, the nano-CP layers on a Pt microelectrode lowered the oxidation potential of H_2O_2. Even, at this low oxidation potential, the oxidation of biological compounds such as ascorbate and dopamine did not significantly occur.

Improving the enzyme efficiency may also help to increase the response speed of sensors. Protection membrane that is highly selective for glutamate or H_2O_2 (depending on protection layer out- or inside the enzyme layer) and that prevents interfering substances to reach the bare electrode is a critical requirement for the sensors. At the same time, the protection and enzyme layers should allow a fast diffusion of glutamate and H_2O_2 molecules. During long term implantation, the protective effect of the protection layer is even more important since biofouling needs to be prevented. An alternative could be using sensors with a guide system, as in the microdialysis technique, to overcome biofouling. In addition, ongoing development of more precise (for example, smaller time scaled) recording equipment might be helpful to detect glutamate levels with higher temporal resolution. Other improvements might also be considered. A smoother electrode surface

may cause less damage to brain tissue and decrease the interaction between electrode surfaces.

2.7 Interference and solutions

The interference from different electrochemically active substances in the brain may lead to a decrease in the sensitivity and specificity of glutamate sensors. Most of the interference is from strong reducing agents, such as AA, UA, DA and cysteine. These compounds can be easily oxidized on the surface of the electrodes, especially in the first generation sensors, because a high potential is applied; or they could react directly with the redox enzyme (HRPox), the mediator (Os^{3+}) on the second generation hydrogel sensors [92] and the metabolite (H_2O_2) on both generations of sensors, resulting in reducing the intermediate steps in the redox reaction(s) and interfering the amperometric detection.

Glutamate oxidase is a very selective enzyme. Only one study suggested that it has a slight sensitivity for I-aspartate (0.6%) [106], therefore the interference from unwanted enzymatic reactions is not a main concern for glutamate sensors. There are several studies on preventing the non-specific interference. One of the methods predominately used with both types of sensors is the inclusion of background sensors. As the term implies, background sensors are prepared in the same way as glutamate sensors but without applying glutamate oxidase. During the calibration and *in vivo* experiment, the background and glutamate sensors are placed in a proximate distance (100 to 200 µm) to insure the equality of detection environments; hereby the non-specific signal recorded through the background sensors can be subtracted from the signal of glutamate sensors. In this way, most of the interference is filtered out. However, the background and glutamate sensors do not react always exactly the same. Strong effects from interference increase the probability that background and glutamate sensors perform differently. Therefore attention should still be paid to prevent direct reaction of interfering compounds with sensors.

Weite H. Oldenziel et al. [82] described that increasing the redox polymer (POs-EA) concentration improved the glutamate detection properties. A concentration of 5 mg/mL is optimal, showing highest sensitivity with optimal response characteristics. A further increase of the POs-EA concentration tended to decline the sensitivity again, which may

be explained by dilution of the enzyme content due to excess POs-EA. Unfortunately, the interference by AA also increased dramatically with increasing POs-EA concentration.

Poly(ethylene-glycol) diglycidyl ether PEDGE is a commercially available diepoxide cross-linker that wires enzymes to the pendant amine groups of the POs-EA, forming the hydrogel network. The influence of different amounts of PEDGE on the sensitivity and interference of the microsensor was investigated. The amount of PEDGE was varied between 6.3 and 26.1 wt % of the coating solution. No changes in microsensor performance were observed (results not shown). Likely, due to its chain length (about 48Å), PEDGE does not restrict the short-range polymer segmental motion, and as a result, the electron-transfer process within the hydrogel is not affected. [107, 108] The PEDGE quantity described in the reference method was maintained in the next experiments.

Nafion is one of the first polymers applied to electrochemical biosensors [109, 110] and has been reported to have an excellent barrier effect for interferences such as ascorbate. It is a sulfonated tetrafuorethylene copolymer. Because of its tetrafuorethylene (Teflon) backbone, Nafion possesses excellent thermal and mechanical stability. The combination with sulfonic acid group results in its highly cation conductive property. Nafion membrane coated on the electrodes can prevent interference mainly via two mechanisms: firstly its complex polymer structure (with small pores) only allows small molecules to pass through; and secondly its positive charge limits the diffusion of anionic components such as AA across the membrane. To obtain a Nafion coated surface, the electrodes are dipped in Nafion polymer solution and then dried. Previous studies have shown that different dipping times, concentration of Nafion and annealing with high temperature can influence the structure of Nafion and therefore affect the permeability and stability. Annealing Nafion provides a more crystal-like polymer structure which is less permeable [111-112]. When Nafion is applied to the first generation sensors, it is often annealed at high temperature.

Polypyrrole (PPy) is another polymer attracting considerable attention in the development of biosensors. It is a conducting polymer, therefore its electrical, electrochemical and catalytic properties can be easily controlled by the electrochemical oxidation process. Because of its polyacetylene like structure, oxidized PPy has a very high conductivity and

electrochemical redox activity even in pH-neutral solution. But over-oxidized PPy loses its electronic conductivity and becomes an ion-exchange membrane. On Pt electrodes pyrrole forms an ultra-thin film that is ion selective against anions, which means it only allows cations to pass through the film. Over-oxidized PPy coating can suppress effectively anionic AA but not cationic dopamine [113]. To obtain an over-oxidized PPy layer, relatively high electrode potentials applied to control anodic oxidation. Size-selective polymer behavior was also observed by Wang et al. [114]. During polymer electro-deposition, a specific enzyme can be coated on the electrode together with the polymer in a one-step loading procedure: the enzyme can be mixed within the monomer pyrrole solution and co-deposited onto the electrode within the electro polymerized PPy. In this way, the enzyme is tightly entrapped in the polymer structure and the amount of enzyme and thickness of the polymer film can be well controlled [115]. However, this one-step loading procedure requires high concentrations of monomer and enzyme; therefore it is not an economic method to immobilize expensive glutamate oxidase on the electrode.

The review has highlighted some novel approaches to the fabrication of electrochemical glutamate sensors. The performance characteristics of the glutamate sensors discussed are summarized within Table 2.1. Several methods for the detection and measurement of glutamate have been described and compared. These sensors are scientifically relevant because they can be used for monitoring brain activity levels and other activities. Some method enables multiple measurements and great sensitivity, but has very poor lateral and temporal resolution. Therefore the measurement itself generates it sown measure and, which is very unfavorable.

The use of enzymes is very popular, but it increases sensor costs. However, recent trends in micro technology may enable new advances in non-enzymatic glutamate sensing. Another disadvantage is that the absorption of oxygen may interfere with the measurements, because glutamate levels increase in ischemic patients. The last type of sensor that was discussed is the optical sensor. These sensors usually have a lower sensitivity than electrochemical sensors, and are more difficult to use in-vivo. In conclusion, the development of glutamate sensors is still essential for their use in neuroscience. In the next chapter we will be described the experimental section of this study.

Table 2.1: Characteristics of several electrochemical glutamate sensors.

Immobilization Method	Limit Of Detection	Optimal pH	Applied Voltage	Sensitivity	Linear Range	Respon-se time	Ref
Poly(carbamoylsulphonat) (PCS) hydrogel mixed with GluOx	1.01µM	6.86	+400 mV	1.94 nA/µM	100 - 5000µM	NS	[29]
Microelectrode array in Pt site	1.82 ±0.17 µM		+700 mV	0.016 ± 0.001(nA/µM)		~ 1s	[78]
CFE	1 ~ 3 µM	-	-100 mV	0.0034 ± 0.001(nA/µM)	-	20 ~ 40s	[87]
Pt nanoparticles modified Au nanowire arrayn electrode	14µM	7.4	+650 mV	194.6 µA $mM^{-1}cm$	200 - 800 µM	4.8s	[89]
CFE	5 µM		-150 mV	0.0055 ± 0.00007(nA/µM)		~ 8s	[92]
RU coated CFE	2.5 µM		+400 mv	0.029(nA/µM)		-	[94]
MEA biosensors coated with PPy/Nafion/GluOx	0.79 ± 0.16 µM	-	-	2.46 ± 0.48 pA/µM	-	-	[100]
Polyion complex-bilayer Membrane	0.2 nM	7.0	+800 mV	1.85 nA/µM	3 – 500 µM	NS	[97]
carbon nanotube nanoelectrode array (VACNT-NEA) by photolithography method	57nM	-	-	0.182 mA $mM^{-1}cm$	20 – 300 µM	-	[102]
Mixed ceria and titania nanoparticles for the detection of glutamate in hypoxic environments	0.594µM	7.4	+600 mV	0.7937 nA/µM	5 – 50µM	~ 5s	[101]
Alternatively assembling layers of glutamate dehydrogenase and Pt-PAMAM.	100 µM	7.4	+200 mV	433 µA/mM^1/cm2	0.2 - 250 µM	3s	[104]

CHAPTER III

Experimental

The electrochemical behavior of different nickel oxide nanoparticle modified glassy carbon electrode (NiO/GCE) has been observed using Cyclic Voltammetry (CV) at glassy carbon electrode. The sensitivity of electrode reactions has been improved by modifying the electrode with nickel oxide nanoparticle. Nickel oxide nanoparticle was prepared by two different processes. It has been characterized by XRD and Scanning Electron Microscope (SEM). Amperometry has been employed for the quantitative estimation. Details of the instrumentation are given in the following sections. The source of different chemicals, the instruments and brief description of the methods are given below.

3.1 Reagent and material

L-Glutamic Acid, Nickel Chloride, Nickel acetate and Ethanol were purchased from E. Merck Germany. Glycerine, Chitosan were obtained from Sigma-Aldrich. Ascorbic acid, uric acid were obtained from British Drug House (BDH), England. NaOH pellets, Chitosan were of analytical grade, purchased from Loba Chemie Pvt. Ltd., India.

3.2 Equipment

Voltammetric and amperometric measurements were performed with a potentiostat/ galvanostat (model: µStat 8400, Drop Sens, Spain). Three electrode cells has been used, where Nickel oxide modified glassy carbon electrode (NiO/GCE) electrodes were employed as a working electrode with Ag/AgCl and Pt wire as reference and counter electrodes, respectively. Morphology of the nanoparticle was examined using SEM (model: JEOL/EO, 2300 instrument operating at an acceleration voltage of 200 kV). The crystal structures of nanoparticle were characterized by XRD (Philips PW3710-MPD diffractometer with CuK_{α} raradiation, λ =1.54˚A**).** For the sysnthesis of crystal, steel autoclave has been used.

3.3 Preparation of NiO nanoparticle

Sol-gel process

In the sol-gel process [116], $NiCl_2.2H_2O$ (1.5g) was transferred into to a 250 mL round bottom flask and dissolved in 70 mL of absolute ethanol at room temperature, leading to a clear green colored solution. In another beaker, NaOH (0.5g, 0.0125 mol) was dissolved in 100 mL absolute ethanol and the NaOH solution was added to the nickel chloride solution drop wise. The mixture was stirred at room temperature for 2 h. during this time, the reaction mixture was found to form a light green colored gel. After 2h, the gel was filtered, washed thoroughly with distilled water and then finally with ethanol. The precipitate was air- dried, yielding a light green colored powder. The precursor powder was taken in a porcelain crucible and calcined for 30 min at 290 °C in a muffle furnace leading to a dark green color nanocrystal. The reactions involved in the preparation are shown below.

$$NiCl_2 + 2NaOH \longrightarrow Ni(OH)_2 + NaCl + 6H_2O$$

$$Ni(OH)_2 \longrightarrow NiO + H_2O$$

Hydrothermal method

Nickel oxide hollow sphere (NiO-HSs) were synthesized by a glycerin-assisted hydrothermal synthesis route [117]. 0.3 g of $NiCl_2.2H_2O$ /$Ni(CH_3COO)_2 \cdot 4H_2O$ was added into 25 mL of H_2O, followed by addition of 1.25 g of glycerin. After sonication for 30 min, the solution was transferred into a 40 mL Teflon-lined stainless steel autoclave and then it was heated at 200 ^{0}C for 2 h. The products was washed with water twice by centrifugation (model: EBA 21) at 6,000 rpm for 30 min, and dried at 60 ^{0}C over night. The NiO-HSs was obtained by calcination in air at 600 ^{0}C for 2 h. The resulting NiO-HSs were dispersed in water before characterization.

3.4 Modification of working electrode

Glassy carbon electrode is used in this study for electrode modification using NiO nanoparticle obtained using both sol-gel and hydrothermal methods. The modified electrode was prepared by a simple casting method (Fig. 3.1).

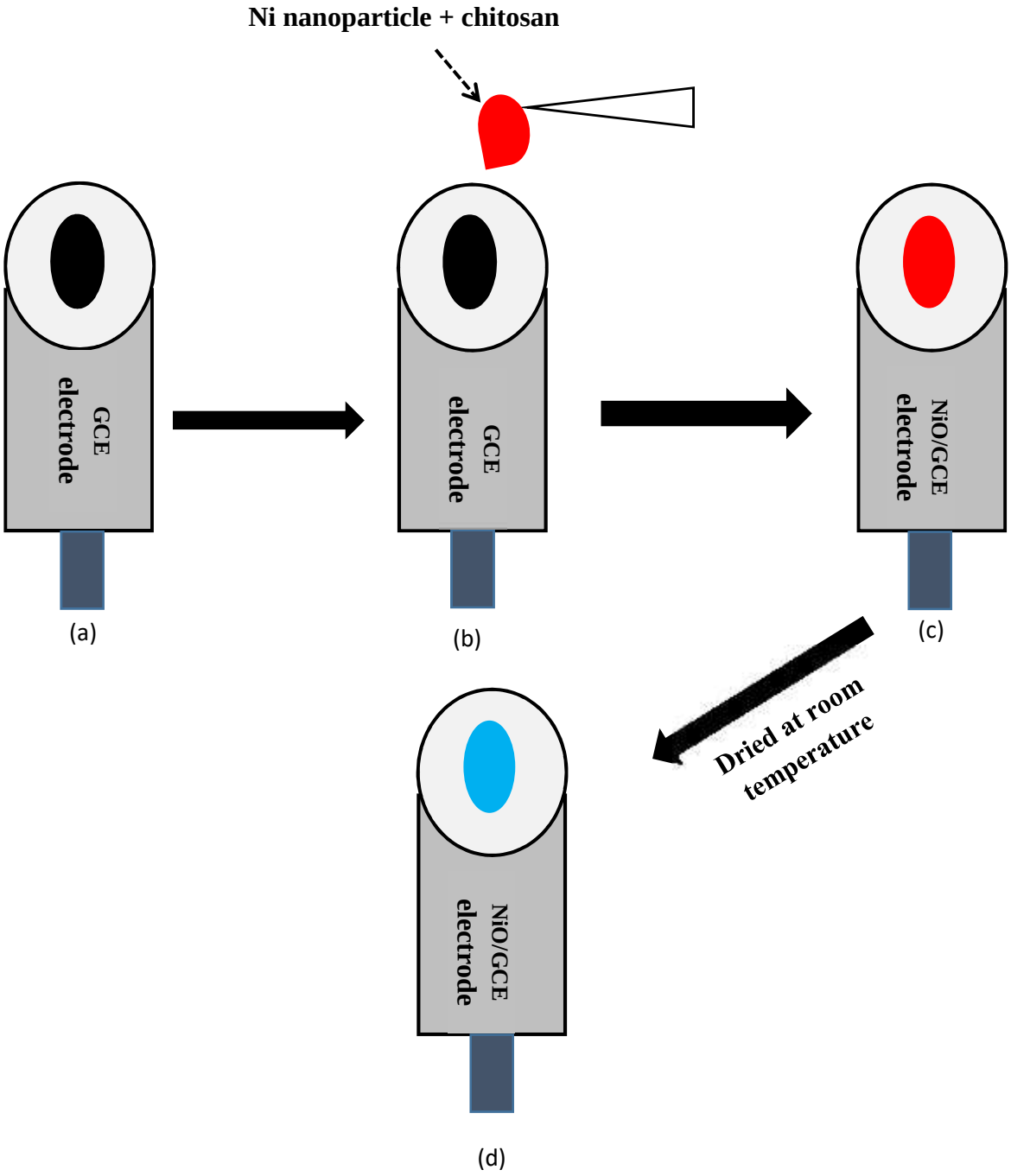

Fig. 3.1: A step-by-step diagram of modification of working electrode. a) bare GCE b) drop coating of Nickel nanoparticle + chitosan c) drying d) NiO/GCE.

Prior to the surface coating, the GCE was polished with 1.0 and 0.3 μm alumina powder, respectively, and it was rinsed with water, followed by sonication in ethanol solution and water successively. Then, the electrode allowed drying in a stream of nitrogen. After that, 10 μL of NiO nanoparticle and 5 μL of 1% chitosan was droped on the clean surface of GCE, and it was dried at room temperature for overnight.

3.5 Preparation of buffer solutions

Phosphate buffer solution was prepared by mixing a solution of 0.2 M NaOH with a solution of 0.2 M KH_2PO_4. The pH of the prepared solution was measured with Orion 2 Star pH meter. To prepare acetate buffer solution definite amount of sodium acetate was dissolved in 2N acetic acid in a volumetric flask and the pH was measured. The pH of the buffer solution was adjusted by further addition of acetic acid and/or sodium acetate.

3.6 Standardization of the electrochemical System

The whole electrochemical set-up was tested using a standard experiment. In the standard experiment we have studied the following redox couple at a glassy carbon (GC) electrode.

$$[Fe(III)(CN)_6]^{3-} + e^- \rightleftharpoons [Fe(II)(CN)_6]^{4-}$$

The reaction above was studied electrochemically by pumping electrons into the system from a GC electrode and by measuring the change in the flow of current during the reaction. This is done most conveniently by scanning the potential of the electrode at a constant rate.

In general, the peak current of diffusion controlled reversible or quasi-reversible electro - chemical reaction follows Randles–Sevcik equation;

$$Ip = 0.4463nF\sqrt{\frac{n}{R}}AC\sqrt{v}$$

where ip: the peak current, n: the number of electrons, F: Faraday constant, T: the temperature in Kelvin, R: the gas constant, A: the surface area of the working electrode,

D: the diffusion coefficient of the electroactive species, C: the bulk concentration of the electroactive species and *v*: the scan rate of voltammograms.

3.7 Electrochemical measurements

Cyclic voltammograms were performed over the definite potential range vs. Ag/AgCl in a cell containing 10.0 mL of 0.1 M NaOH solution. The surface of the electrodes is completely immersed. The cell is deaerated for 5 minutes with high purity nitrogen gas. The solution has been kept quite for 10 seconds. To determine the potential window, electrochemical scanning is carried out with the supporting electrolyte to obtain the background voltammogram.

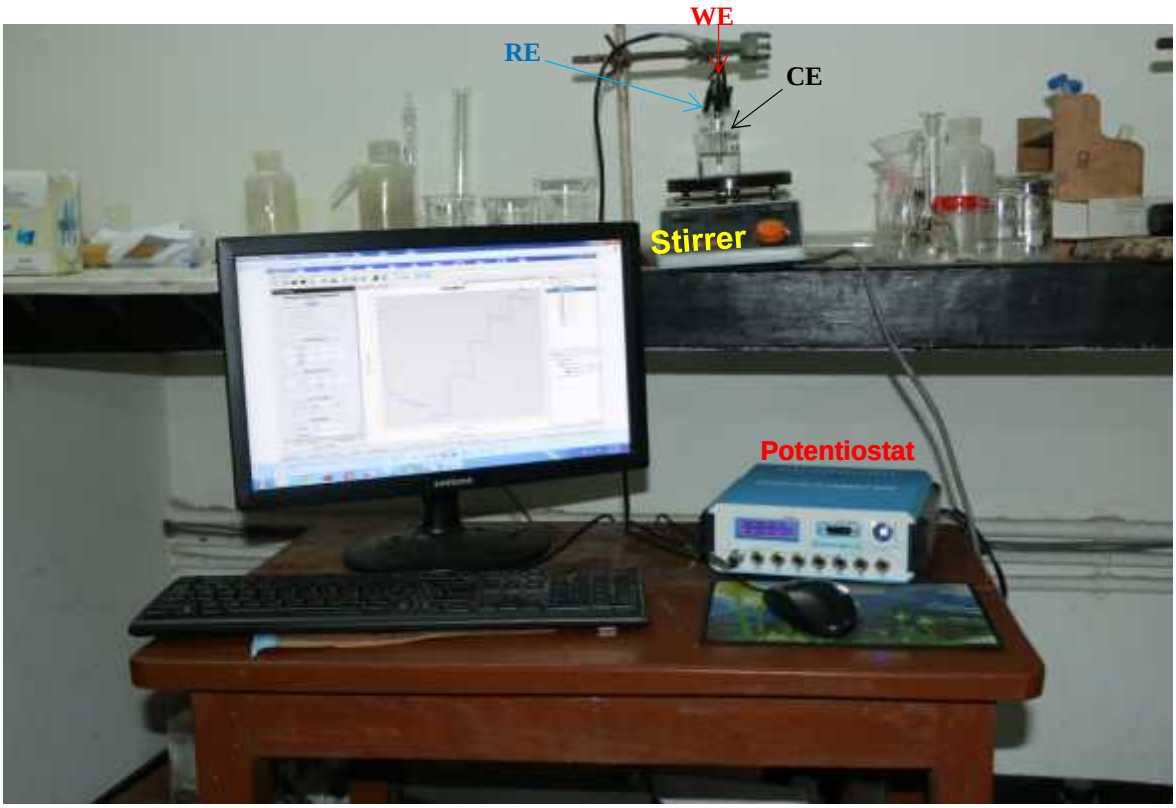

Fig 3.2: Electrochemical experimental setup.

For amperometric experiments, the voltage was switched directly from open circuit to the appropriate applied potential (vs. Ag/AgCl). The experimental setup is shown in fig (Fig. 3.2). Solutions were agitated with a stirrer at a fixed speed for both NaOH solution and cell media studies. This was in order to facilitate diffusion and improve the homogeneity of the solution. Initially, studies were carried out with the modified electrode in 0.1 M NaOH

solutions containing glutamate in order to determine whether the performance is suitable for the subsequent monitoring of the glutamate response. Amperometry was performed by applying a potential to the electrode immersed in a 10 ml of 0.1M NaOH stirred solution with the addition of definite amount of glutamate. The resulting real time current responses were recorded over a period of time.

3.8 Interference studies

A three electrode system was employed where NiO/GCE electrodes were employed as a working electrode with Ag/AgCl and Pt wire as reference and counter electrodes, respectively. L-glutamic acid, ascorbic acid and uric acid were added (over their physiological concentration range) and current response measured at room temperature, E_{app} = 0.55V vs. Ag/AgCl in the presence of 0.1M NaOH solution.

3.9 Stability studies

Electrode stability was evaluated using amperometry at potential 0.55 V vs. Ag/AgCl by addition of 2 mM L-glutamate at room temperature (298K). Testing was performed every day for a period of one week. In between measurements the electrode was stored at room temperature.

The next chapter we will describe more about result and discussion on the development of a non-enzymatic glutamate sensor.

CHAPTER IV

Results and Discussion

4.1 Electrochemical setup standardization

Cyclic voltammograms (CVs) of ferricyanide at glassy carbon electrode were performed at concentration of 2mM of ferricyanide in 0.1 M KNO_3 as supporting electrolyte, each solution was scanned at different scan rate equal to 20, 40, 60, 80, 100, 120, 140, 160 mV/s. The resultant CV curves and the electrochemical parameters are shown respectively in Figure 4.1 and Table 4.1.

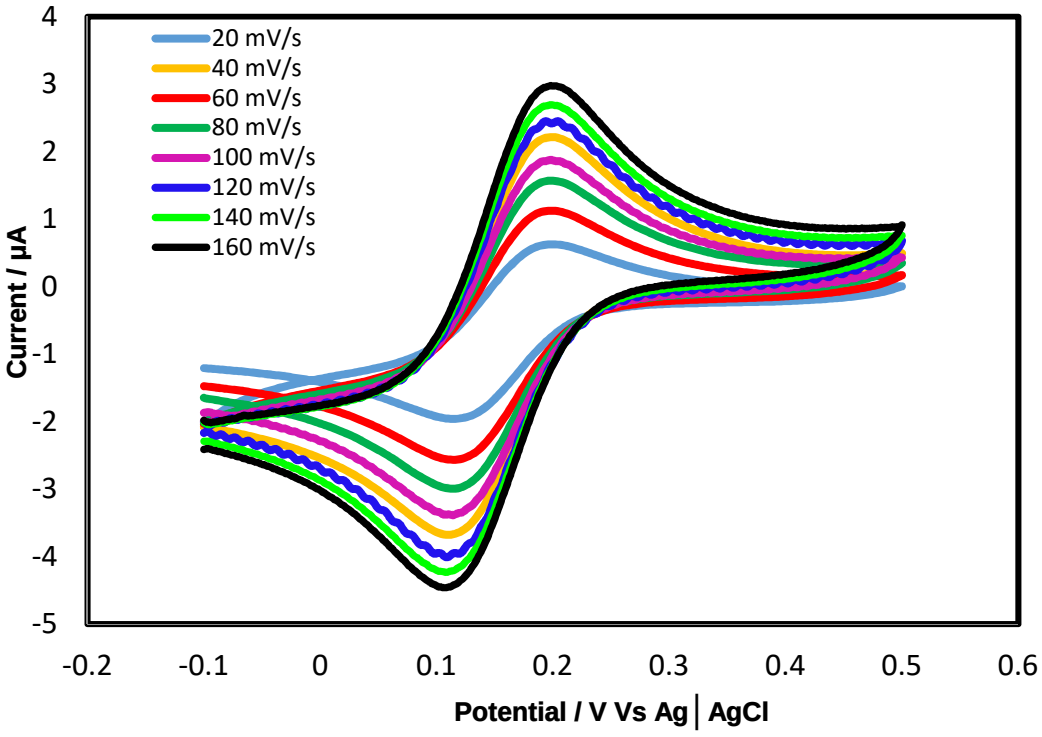

Fig. 4.1: Cyclic voltammograms (CVs) of 2mM ferricyanide on GCE at scan rate of 20, 40, 60, 80, 100, 120, 140, 160 mV/s, electrolyte: 0.1 M KNO_3.

Table 4.1: Electrochemical parameters obtained from CVs of ferricyanide on GCE.

ν Vs^{-1}	$\nu^{1/2}$	E_{pa} V (+)	E_{pc} V (+)	i_{pa} µA (+)	i_{pc} µA (-)	i_{pa}/i_{pc}
0.02	0.14	0.21	0.12	1.34	1.25	1.07
0.04	0.2	0.20	0.12	1.86	1.77	1.05
0.06	0.24	0.20	0.12	2.30	2.88	1.00
0.08	0.28	0.20	0.12	2.64	2.49	1.06
0.1	0.31	0.20	0.12	2.91	2.80	1.03
0.12	0.34	0.20	0.12	3.09	3.03	1.02
0.14	0.37	0.20	0.12	3.44	3.30	1.04
0.16	0.4	0.20	0.12	3.67	3.52	1.04

ν= scan rate; $\nu^{1/2}$= SQRT of scan rate; E_{pa}= anodic peak potential; E_{pc}= cathodic peak potential; i_{pa}= anodic peak current; i_{pc}= cathodic peak current.

In general, the peak current of diffusion controlled reversible or quasi-reversible electro - chemical reaction follows Randles–Sevcik equation [118]

$$I_p = 0.4463nF\sqrt{\frac{n}{R}}AC\sqrt{v} \qquad \text{----------} \qquad (1)$$

Where ip: the peak current, n: the number of electrons, F: Faraday constant, T: the temperature in Kelvin, R: the gas constant, A: the surface area of the working electrode, D: the diffusion coefficient of the electroactive species, C: the bulk concentration of the electroactive species and *v*: the scan rate of voltammograms.

Thus, if we know the value of diffusion coefficient of ferricyanide at 298K the surface area for ferricyanide are calculated from the slope of the plot of peak current versus √scan rate (Fig. 4.2).

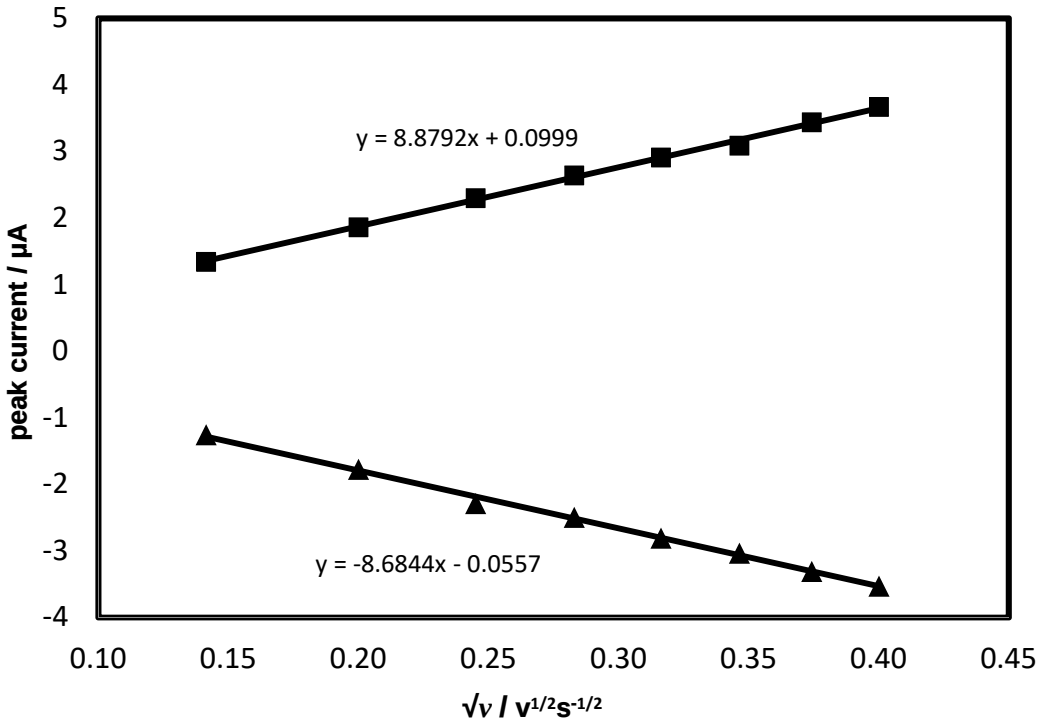

Fig. 4.2: The anodic and the cathodic peak current as function of the square root of the scan rate on GCE.

From Equation (1) we get,

$$\text{Slope} = 0.4463nF\sqrt{\frac{n}{R}}AC$$

$$A = \frac{S}{0.4\sqrt{\frac{n}{R}}C}$$

From the curve (Fig 4.2) the value of slope is ~9×10^{-6} and the standard value of diffusion coefficient for ferricyanide on GCE is 1.52×10^{-6} cm^2/s. where concentration C = 2×10^{-6} mol/cm^3 so we get,

$$A = \frac{9\times1^{-6}}{0.4\times1\times9\sqrt{\frac{1\times9\times1.5\times1^{-6}}{8.3\times2}}\times2\times1^{-6}}$$

$$A = 0.013\ cm^2$$

From the theoretical value the surface area of GC electrode i.e used for experiment is $0.01cm^2$. We show that the experimental value of surface area is very close to theoretical value. This calculated result has been used in further studies.

4.2 Synthesis of nanoparticle and its physical characterizations

The NiO nanocrystals were prepared using sol-gel synthesis method. Fig. 4.3 shows the XRD patterns of nanocrystals thus obtained. It is seen that the sample exhibits four strong well defined diffraction peaks at 2θ of 37.07, 43.22, 62.18 and 75.12° (Fig. 4.3) which are attributed to (111), (200), (220) and (311) planes of face-centered cubic (fcc) NiO phase (JCPDS file no. 73-1519, Fig. 4.4).The average crystallite size (D) of nanoparticles was calculated using the Scherer formula as follows [119]:

$$D_{h,k,l}=0.9\lambda/ (\beta_{h,k,l}\cos\theta)$$

Where λ is the wavelength (λ = 1.542 Å) (CuK_α), β is the full width at half maximum (FWHM) of the line, and θ is the diffraction angle.

The size of NiO nanostructure using the (111) plane reflection in XRD patterns was 24 nm, as seen in Fig. 4.3. and Table 4.2 shows Data of X-ray diffraction (XRD) pattern from NiO nanocrystal.

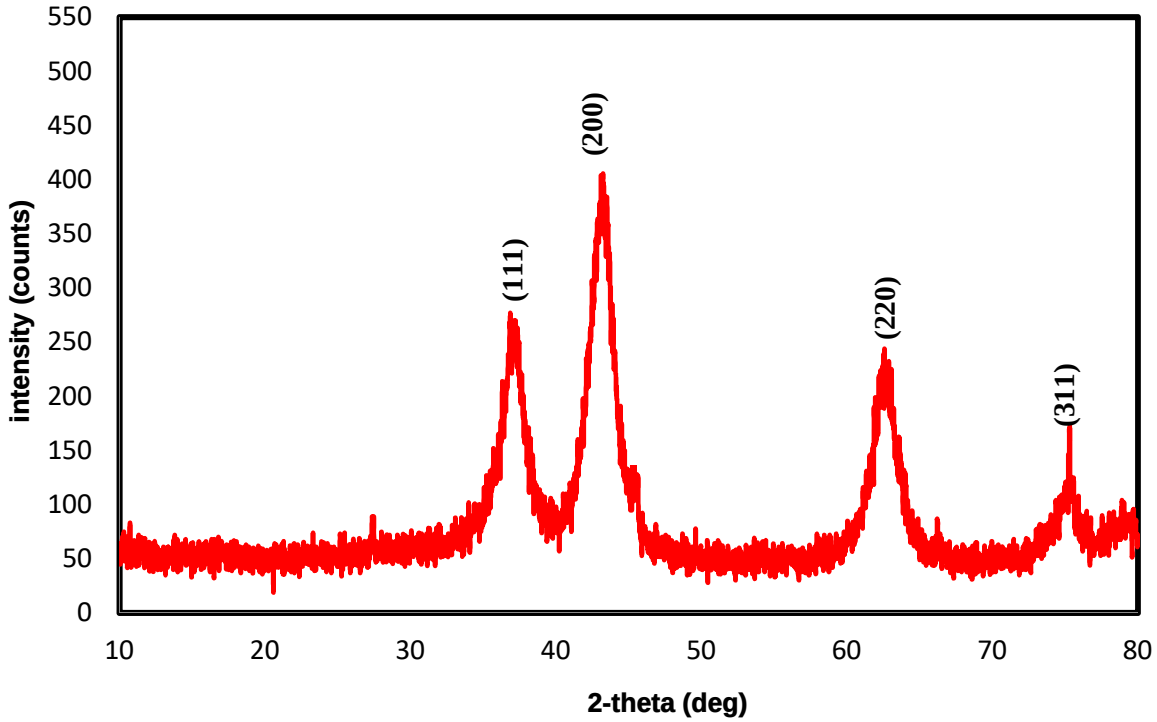

Fig. 4.3: XRD pattern of NiO nanocrystal.

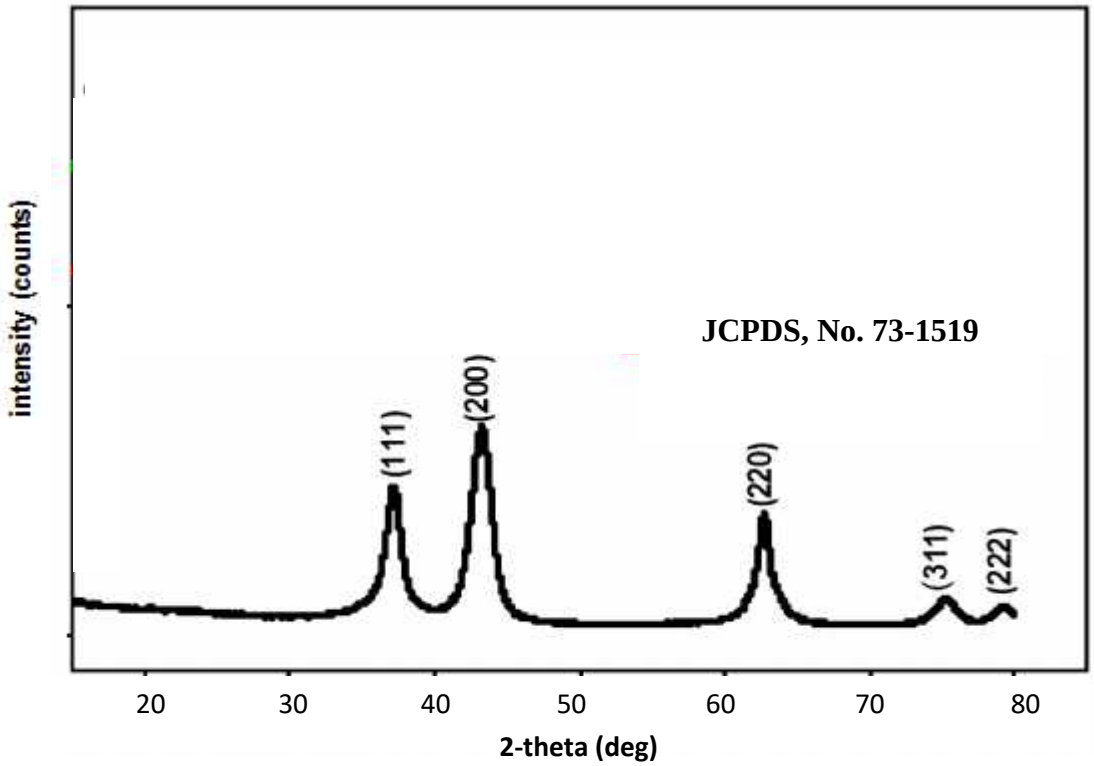

Fig. 4.4: Standard XRD pattern of NiO nanocrystal

Table 4.1. Data of XRD for NiO nanocrystals .

Hkl	2-theta(deg)	FWHM(deg)	Rel. int. I(a.u.)
111	37.07	0.59	54.40
200	43.22	1.71	100.00
220	62.186	1.46	51.95
311	75.12	0.73	13.13

The broad peak of XRD pattern indicates nanocrystalline behavior of the particles. In Fig 4.3 the noise of the signal is obtained which could be eliminated by further heating at higher temperature.

The morphology of NiO samples was characterized by FE-SEM technique. Fig. 4.5 shows the SEM images of NiO thus obtained.

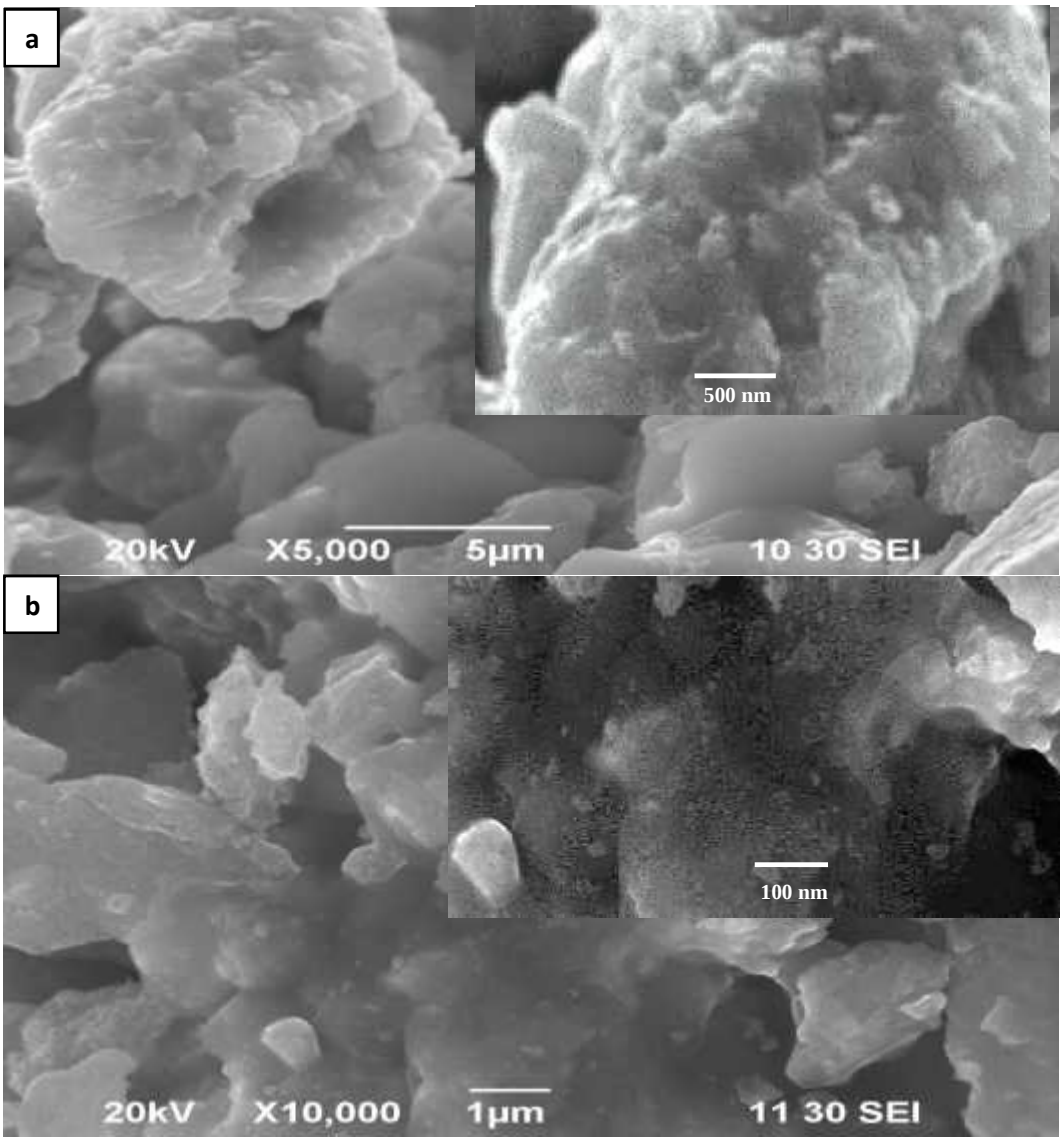

Fig. 4.5: SEM images of NiO nanocrystal.

The image (Fig.4.5) reveals that the NiO particles are in agglomerated form. However, a range of nanoparticles were obtained with the crystal size of 500 nm. From both XRD and SEM analysis, it is also observed that the average crystallite size of NiO nanoparticle is around 60 nm.

4.3 Sensor fabrication

Sensors were fabricated by modified drop casting method [117]. In brief, 10µL of NiO mixed with 5 µL of 1% chitosan, stirred for 10 min. 5µL of this mixture was placed onto the electrode surface and dried for overnight at room temperature. A schematic diagram of this modification has been shown in Fig. 4.6.

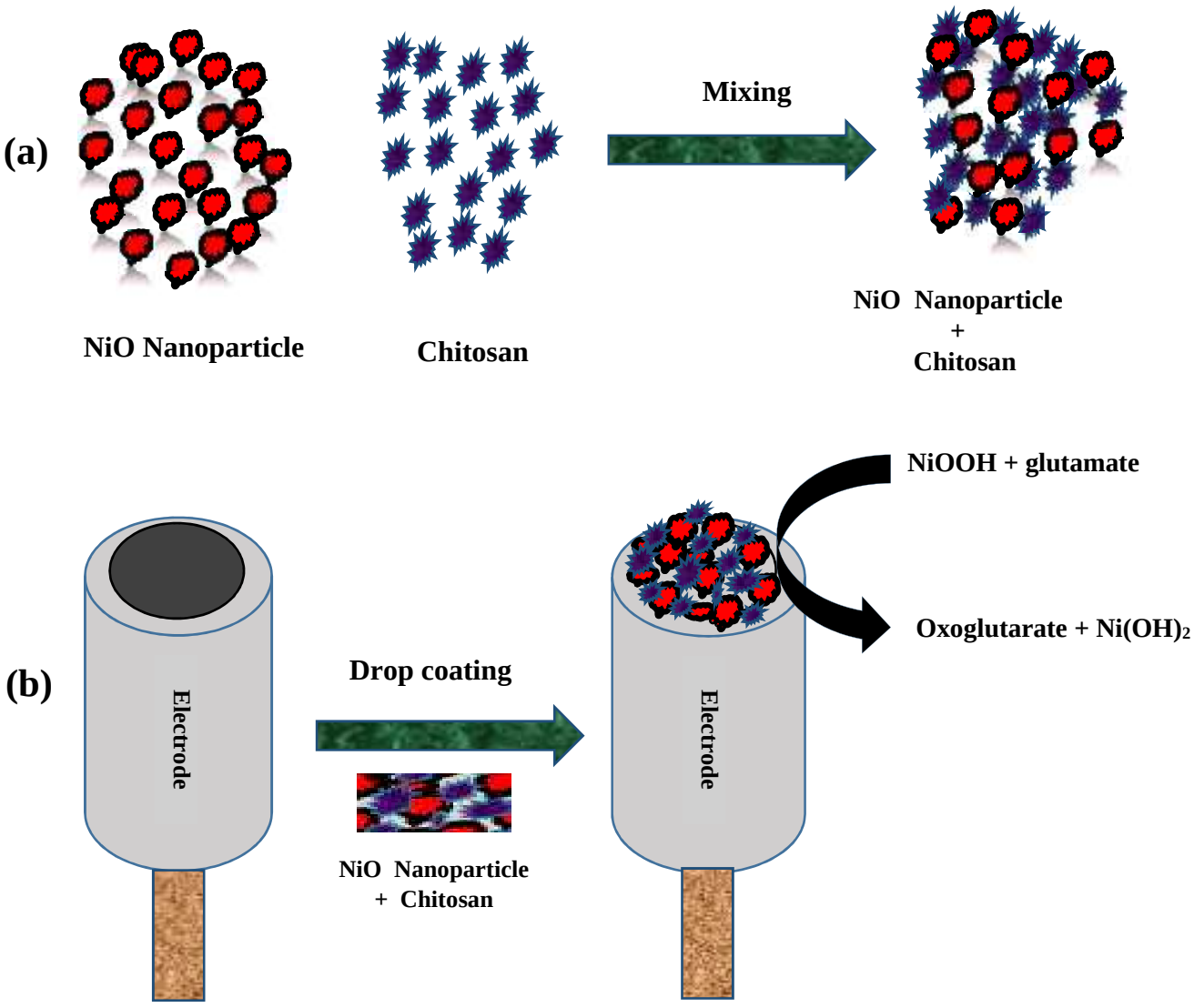

Fig. 4.6: Schematic illustration of stepwise fabrication of the glutamate sensor. a) mixing of 10 µL of NiO nanoparticle aqueous dispersion in presence 5 µL of 1% chitosan b) drop coating of NiO nanoparticle + chitosan.

4.4 Electrochemical characterisation of NiO nanoparticle modified GCE

To demonstrate the sensing application of the nickel oxide nanoparticle, a non-enzymatic glutamate sensor was constructed by deposition of the aqueous dispersion of NiO nanoparticle on a glassy carbon electrode (GCE) surface in the presence of chitosan.

Prior to the implementation of the as prepared NiO Nano crystal as a non-enzymatic sensor, their electrochemical behavior was investigated using cyclic voltammograms (CV). Fig. 4.7 shows the CVs of bare GCE and NiO nanocrystal modified GCE (designated as NiO/GCE) in 0.1 M NaOH at a scan rate of 0.05 VS^{-1}.

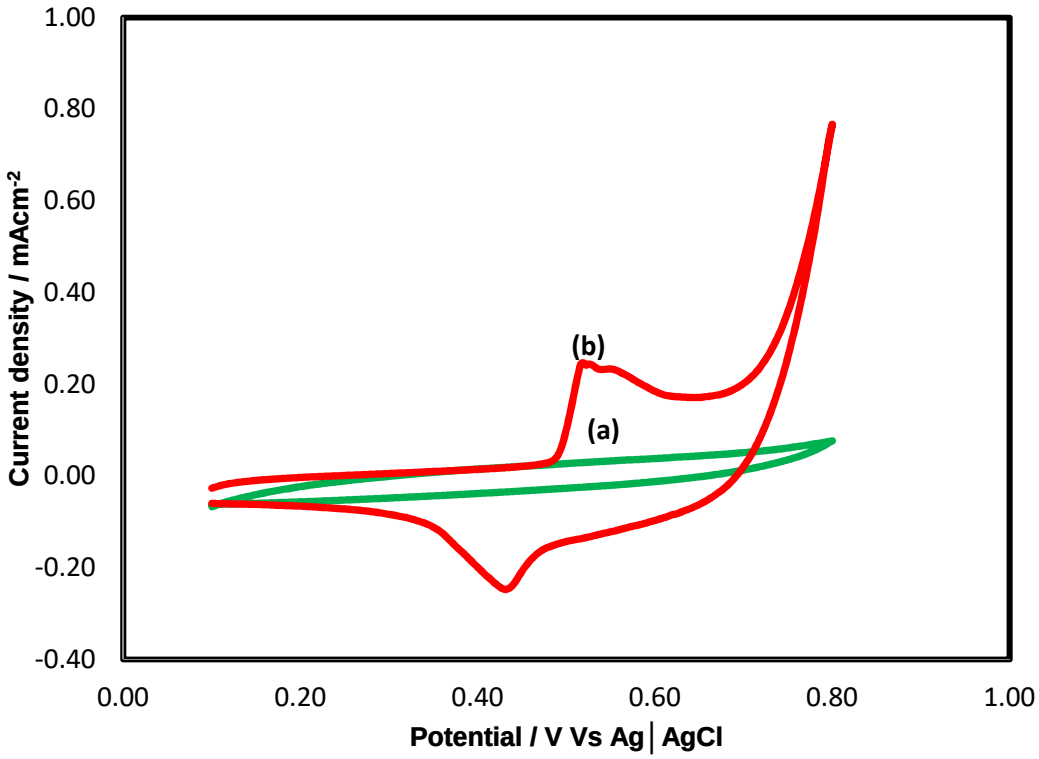

Fig. 4.7: CVs of 0.1 M NaOH (a) in bare GCE (b) in the presence of NiO/GCE (scan rate: 0.05 V/s).

It is seen that bare GCE exhibits no obvious oxidation peak in 0.1 M NaOH , indicating that the response of bare GCE toward the 0.1 M NaOH is pretty weak. In contrast NiO nanocrystal, exhibit a pair of anodic and cathodic peak at 0.51 and -0.23 V which attribute to the oxidation reactions due to the surface corrosion of metallic Ni [120].

However, pair of redox peaks may be correlated with the oxidation–reduction reaction showing to the presence of species in the metallic NiO nanocrystal. This is due to the fact

that in crystalline nanoparticle is arranged in a three dimensional order lattice. The nanocrystal is a well-ordered and stable structure contrary to an amorphous from based on the same element. Nanocrystal shows a high surface to volume ratio due to their small size [121]. As chemical reaction take place at the surface will also result in a more reactive material when in nano-size compare to bulk size.

It is also reported that [122] two pair of redox peaks is observed in the metallic NiNAE. It may be correlated with the oxidation–reduction reaction which is showing to the presence of multiple species. Two redox peaks can be attributed to the difference in chemical reactivity of polycrystalline phases of Ni towards oxidation–reduction reactions (Ni^{2+}/Ni^{3+}) [123]. In Fig 4.7 shows only one pair of redox peak which is indicating to the presence of on its own chemical reactivity of polycrystalline phases of the nickel oxide nanocrystal.

However, the anodic and cathodic peaks complied with other publications and can attribute to the formation and reduction of a few monolayers of NiOOH by the surface corrosion of metallic Ni [124-125]. Therefore, the reactions which occurred on the surface can be described as follows:

1. $Ni(OH)_2 + OH^- \longrightarrow NiOOH + H_2O + e^-$
2. $NiOOH + H_2O + e^- \longrightarrow Ni(OH)_2 + OH^-$

According to Fig. 4.7, the total current is increased by 20% in NiO/GCE compare to the bare GC electrode which indicate that the NiO/GCE is highly efficient. The electrochemical performance of NiO nanostructures is highly dependent on the morphology and size. A number of works have been reported on various strategy of modifying electrode surface [29, 65, 82, 116]. However, majority of them involved complicated processing steps. In this work, we have constructed NiO nanocrystal modified GCE where fabrication method is facile and cost effective.

We also have prepared another two types of modified GC electrodes using NiO hollow sphere obtained from $NiCl_2$ as well as Ni $(CH_3COO)_2$ using hydrothermal methods. We

also have tested graphite (pencil) instead of GC as sensing platform for the modification which is discuss in the next section.

Figure 4.8 shows the cyclic voltammograms of bare GCE and NiO hollowsphere prepared from $NiCl_2$ modified GCE (designated as NiO(NC)/HSs/GCE) in 0.1 M NaOH at a scan rate of 0.05 Vs^{-1}. It is seen that in contrast to NiO nanoparticle, NiO hollowsphere, exhibit a pair of anodic and cathodic peak at 0.602 V and -0.17 V respectively, which are attributed to Ni(II)/Ni(III) couple. According to Fig. 4.8, the total current is increased by 15% in NiO(NA)/HSs/GCE electrode compare to the bare GCE electrode indicating the NiO(NC)/HSs/GCE less efficient compare to the NiO/GCE.

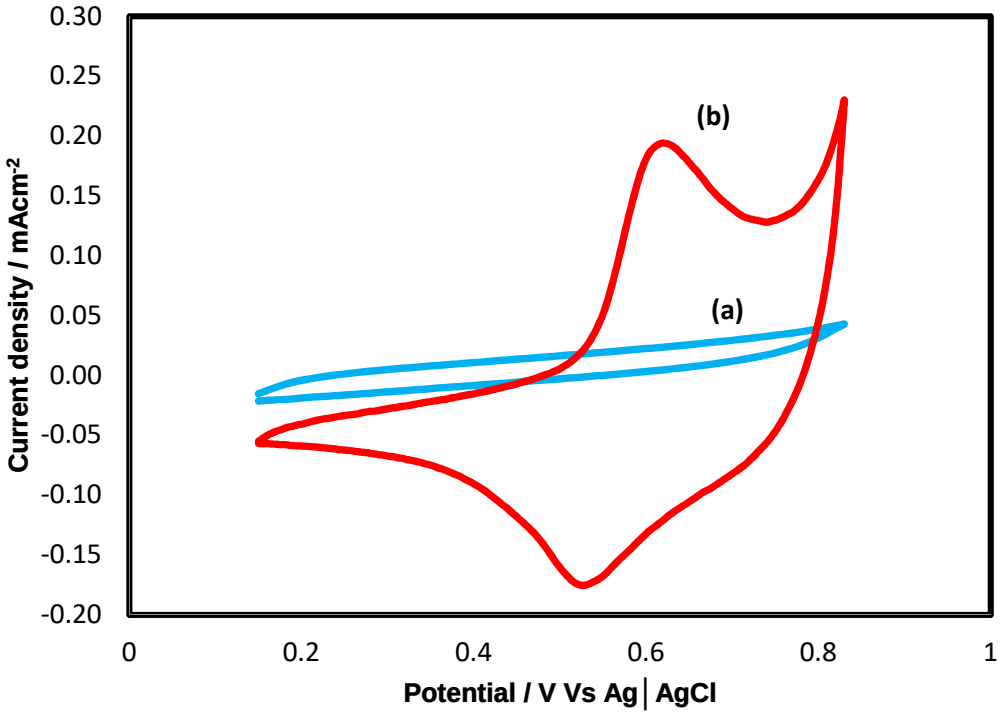

Fig. 4.8: CVs of 0.1 M NaOH (a) in bare GCE (b) in the presence of NiO(NC)/HSs/ GCE (scan rate: 0.05 V/s).

On the other hand NiO hollowsphere prepared from $Ni(CH_3COO)_2$ modified GCE (elected as NiO(NA)/HSs/GCE) show a pair of anodic and cathodic peak at 0.401V and -0.04 V in Fig. 4.9 can also be attributed to the surface deterioration of metallic Ni.

The cyclic voltammograms (CV) of 0.1 M NaOH at NiO(NA)/HSs/GCE electrode shows that the total current is increased by 4.5% in NiO(NA)/HSs/GCE electrode compare to the bare GCE electrode.

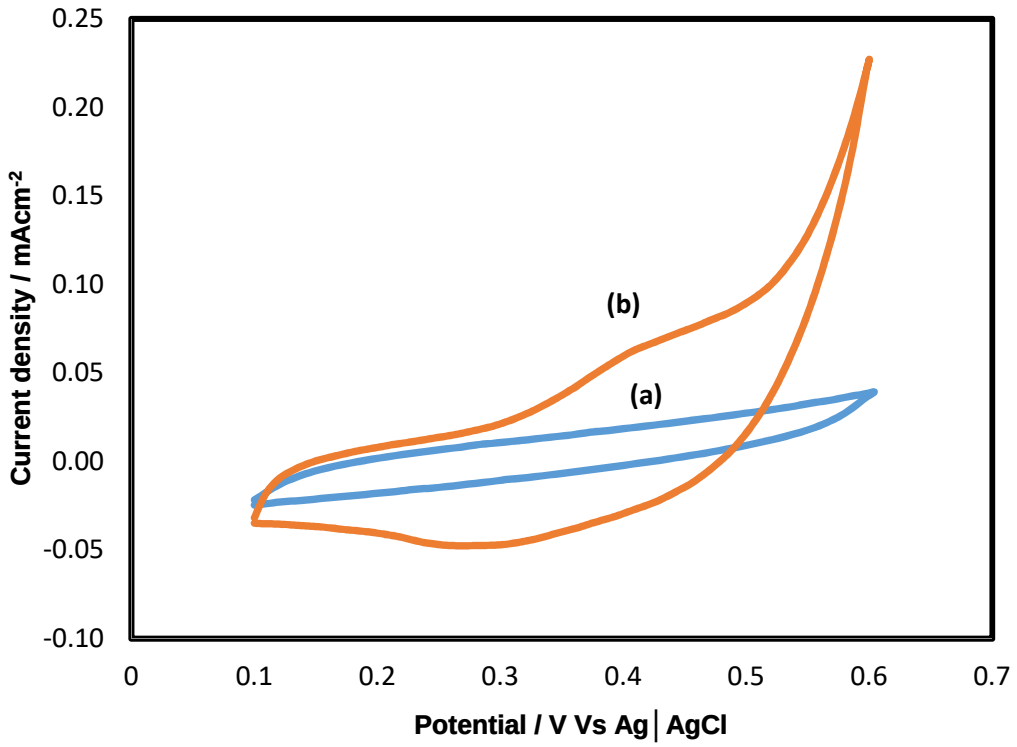

Fig. 4.9: CVs of 0.1 M NaOH (a) in bare GCE (b) in the presence of NiO(NA)/HSs /GCE (scan rate: 0.05 V/s).

It can be observed that the total current is increased for NiO/GCE 5 times compare to the NiO(NC)/HSs/GCE and NiO(NA)/HSs/GCE electrode which can be attribute to the good competence of NiO/GCE electrode. It is also seen that the reaction process is diffusion controlled on both electrodes.

4.5 Electrochemical characterisation of NiO nanoparticle modified graphite (Pencil) electrode

Previously we discuss the electrochemical behavior of NiO/GCE, now we discuss the electrochemical behavior of nickel oxide nanoparticle modified graphite (pencil) electrode.

To establish the analytical application of the nickel oxide nanoparticle, towards the graphite (pencil) electrode, the surface of the electrode was constructed by deposition of the aqueous dispersion of NiO nanoparticle in the presence of chitosan. Fig. 4.10 represents the CVs of bare graphite (pencil) and NiO nanocrystal modified graphite (pencil) electrode in 0.1 M NaOH at a scan rate of 0.05 Vs^{-1}.

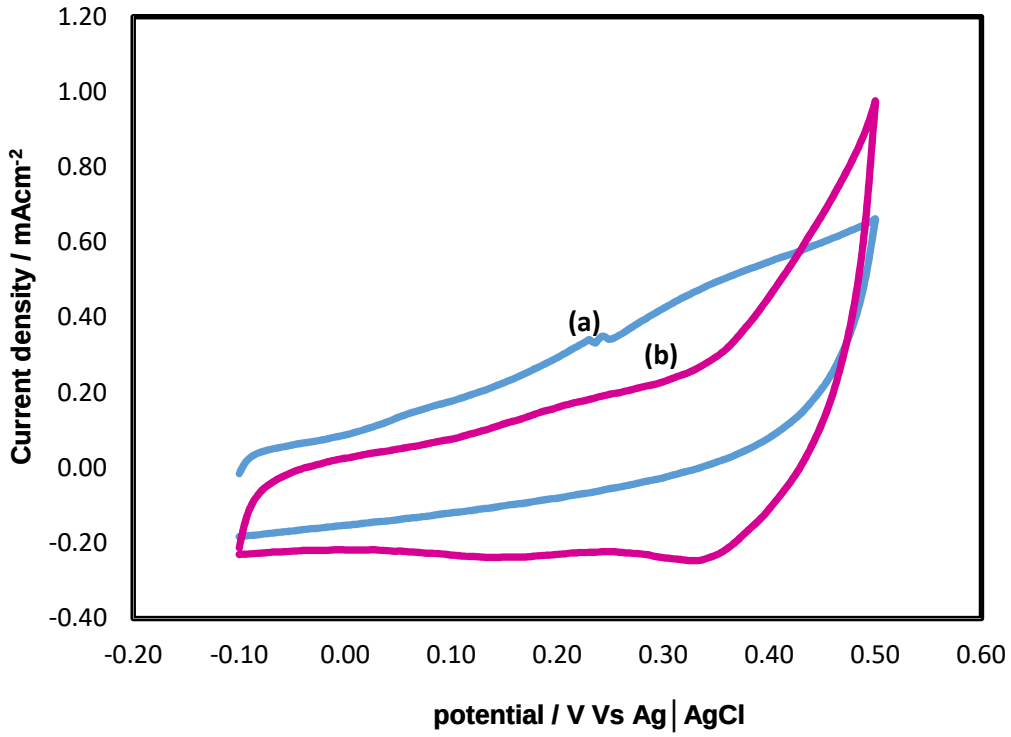

Fig. 4.10: CVs of 0.1 M NaOH (a) in bare graphite (b) in the presence of NiO naocrystal modified graphite electrode (scan rate: 0.05 V/s).

It is seen that bare graphite electrode exhibits no obvious oxidation peak in 0.1 M NaOH , indicating that the response of bare graphite electrode toward the 0.1 M NaOH is pretty weak. In contrast NiO nanocrystal, exhibit a pair of anodic and cathodic peak at

0.25 and -0.38V which attribute to the oxidation reactions due to the surface corrosion of metallic Ni [120].

According to Fig. 4.10, the total oxidation current is decreased in NiO nanocrystal, modified pencil electrode compare to the bare GCE electrode which indicate that the electrode is not efficient.

Fig. 4.11 represents the CVs of bare GCE and NiO hollowsphere prepared from $NiCl_2$ (NiO(NC)/HSs) modified graphite (pencil) electrode in 0.1 M NaOH at a scan rate of 0.05 Vs^{-1}. From Fig. 4.11 it is seen that no oxidation peak in bare and modified graphite electrode. It is also shows that the total current decreased in modified graphite (pencil) electrode than the bare graphite electrode.

Similar behavior occurred in Fig. 4.12 which represents the CVs of bare pencil electrode and NiO hollowsphere prepared from $Ni(CH_3COO)_2$ (NiO(NA)/HSs) modified graphite (pecil) electrode in 0.1 M NaOH at a scan rate of 0.05 VS^{-1}.

From the elementary analysis it is seen that pencil is not contain pure graphite. It is also found that some species such as Al, Ca, Mg, Si, gluing agent etc. usually co-exist with graphite (Fig. 4.13). In our opinion this species may interfere the reactivity of nickel oxide nanoparticle inhibit the sensitivity towards glutamate. That's why the formation and reduction of monolayers of NiOOH by the surface corrosion of metallic Ni cannot ensue successfully on graphite electrode. That's why the total current response is irregular for modified graphite electrode.

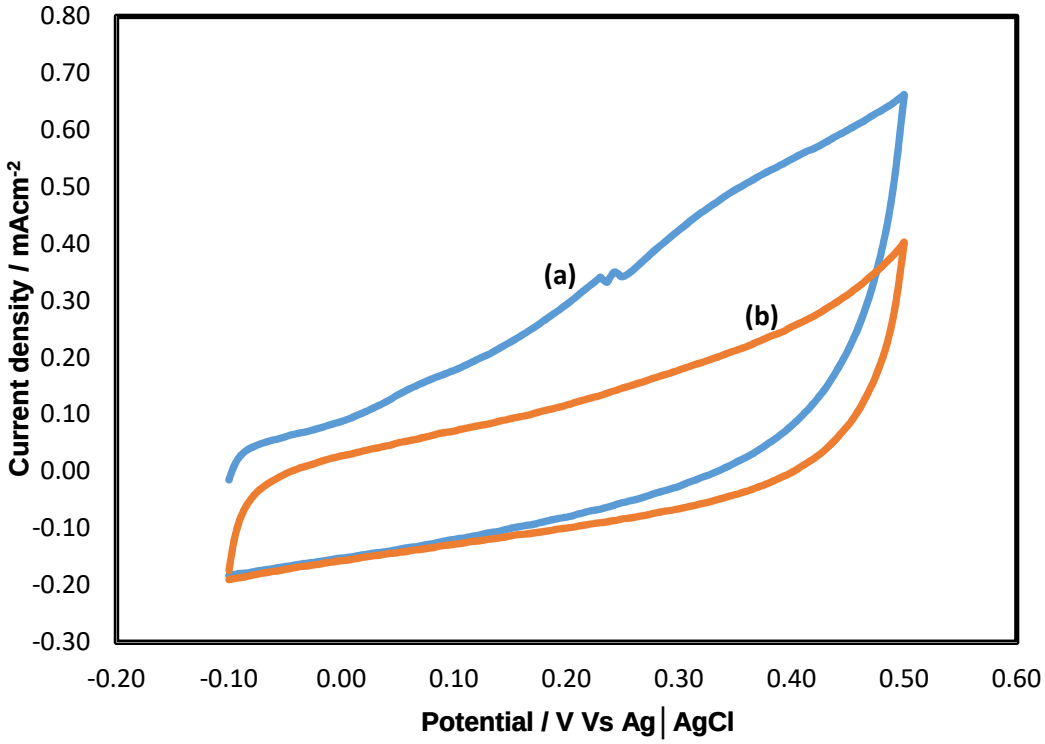

Fig. 4.11: CVs of 0.1 M NaOH (a) in bare graphite (b) in the presence of NiO(NC)/ HSs modified graphite electrode (scan rate: 0.05 V/s).

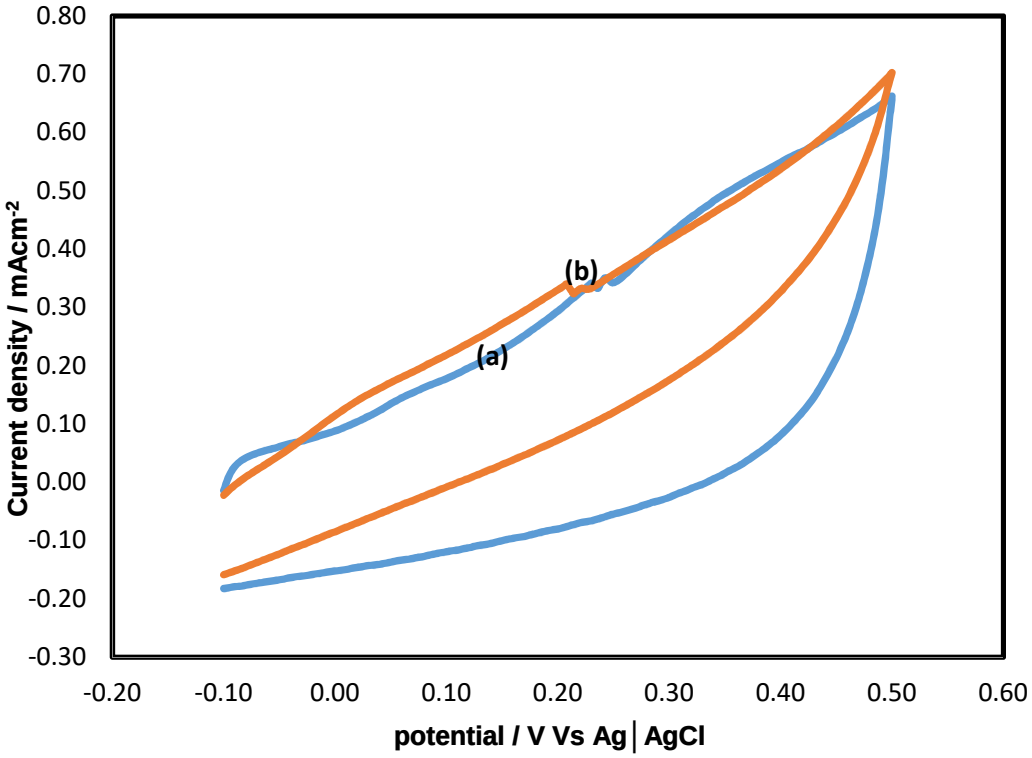

Fig. 4.12: CVs of 0.1 M NaOH (a) in bare graphite (b) in the presence of NiO(NA)/ HSs modified graphite electrode (scan rate: 0.05 V/s).

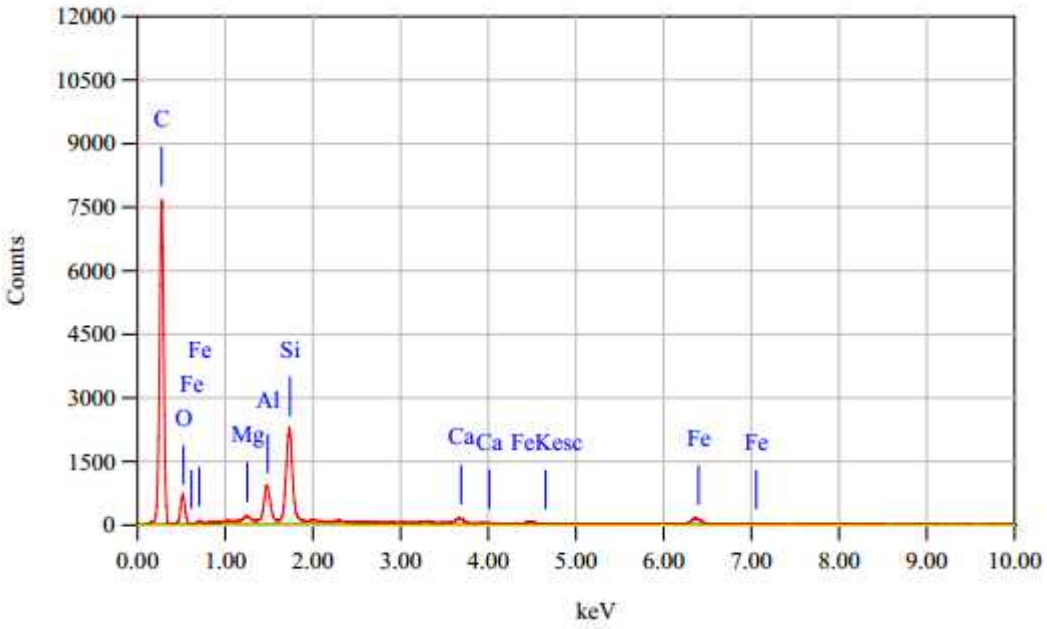

Fig. 4.13 : EDX of bare graphite electrode.

4.6 Electrocatalytical oxidation of L-glutamate at NiO nanoparticle GCE.

In order to address the analytical applicability of the NiO/GCE, NiO(NC)/HSs/GCE and NiO(NA)/HSs/GCE electrodes, we investigated the electrocatalytic activity of these electrodes towards glutamate.

Fig. 4.14 presents the CV responses of NiO/GCE in 0.1 M NaOH without (a) and with L-glutamate of 10 mM (b). In the absence of glutamate, a redox peak of Ni (II) / Ni (III) was observed. Upon the addition of glutamate, an increase of the anodic peak current density can be observed for NiO/GC electrode.

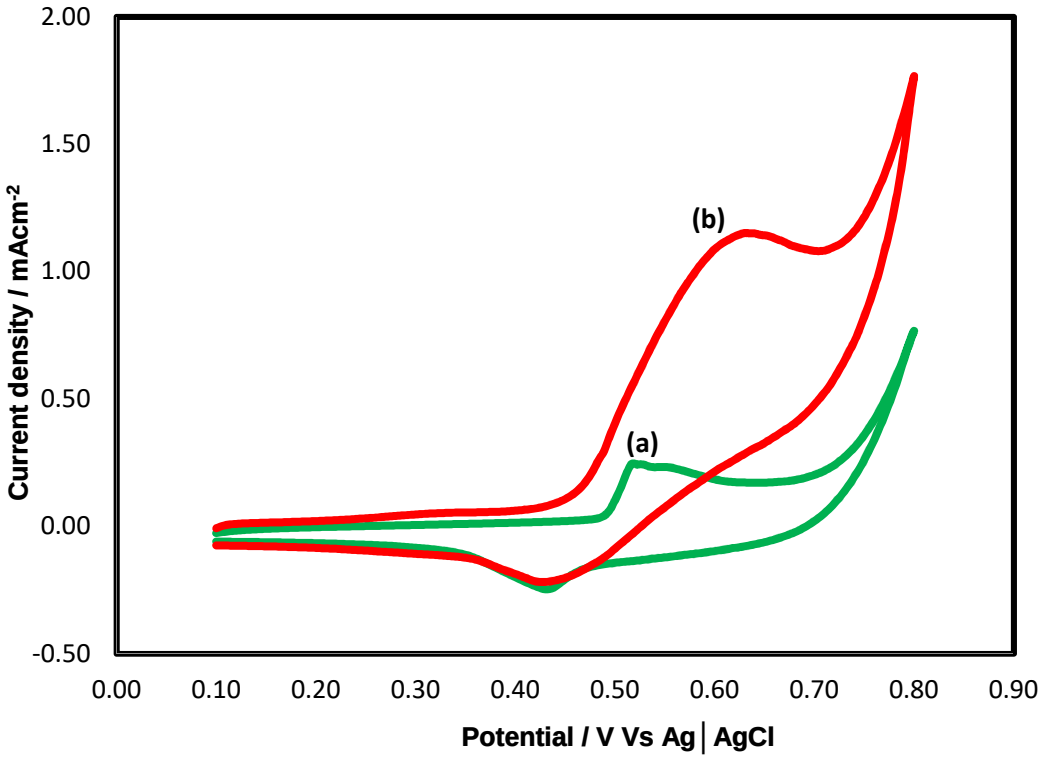

Fig. 4.14: CVs of, NiO/GCE (a) without glutamate and (b) with 10 mM glutamate in 0.1 M NaOH (scan rate: 0.05 V/s).

This indicates that NiO-nanocrystal can catalyze oxidation of glutamate in NaOH solution, which is similar to the previously reported results on detection of glutamate based on NiO-based materials [88]. This specifies that NiO/GCE exhibit excellent electrocatalytic activity towards the oxidation of glutamate without using any enzyme.

It also can be seen that with the addition of glutamate, the anodic peak shifts to the higher potential, which may attribute to the diffusion limitation of glutamate at the electrode surface. Similar behavior was obtained in other literatures for Ni electrode [126-127].

The mechanism for oxidation of glutamate by NiO-based materials could be represented by the following reactions: First, Ni^{2+}could be electro-oxidized to Ni^{3+} in alkaline solution, where the release of electron resulted in the formation of oxidation peak current. Then, of glutamate could be oxidized to oxoglutarate by Ni^{3+}, which was deoxidized to Ni^{2+} at the same time according to the following reactions:

1. $Ni(OH)_2 + OH^- \longrightarrow NiOOH + H_2O + e^-$
2. $NiOOH + glutamate \longrightarrow Ni(OH)_2 + Oxoglutarate$

Fig. 4.15 shows after addition of 10 mM glutamate, the intensity of oxidation peak increases which indicates that NiO/HSs can catalyze oxidation of glutamate in NaOH solution. It also can be seen that, the anodic peak shifts to the higher potential, with the addition of glutamate which may associate to the diffusion limitation of glutamate at the electrode surface.

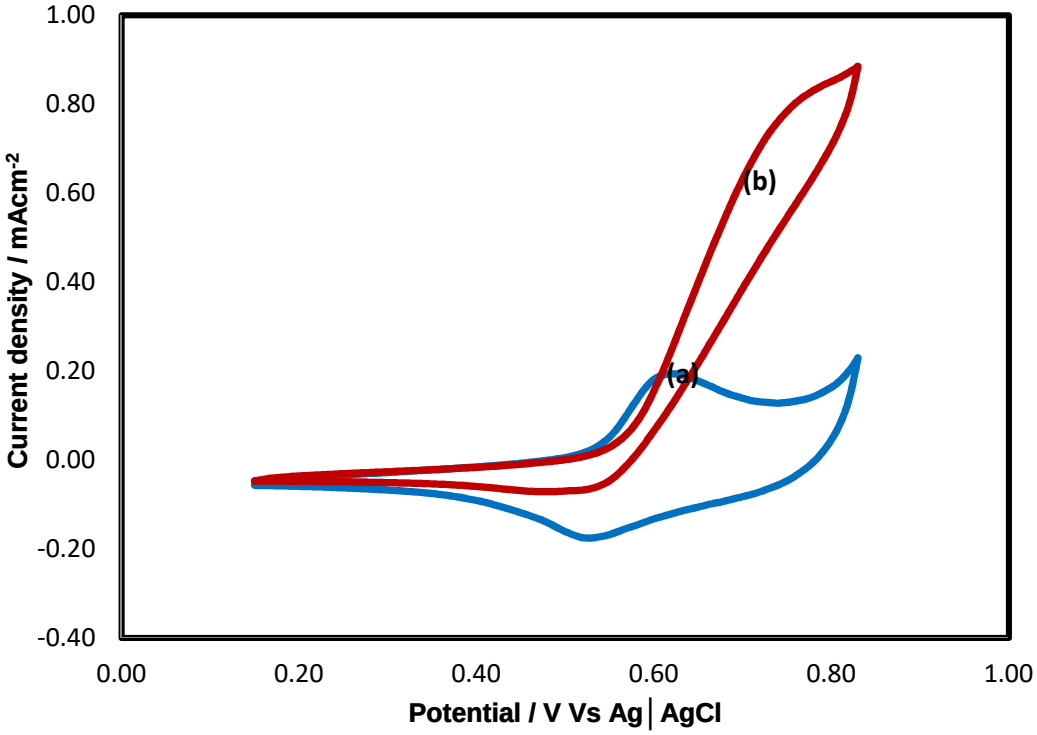

Fig. 4.15: CVs of, NiO(NC)/HSs/GCE (a) without glutamate and (b) with 10 mM glutamate in 0.1 M NaOH (scan rate: 0.05 V/s).

Fig. 4.15 presents the CV responses of NiO(NA)/HSs/GCE electrode in 0.1 M NaOH without (curve a) and with L-glutamate of 10 mM (curve b). It is seen that after addition of 10 mM glutamate the anodic peak current increase at potential 0.402V which indicate that this electrode shows catalytic activity.

In NiO/HSs surface glutamate also oxidized to oxoglutarate by Ni^{3+}. However, total catalytical current due to the addition of 10 mM glutamate is increased in NiO(NC)/ HSs/GCE electrode compared to the NiO(NC)-HSs electrode (according to cyclic voltammogram).

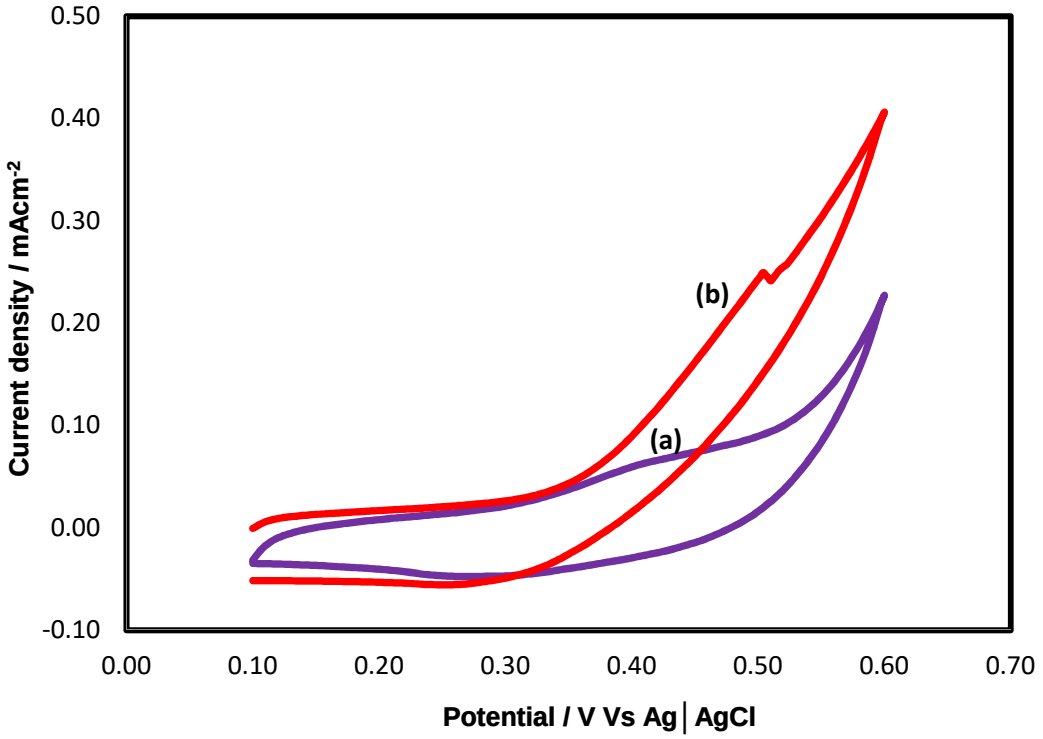

Fig. 4.16: CVs of, NiO(NA)/HSs/GCE (a) without glutamate and (b) with 10 mM glutamate in 0.1 M NaOH (scan rate: 0.05 V/s).

In case of NiO(NA)/HSs/GCE electrode a little decrease in cathodic peak current can be seen and therefore, in our opinion it can be attributed due to the difference in chemical reactivity of crystalline phases of Ni towards oxidation–reduction reactions (Ni^{2+}/ Ni^{3+}) [123].

It also can be seen that with the addition of glutamate, the anodic peak shifts to the higher potential in both the NiO/GCE, NiO(NC)/HSs/GCE and NiO(NA)/HSs/GCE electrodes, which may be indicating to the diffusion limitation of glutamate at the electrode surface. Similar behavior was obtained in other literatures for Ni electrode [126-127].

It also can be observed that catalytic peak potential for NiO(NC)/HSs/GCE shifted towards higher potential compare to the NiO/GCE and NiO(NA)/HSs/GCE for 10 mM glutamate addition. Decrease in cathodic peak current can be observed for NiO(NA)/HSs/GCE but in case of NiO/GCE the anodic and cathodic peak current both increase at lower potential indicating that NiO/GCE electrodes exhibit excellent electrocatalytic activity towards the oxidation of glutamate without using any enzyme than other electrodes.

4.7 Electrocatalytic oxidation of L-glutamate on NiO nanoparticle modified graphite electrode

We also investigate the electrocatalytic activity of nickel oxide modified graphite electrode towards the oxidation of glutamate. To establish the sensing application of modified pencil electrode we investigated the electrocatalytic activity of the electrodes towards glutamate. Fig. 4.17, Fig. 4.18 and Fig. 4.19. presents the CVs of current responses of modified graphite (pencil) electrode in 0.1 M NaOH without (a) and with L-glutamate of 10 mM (b).

From these Fig. it reveals that NiO-nanoparticle cannot catalyze oxidation of glutamate in NaOH solution at the surface of graphite (pencil) electrode, which indicate that Ni^{2+}could not be electro-oxidized to Ni^{3+} in alkaline solution.

These specify that the nickel oxide nanoparticle cannot totally modify the surface of the graphite (pencil) electrode because of interferents (Fig. 4.13).

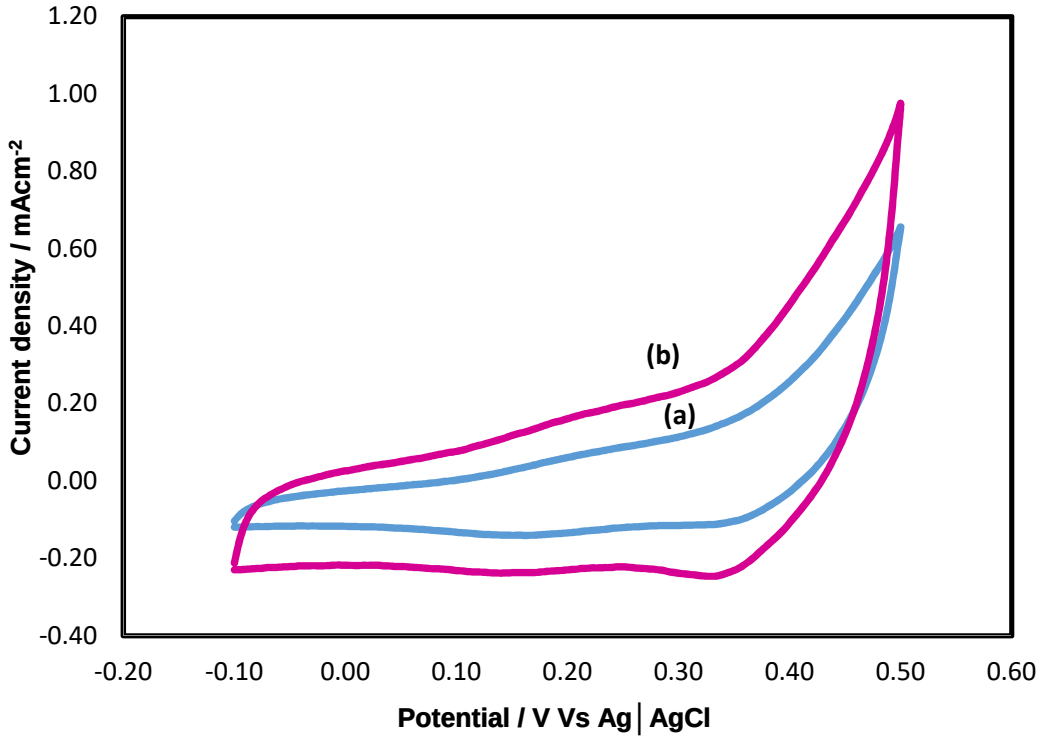

Fig. 4.17: CVs of, NiO nanocrystal modified graphite electrode (a) without glutamate and (b) with 10 mM glutamate in 0.1 M NaOH (scan rate: 0.05 V/s).

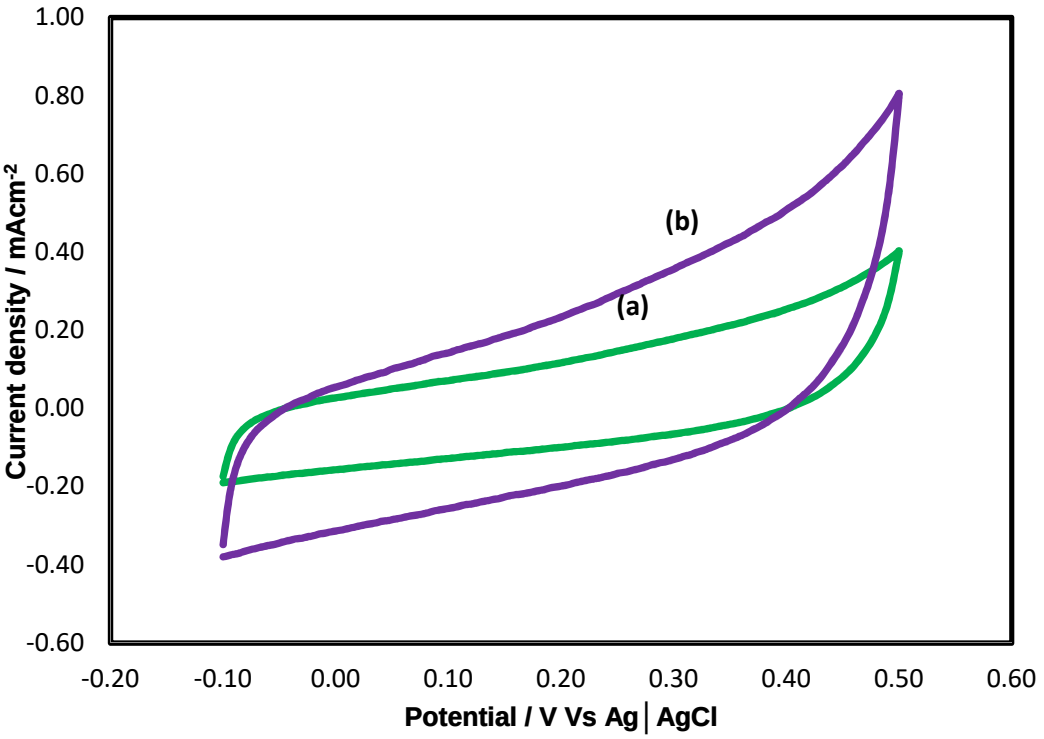

Fig. 4.18: CVs of, NiO(NC)/HSs modified graphite electrode (a) without glutamate and (b) with 10 mM glutamate in 0.1 M NaOH (scan rate: 0.05 V/s).

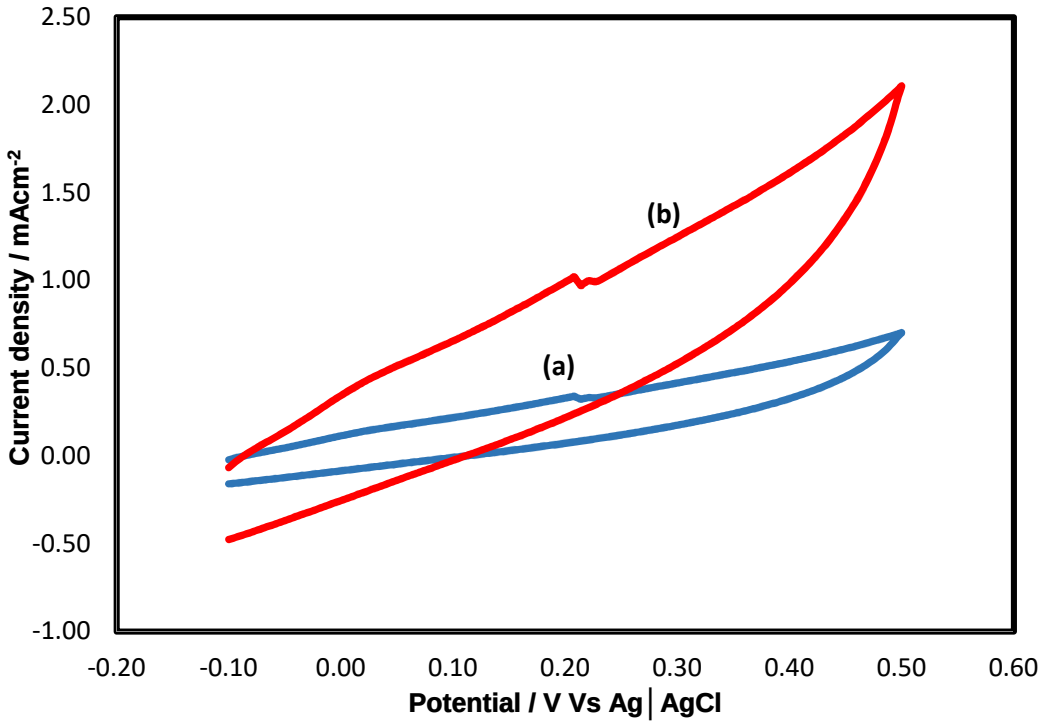

Fig. 4.19: CVs of, NiO(NA)/HSs modified graphite electrode (a) without glutamate and (b) with 10 mM glutamate in 0.1 M NaOH (scan rate: 0.05 V/s).

It is observed that the nickel oxide nanoparticle exhibit excellent electrocatalytic activity towards the oxidation of glutamate on GCE compare to the pencil electrode. Because GCE contain pure graphite which has excellent mechanism and electrical properties, wide potential window, chemical inertness (solvent resistance), and relatively reproducible performance. In GCE the improved electron transfer reactivity has been attributing to the removal of surface contaminants, exposure of fresh carbon edges, and an increase in the density of surface oxygen groups (which act as interfacial surface mediators).

4.8 Amperometric sensing and analytical performance of the glutamate sensor

In order to obtain a better understanding of the sensitivity of the glutamate sensor the current response change with glutamate concentrations was investigated.

For the amperometric sensing application, NiO nanocrystal is generally evaluated by measuring the current response for glutamate into stirred 0.1 M NaOH. Fig.4.20 presents the amperometric responses for the NiO nanocrystal during the successive addition of 1.0

mM glutamate in 0.1M NaOH at an applied potential of 0.55 V. The electrode could successfully catalytically detect electron transition from Ni (II) / Ni (III). When an aliquot of glutamate was added into the stirring NaOH solution, the NiO/GCE responded rapidly to the substrate and the current rose steeply to reach a stable value. At the applied potential of 0.55 V, the anodic current of the sensor increased dramatically and achieved 95% of the steady-state current within 5 s, revealing a fast amperometric response behavior.

For calibration graph, where standard deviation found to be minimum compare to the current obtained in a single point. However, sensitivity has been calculated using the current density value obtained at each concentration. Sensitivity of glutamate obtained was 11 μA/mM/cm^2 for NiO/GCE. Glutamate sensitivity for NiO/GCE is significantly higher than the majority of the reported glutamate [29, 82, 88, 97, 116, 127, 128, 129, 130, 131] where the sensitivity varies between 0.001 and 10.76 μA/mM /cm^2.

The detection limit is estimated to be 272 μM at a signal-to-noise ratio of 3. Furthermore, the NiO/GCE sensor was also used for detection of glutamate with a relatively wide concentrations ranging from 1 to 8 mM.

Fig. 4.21 shows the plot of electrocatalytic current of glutamate versus the corresponding concentrations of glutamate in NiO/GCE. It is seen that NiO nanocrystal electrode is linear for glutamate detection up to 8 mM, with a sensitivity 11 μA/mM/cm^2, which is more sensitive than other glutamate sensor. The performance of previously reported sensor platform for glutamate detection where majority of them involved complicated processing steps, which are not efficient to improve the sensitivity, response time and overall reliability of the system compare to the NiO/GCE.

In order to investigate the sensing application of NiO(NC)/HSs/GCE and NiO(NA)/ HSs/GCE electrodes the current response is measured for glutamate into stirred 0.1 M NaOH solution.

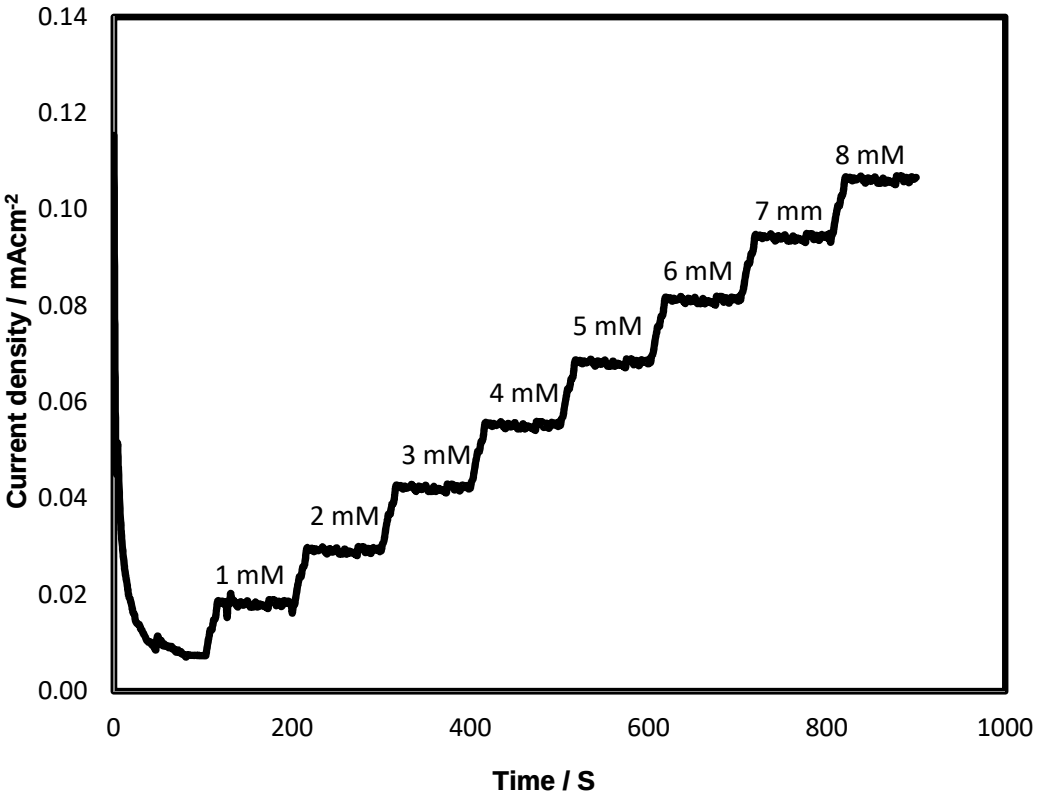

Fig. 4.20: Typical amperometric current response of the NiO/GCE upon the successive addition of glutamate with concentrations from 1 to 8 mM into stirred 0.1 M NaOH solution.

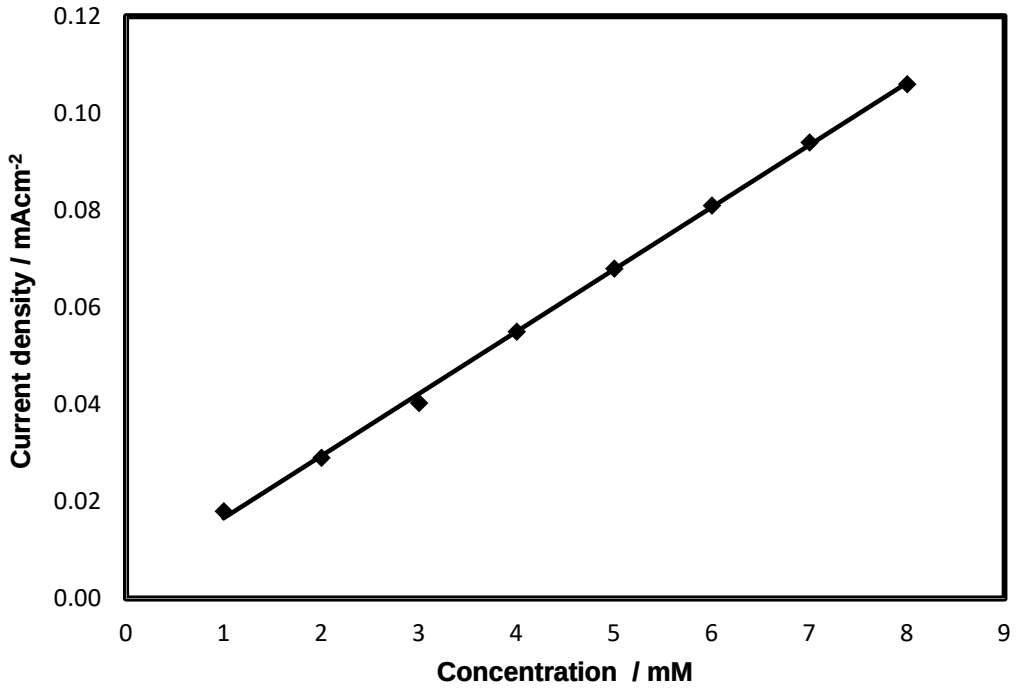

Fig. 4.21: The plot of electrocatalytic current of glutamate versus the corresponding concentrations of glutamate in NiO/GCE.

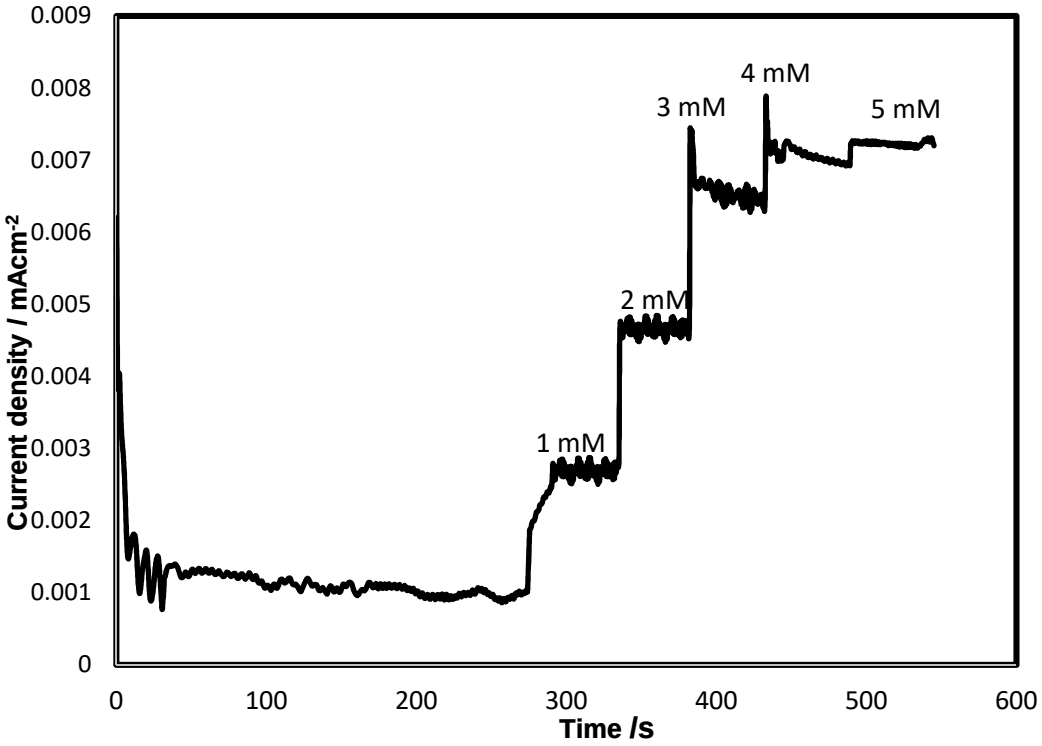

Fig. 4.22: Typical amperometric current response of the NiO(NC)/HSs/GCE upon the successive addition of glutamate into stirred 0.1 M NaOH solution.

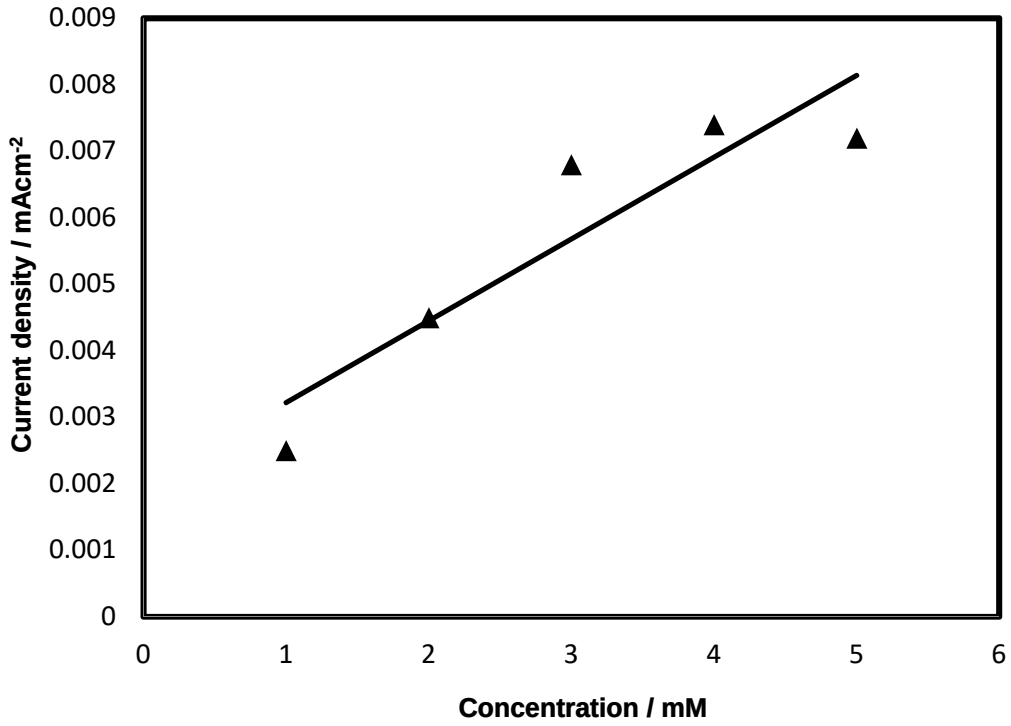

Fig. 4.23: The plot of electrocatalytic current of glutamate versus the corresponding concentrations of glutamate in NiO(NC)/HSs/GCE.

Fig. 4.22 shows a typical amperometric response of the NiO(NC)/HSs/GCE upon the successive addition of a certain concentration of glutamate into stirred 0.1 M NaOH solution. At the applied potential of 0.65 V, the anodic current of the sensor increased dramatically and achieved 95% of the steady-state current within 5 s, revealing a fast amperometric response behavior.

The plot of electrocatalytic current of glutamate versus the corresponding concentrations of glutamate (Fig 4.23). It shows that NiO(NC)/HSs/GCE electrode is linear for glutamate detection 3 mM with sensitivity ~2 μA/mM/cm^2 which indicate that NiO(NC) /HSs/GCE electrode is low sensitive compared to NiO/GCE on addition of 1 mM glutamate in 0.1 M NaOH solution. This is attributed to the lower electrocatalytic properties of the NiO(NC)/HSs/GCE electrode in the basic medium. The detection limit of NiO(NC) /HSs/GCE is estimated to be 335 μM at a signal-to-noise ratio of 3.

Sensitivity has been calculated using the current density value obtained at each concentration. Sensitivity of glutamate obtained was ~2 μA/mM/cm^2 for NiO(NC)/HSs /GCE electrode which is significantly 5.5 times lower than the NiO/GCE.

Fig. 4.24 shows a typical amperometric response of the NiO(NA)/HSs/GCE upon the successive addition of a certain concentration of glutamate into stirred 0.1 M NaOH solution.

At the applied potential, initially the anodic current of the sensor increased dramatically after addition of 1mM glutamate. When another 1 mM glutamate is added to the stirred 0.1 M NaOH solution the sensitivity decreased. After addition of 4 mm glutamate the sensor is stopped to response towards glutamate. In our opinion this is occurred due to the reactivity of crystal. This is attributed to the lower efficiency of the NiO(NC)/HSs/GCE electrode in the basic medium. The detection limit of NiO(NA)/HSs/GCE is estimated to be 290 μM at a signal-to-noise ratio of 3.

The insets of Fig. 4.25 show electrocatalytic current is decreased for glutamate detection, which indicate that NiO(NA)/HSs/GCE electrode is electrocatalyticaly weak towards the glutamate detection.

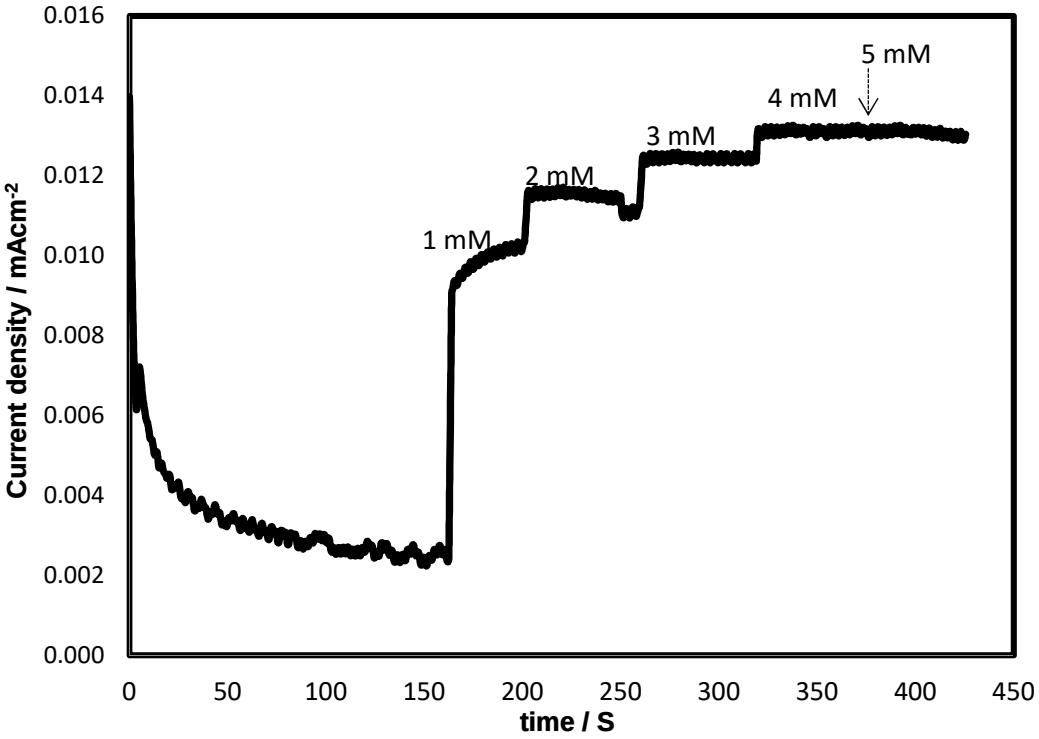

Fig 4.24: Typical amperometric current response of the the NiO(NA)/HSs/GCE upon the successive addition of glutamate into stirred 0.1 M NaOH solution.

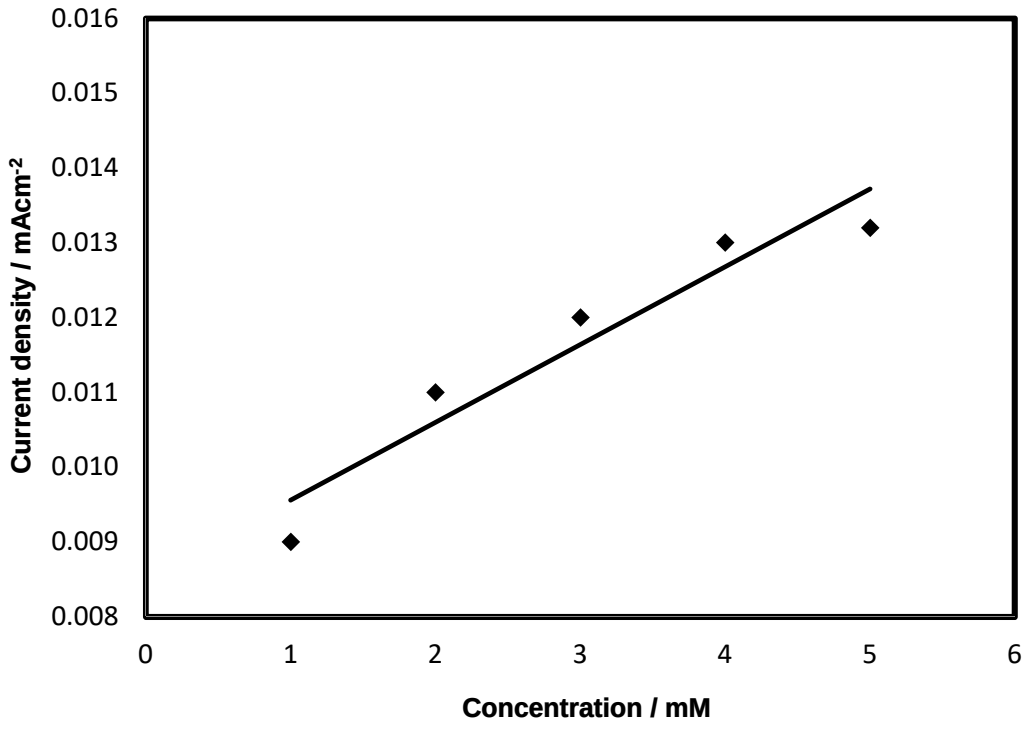

Fig. 4.25: The plot of electrocatalytic current of glutamate versus the corresponding concentrations of glutamate in NiO(NA)/HSs/GCE.

A comparison of nickel oxide modified GC electrodes base on sensitivity, linearity range, limit of detection are shown in Table 4.3. Table 4.3 reveals that NiO/GC electrode has high sensitivity with low detection limit with a high linearity range towards the oxidation of glutamate compare to the other two electrodes.

Table 4.3: Comparison of analytical performance of nickel oxide modified GC electrodes.

Electrodes	Limit of detection (µM)	Linearity range (mM)	Sensitivity µA/mM/cm^2
NiO /GCE	272	1-8	11
NiO/HSs/GCE (prepared from $NiCl_2$)	335	1-3	~2
NiO/HSs/GCE [prepared from $Ni(CH_3COO)_2$]	290	-	3

Table 4.4: A comparison of the performance of some sensor platform for glutamate detection.

Electrodes	Linearity range (mM)	Sensitivity µA/mM/cm^2	Enzyme	References
PtNP/AuNAE	0.1-1.4	10.76	GlutOX	[89]
Planar Pt	0.2–6.0	1.43	GlutOX	[88]
Pd Electrode		12.1	GlutOX	[97]
Au Electrode	0.05–0.15	2.5	GlutOX	[130]
Planar Pt	0.005–1.0		GlutOX	[131]
PtNP–TiO_2nanotube arrays	4×10^{-3}–1.25	1.68	GlutOX	[132]
PtNP–CNT TiO_2nanotube arrays	1×10^{-3}–2	0.134	GlutOX	[133]
Pt–AuNP TiO_2nanotube arrays	-	2.92	GlutOX	[134]
NiO nanocrystal on GCE	1-8	~11	No Enzyme	(this work)

Table 4.4 shows Comparison of analytical performance of our proposed Glutamate sensor sensor with other published glutamate sensors where we show that a number of works have been reported on various strategy of employing modified electrode surface to improve the sensitivity. However, majority of them involved complicated processing steps, which are not efficient to improve the sensitivity and overall reliability of the system. In this work, we fabricated a novel NiO nanocrysatl modified electrode and evaluated them in glutamate detection without using any enzyme. Moreover, we have developed a new, cost effective; highly sensitive (11 μA/mM/cm^2) with a linear range 1 to 8 mM sensing platform compare to a large number of reported glutamate sensor.

4.9 Effect of pH in NiO/GCE

The effect of pH was determined by carrying out over the pH range 3–9 at a temperature of 25°C. The response of the current density NiO/GCE for different pH is shown in Fig. 4.26.

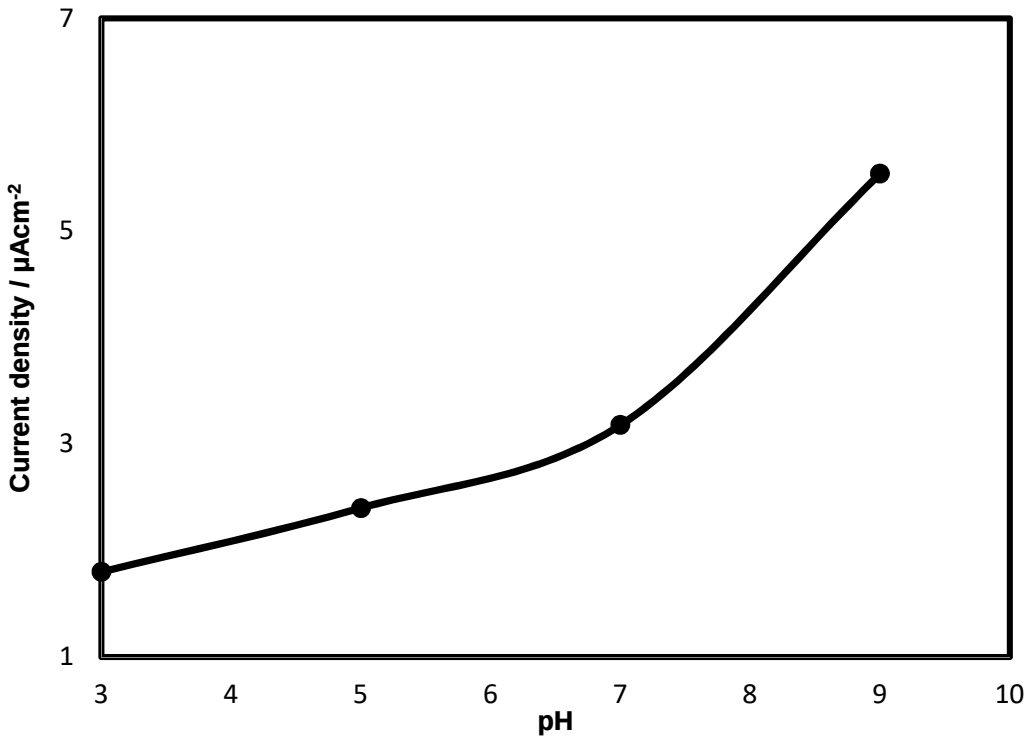

Fig. 4.26: Response of the current density NiO/GCE at different pH.

It is seen that the response of current increase with the increasing of pH. The total current is maximum at basic media, which indicate that the electrocatalytic activity towards the

oxidation of glutamate NiO nanoparticle modified GCE is highly increased in basic media. Because in basic media Ni^{2+}could be easily electro-oxidized to Ni^{3+} resulted in the formation of oxidation peak current and then, glutamate could be oxidized to oxoglutarate by $Ni^{3+.}$

4.10 Interferences studies

It is well known that some easily oxidative species such as AA, and UA usually co-exist with glutamate in human blood. One of the major challenges in non-enzymatic glutamate detection could be electrochemically active interferents, which generate electrochemical signals at the same potential as glutamate. However, for the non-enzymatic sensor, investigation needs to be done whether background subtraction method would work or not to eliminate electrochemical interferents [82].

Therefore, we have examined the amperometric responses of the NiO/GCE at an applied potential of 0.55 V in 0.1 M NaOH solution with continuous additions of 2 mM glutamate, 100 µM uric acid, 100 µM ascorbic acid and 1 mM glutamate. From the current response in Fig. 4.27, a significant signal was obtained for glutamate compared to the uric acid and ascorbic acid.

We also investigate the amperometric responses of the NiO(NC)/HsS/GCE and NiO(NA)/ HsS/GCE at an applied potential of 0.65 and 0.401V respectively in 0.1 M NaOH solution with continuous additions of 2 mM glutamate, 100 µM uric acid, 100 µM ascorbic acid and 1 mM glutamate as shown in Fig. 4.28 & Fig. 4.29 respectively.

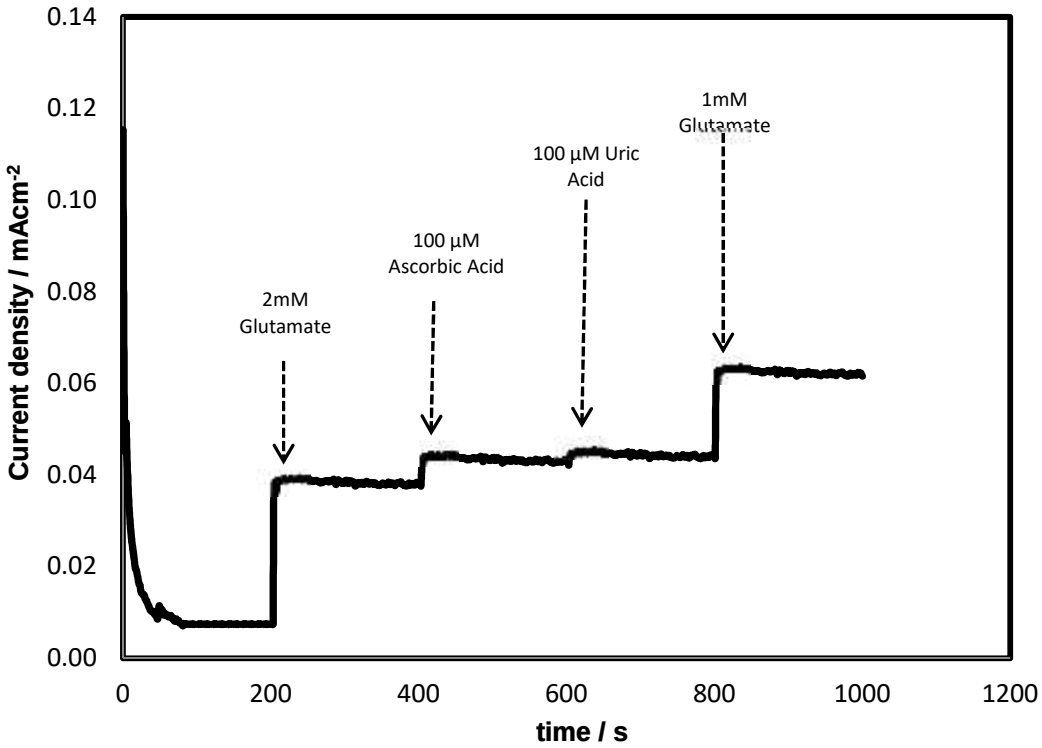

Fig.4.27: Interference test of NiO/GCEin 0.1 M NaOH at +0.55 V with glutamate and other interferents including AA,and UA.

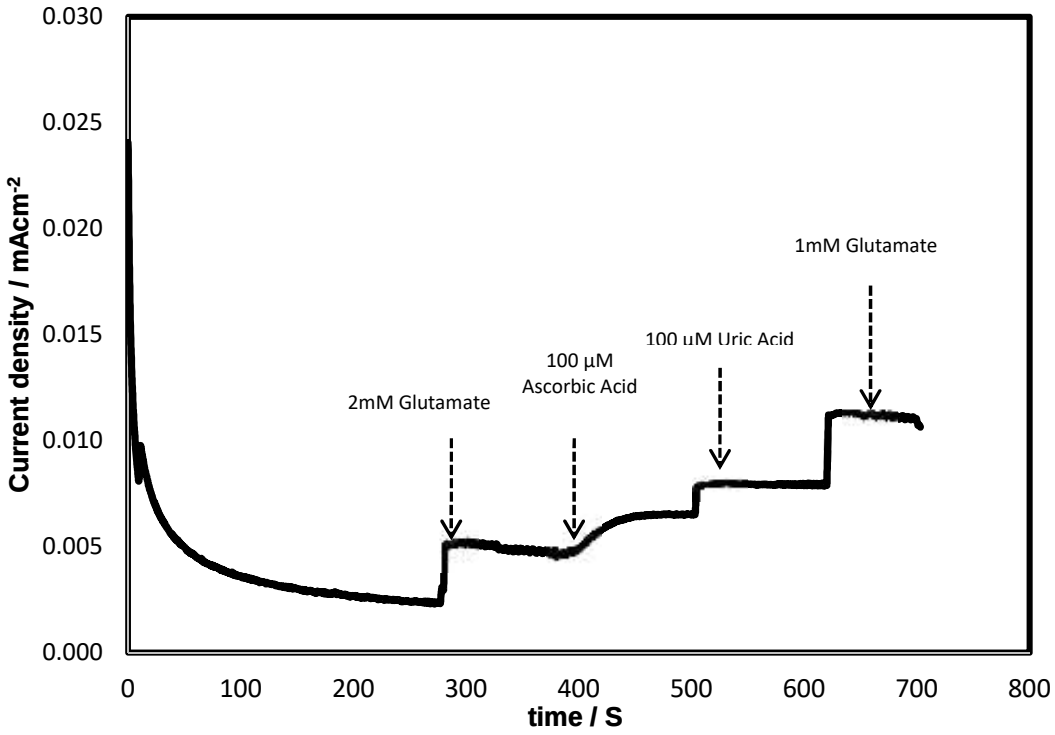

Fig. 4.28: Interference test of NiO(NC)/HsS/GCE in 0.1 M NaOH at +0.65 V with glutamate and other interferents including AA,and UA.

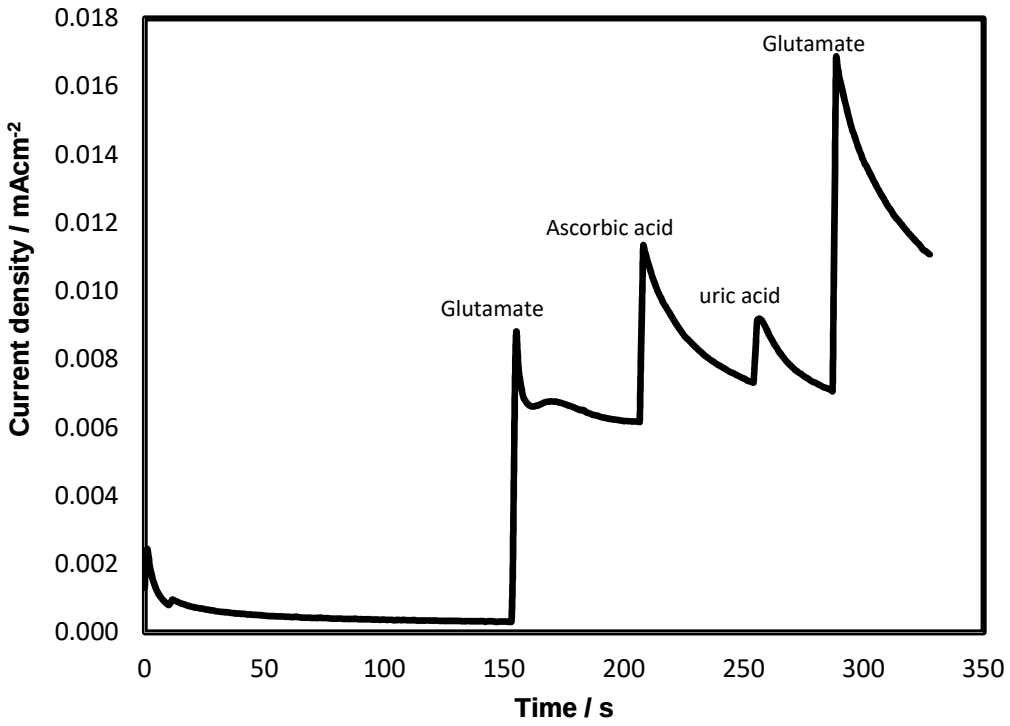

Fig. 4.29: Interference test of NiO(NA)/HSs/GCE in 0.1 M NaOH at +0.401 V with glutamate and other interferents including AA, and UA.

From interference studies we show that in NiO/GCE the change of current response due to addition of AA and UA is lower compare to NiO/HSs/GCE. It indicates the high selectivity of NiO/GCE than NiO/HSs/GCE.

Although the addition of AA and UA also induce the increasing current of NiO/GCE, compared to 2 mM glutamate, the interfering species of 100 μM ascorbic acid yielded current response of ~15 % and 100 μM uric acid of ~ 3 % for the intensity increased is much smaller than that of glutamate. These results indicate that NiO/GCE shows good selectivity toward glutamate and could be used as a good sensing material for highly selective and sensitive detection of glutamate in the practical conditions.

In this study mM range glutamate has been taken as a consideration during calculation; it is because average daily intake of glutamate which is safe for human is 0.3–1.0 g [133]. Therefore, detecting glutamate below this level is important and more relevant for interference study.

4.11 Stability of the NiO modified GC electrode

The stability of the NiO nanoparticle modified electrodes was determined over a period of one week, with analysis carried out every day, 5 assays each day with 1.0 mM glutamate addition (Fig 4.30, Fig 4.31, & Fig 4.32). In between the testing, the electrode was stored in air at ambient conditions. Electrode was found to retain high activity after 1 week.

From Fig 4.30, it exposes that the stability of NiO/GCE is 89 % after 4 days of its initial activity and 65 % activity was retained after 7 days. On the other hand stability of NiO(NC)/HSs/GCE is decreased 49 % after 4 days of its initial activity and after 7 days it was taken only 10 % (Fig. 4.31). Similar behavior has been observed for NiO(NA)/HSs /GCE (Fig. 4.32).

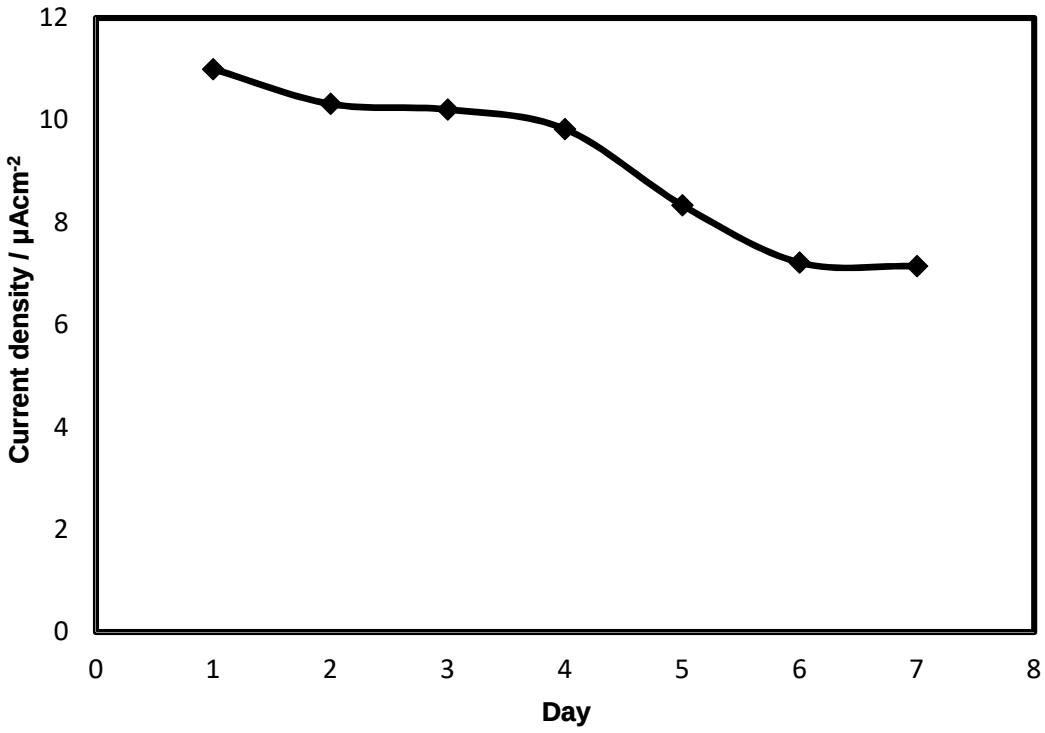

Fig. 4.30: Stability of the NiO/GC electrode over a period of one week.

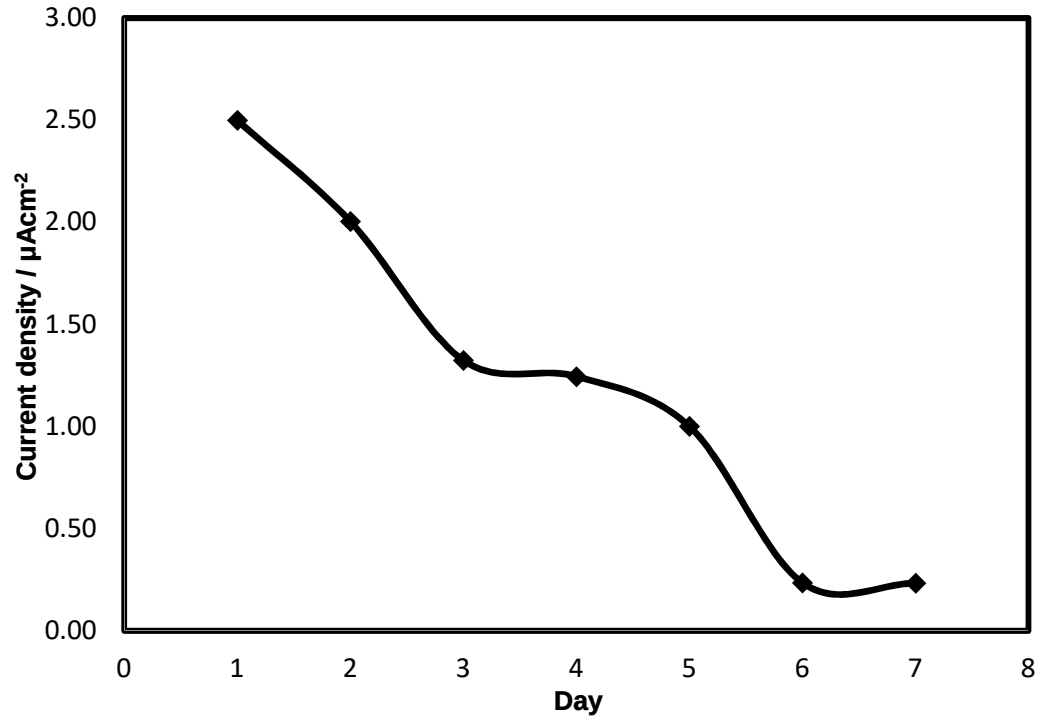

Fig. 4.31: Stability of the NiO(NC)/HSs/GC electrode over a period of one week.

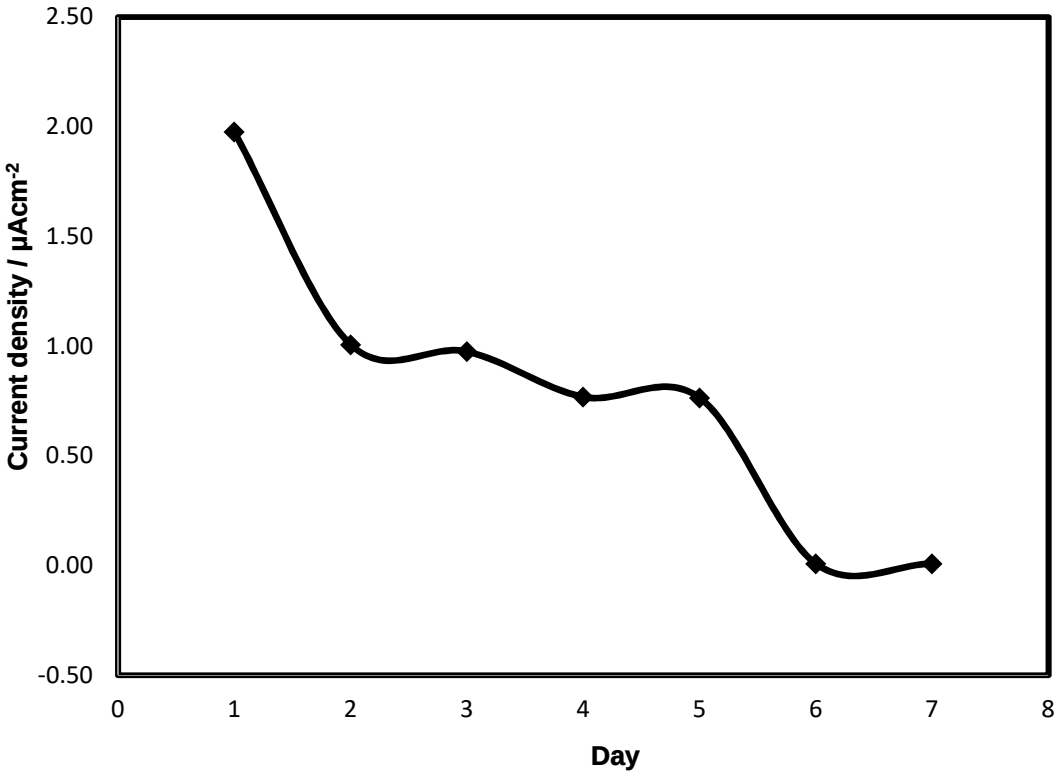

Fig 4.32: Stability of the NiO(NA)/HSs/GC electrode over a period of one week.

The NiO/GCE is more stable compare to NiO/HSs/GCE. This is due to the fact of the crystalline which shows a high surface to volume ratio due to their small size. Because of their high surface-to-volume ratio and tunable electron transport properties due to quantum confinement effect, their electrical properties are strongly influenced by minor perturbations.

In this study, we have developed a sensitive and selective glutamate sensor using novel NiO nanocrystal. The results of electrochemical detection of glutamate indicate NiO nanocrystal exhibit high selectivity, high sensitivity and low detection limit toward the oxidation of glutamate. Our present study is important because it provides us a novel method for non-enzymatic detection of glutamate by using metal oxides nanocrystal as sensing materials. The fabrication method is very cheap and easy compares to the previously reported some sensing platform.

CHAPTER V

Conclusions

In summary, a novel non-enzymatic glutamate sensor has been successfully fabricated using NiO nanoparticle as sensing materials in presence of chitosan.We have described a new, cost effective and sensitive sensor platform to detect glutamate.

In the present work, NiO nanoparticle has been synthesized using sol-gel method. The resulting NiO nanostructures have been used here for the development of an enzyme-free glutamate sensor. The synthesized NiO nanocrystals obtained diffraction peaks are in accordance with the reported standard spectrum JCPDS, No. 73-1519. Scanning electron microscopy is used for the study of the morphology of the prepared NiO nanostructures. It can be inferred that the nanostructures appeared like as nanocrystal having an average particle size of 50 nm.

Excellent catalytic activity has been found for glutamate detection using NiO/GCE. The sensitivity of NiO/GCE, has been found to be 11μA/mM/cm^2, and exhibited linear behavior for glutamate detection in the concentration range up to 8 mM with a limit of detection of 272 μM. The stability of NiO/GCE retain up to 65% after 1 week of regular use.

In this study we have also developed another sensing platform based on nickel oxide hollowsphere (NiO-HSs) that are prepared using a glycerin-assisted hydrothermal method. Catalytic activity has been found for glutamate detection using NiO-HSs/GCE is lower compare to NiO/GCE. The sensitivity of NiO-HSs/GCE is found ~2 μA/mM/cm^2 and ~3 μA/mM/cm^2 respectively which indicates lower performance in 0.1 M NaOH compare to NiO/GCE.

Moreover, NiO/GCE shows selectivity towards glutamate in the presence of physiological level of uric acid and ascorbic acid. In conclusion, we have developed possibly one of the cheapest sensor platform to detect glutamate which do not require any enzyme.

Recommendations

Further work is needed to improve the glutamate sensor. Recommendations are as follows

- To enhance the stability and sensitivity.
- Fixing nanoparticle on GC electrode.
- Extensive fundamental electrochemical properties will be investigated.
- To improve the sensor platform to enhance the cross reactivity of glutamate in the presence of interferences.
- Enabling to determine glutamate in real sample.